Natural Resources Canada | Ressources Naturelles Canada

GEOCHEMICAL AND STRUCTURAL EVOLUTION OF THE PLEASANT HILLS PLUTON, COBEQUID HIGHLANDS NOVA SCOTIA, CANADA

by

G. Pe-Piper and D.J.W. Piper

GEOLOGICAL SURVEY OF CANADA OPEN FILE

#3372

CONTRIBUTION TO THE CANADA NOVA SCOTIA COOPERATION AGREEMENT ON MINERAL DEVELOPMENT

CONTRIBUTION TO THE MAGDALEN BASIN (NATMAP) PROJECT

Geochemical and structural evolution of the Pleasant Hills pluton, Cobequid Highlands, Nova Scotia, Canada

G. Pe-Piper
Department of Geology, Saint Mary's University, Halifax, B3H 3C3, N.S., Canada

D.J.W. Piper
Atlantic Geoscience Centre, Geological Survey of Canada (Atlantic), Bedford Institute of Oceanography, P.O. Box 1006, Dartmouth, Nova Scotia B2Y 4A2, Canada

Abstract

This open file reports on field mapping and laboratory investigation of the latest Devonian - earliest Carboniferous Pleasant Hills pluton of the Cobequid Highlands of Nova Scotia. The report complements 1:20 000 and 1:10 000 maps and a Fieldlog data base.

Work supported by the Canada Nova Scotia Cooperation Agreement on Mineral Development. Project carried by the Geological Survey of Canada, Atlantic Geoscience Centre. Scientific Authority Dr. P.S. Giles. Some additional funding from the Natural Sciences and Engineering Research Council.

CONTENTS PAGE

TEXT

EXPLANATION OF BACK POCKET MAPS

Three 1:10 000 maps are presented. These were compiled prior to use of Fieldlog. They show all outcrops and sample numbers.

Two 1:20 000 maps are presented. These show outcrops in the Fieldlog data base and interpreted geological boundaries. The boundaries are based on outcrops both on these maps and 1:10 000 maps.

Digital versions of all five maps are available with this Open File.

INTRODUCTION

Geological setting

In the Cobequid Highlands of northern Nova Scotia, granite and diorite plutons of latest Devonian to earliest Carboniferous age occupy a linear belt about 160 km in length and 10 - 20 km wide (Fig. 1), bounded to the south by the Cobequid fault zone (CFZ). This fault zone is part of a major tectonic element, the Cobequid-Chedabucto fault zone, which marks the northern limit of the Carboniferous Minas sub-basin that was reactivated in the Triassic. This fault zone was a Devonian-Carboniferous dextral strike slip system (Mawer and White, 1987), interpreted as the suture between the Avalon and Meguma terranes (Eisbacher 1969, 1970; Williams, 1979; Keppie, 1989). Avalon-Meguma convergent tectonics took place in the early to middle Devonian (405 - 390 Ma: Keppie and Dallmeyer, 1987; Muecke et al. 1988) (Fig. 2). Other authors (Keen et al., 1991) have interpreted the suture zone as lying further south, with the Cobequid-Chedabucto fault zone resulting from late Devonian - Carboniferous transcurrent motion.

The Cobequid fault zone is a complex structural line that shows zones of faults parallel to the main zone (including the Kirkhill, Rockland Brook and Londonderry faults: Fig. 3) and with second order shear zones forming splays. Spatial strain variation, observed in areas of releasing and restraining bends, has probably occurred throughout the period of strong strike-slip motion on the CFZ (Waldron et al. 1989; Koukouvelas et al., in press). The amount of strike-slip motion on the fault is however poorly constrained. Early to mid-Devonian motion may have been sinistral (Keppie and Dallmeyer, 1987), during the main phase of collision of the Meguma and Avalon terranes (Muecke et al. 1988) (the "Acadian orogeny"), but in eastern Nova Scotia dextral shear on the Chedabucto fault has been dated from 359 - 372 $\pm$2 Ma using $^{39}Ar/^{40}Ar$ dating of micas (Keppie and Dallmeyer, 1987). This deformation immediately preceded or overlapped the period of pluton emplacement in the Cobequid Highlands. Post-Visean dextral slip of about 100 km is indicated by offset of the Antigonish and Shubenacadie basins.

The granitic magmas in the Cobequid Highlands could have been derived from melting of lower crust by mafic magma resulting from mid to late Devonian extension of the Magdalen basin (Piper et al., 1993). They are emplaced into Neoproterozoic metasedimentary and metavolcanic rocks and are associated with basaltic and rhyolitic volcanism (Koukouvelas et al., in press). The time of granite emplacement (Fig. 2) corresponds approximately to the development of the major Horton Group basins (Fig. 2). Fault motion along the Cobequid-Chedabucto fault zone can be demonstrated both before emplacement of the plutons (Keppie and Dallmeyer, 1987) and immediately afterwards (Donohoe and

Wallace, 1985).

Much of the mid-Devonian - early Permian Magdalen Basin is interpreted to be underplated by thick mafic lower crust on the basis of seismic and gravity data (Marillier and Verhoef, 1989; Marillier and Reid, 1990). The Pleasant Hills pluton lies immediately southwest of the underplated area. The Pleasant Hills pluton occurs at a bend in the CFZ and its major splays. The Pleasant Hills pluton has yielded U-Pb zircon dates of about 361+-2 Ma (Doig et al., in press).

GEOLOGY OF THE PLEASANT HILLS PLUTON

Contact relationships

The Pleasant Hills pluton (Donohoe and Wallace, 1982) is approximately 20 km long and 5 km wide and lies immediately north of the Cobequid fault zone (Fig. 3). It is a composite pluton that includes diorite, granodiorite, and several granitic phases including high-level porphyry, all cut by at least two generations of mafic dykes (Pe-Piper et al., 1989a). The Rockland Brook fault, a major strike-slip splay off the Cobequid fault zone, cuts the southeastern margin of the pluton (Miller et al., 1989).

Diorite is widespread in the poorly exposed western end of the pluton, where contact relationships indicate that it is older than the central granitic part of the pluton. Diorite also occurs along the southern margin of the pluton, where it commonly grades northward into granodiorite. The main body of the pluton is a coarse-grained granite, locally with rapakivi texture, elongate sub-parallel to the length of the pluton. The northern and northeastern margins of the pluton comprise finer grained granite, locally with diorite and granodiorite bodies that show lobate contacts with the granite (cf. Wiebe, 1993) suggesting almost synchronous emplacement of mafic and felsic magma. Small (ca. 10m wide) gabbro bodies occur locally along the northern margin of the pluton and appear to predate the granite. At the northeastern end of the pluton, several sub-circular porphyritic rhyolite bodies cut the main granite. Some mafic dykes are deformed along with the host granite. Other mafic dykes, up to 10 m wide, are undeformed and cut all other lithologies. Aplite veins cut all other lithologies and are most common in the northern part of the pluton. They are oriented in two conjugate systems, striking NE and NW (H, Fig. 5). Undeformed mafic dykes mostly strike NE.

The northern contact of the pluton is linear, trending 110° and generally dipping southward. In most places, a fine grained phase of the granite is in igneous contact with argillite and sandstone containing granitic clasts. Locally, granodiorite and felsic porphyry intrude the argillite. In places, the granitic magma appears to have been intruded along an older gabbro - argillite thrust contact that has a 1 m wide mylonitic zone with S-C planes and asymmetric folds indicating a top-to-NE sense of movement.

Granitic dykes extend 20 - 100 m from the contact into country rock: most are either parallel or orthogonal to the contact, but millimetre-wide dykes dip northeastward (A, Fig. 5). The dykes are deformed by isoclinal folds and/or by sinistral shear zones in horizontal exposures, whereas vertical exposures show thrusting to the northwest, indicating a sinistral shear component. Northwest-directed thrusting is also shown by mylonitic shear zones in the marginal phase of the pluton (B, Fig. 5).

The southern margin of the pluton is a sharp, subvertical linear contact with the CFZ, which forms a zone of mylonitic rocks up to 600 m wide (F, Fig. 5) of granitic and mafic protolith, and a poorly observed cataclastic zone. The western contact of the pluton is poorly exposed, but appears bounded by a late N-S high-angle fault.

Shear zones

Two main shear zones through the pluton, that are splays of the CFZ, form 400-500 m wide zones of dark ultra-mylonites showing a complex style of deformation and a variety of tectonic elements. Both shear zones separate predominantly mafic rocks to the south from the main granite phase of the pluton. The eastern shear zone continues eastward as the Rockland Brook fault (Miller et al. 1991). The southeastern margin of the pluton is a complex shear zone between the Londonderry and Rockland Brook faults previously mapped as Neoproterozoic basement gneiss (Nance and Murphy, 1988) that we interpret as a mix of Neoproterozoic and late Paleozoic plutonic rocks deformed in the Cobequid fault zone.

Several domains of relatively homogenous shear deformation can be distinguished within the Pleasant Hills pluton itself. (a) The northernmost 250 m of the pluton shows a sinistral sense of movement on NW thrusts occurring in zones typically 20 m wide. (b) The area south of this contact has both sinistral and dextral shears, with the dextral shears becoming predominant southward. Sinistral shears strike 045° and dip SE, whereas dextral shears strike 175° and dip moderately to steeply to the E (E in Fig. 5). The main coarse-grained phase of the pluton has a weak system of dextral (predominant) and sinistral shear zones. (d) The southern margin of the pluton is deformed by dextral shear. Magmatic contacts have been reoriented parallel to the fault zone and a strong mylonitic foliation is developed (F in Fig. 5). (e) The southeastern margin of the pluton (G in Fig. 5) comprises inhomogeneous diorite with planar mylonitic shear zones progressively deformed by ductile folds, producing a scatter in foliation directions (G, Fig. 5) similar to that described by Waldron et al. (1989) from the Cobequid fault zone at Cape Chignecto. Ductile shear zones show a NW sense of movement and overprinted by brittle shears.

Flat to gently dipping planes cut all the lithologies of the pluton and duplexes, s-c structures and small scale asymmetrical folds all indicate a southward direction of movement (Fig. 6A). In the western

part of the pluton, early diorite has acted as a barrier to southward movement of granite (Fig. 6B). These planes typically occur as thrust faults dipping gently northward in the northern part of the pluton and as south-dipping normal faults in the southern part of the pluton.

Relative age of igneous phases

Available geochronology does not allow definition of the sequence of igneous events. The coarse hornblende granite has yielded a U-Pb zircon age of 361±2 Ma (Doig et al., in press). Ar-Ar dating of several granodioritic phases has yielded similar ages (Nearing, 1995).

Sequence of some igneous phases can be inferred from cross-cutting relationships (Table 1). The marginal rhyolites in the eastern pluton are cut by dykes similar to the fine and medium granites. The major diorites in the western pluton are cut by granite, but the lobate contacts (cf. Wiebe, 1993) suggest almost synchronous emplacement of mafic and felsic magma in places. Rapakivi granite in the Gamble Lake area is cut by dykes of gabbro that contain feldspar xenocrysts and small digested granite enclaves. Larger bodies of hybrid granodiorite are common in this area, some with rapakivi texture. Rhyolite bodies 5-20 m wide with a fine gabbro rim are in angular (? stoped) contact with the rapakivi granite in the Toad Lake area.

Diabase sheets occur throughout much of the pluton. Some are deformed along with the host granite, whereas others, up to 10 m wide, are undeformed and cut all other lithologies. Some late pegmatitic veins in the southern part of the pluton are deformed. Aplite veins cut all other lithologies and are most common in the northern part of the pluton. They are oriented in two conjugate systems, striking NE and NW (Fig. 5), in response to the general stress regime. Undeformed mafic dykes mostly strike NE.

Studies elsewhere in the Cobequid Highlands have shown that the oldest gabbros are relatively unevolved olivine tholeiites (Pe-Piper et al., 1989b). Sequences of cross-cutting structures show that younger mafic rocks are progressively enriched in incompatible elements such as Ti, Zr and Nb (Pe-Piper, 1991). Application of this technique (e.g., Fig. 7b) shows that the least evolved mafic rocks are the diorite of the Economy Lake shear zone (unit G), some of the diorite sheets in the western part of the pluton (unit L), some marginal gabbro at the northern rim of the pluton (unit N: sample 4734) and a few dykes in the southern part of the pluton (samples 4854, 7010). These observations are consistent with the inference from structural data that the western part of the pluton is older than the eastern part.

STRUCTURAL INTERPRETATION

Major deformational phases

In the Pleasant Hills pluton, northward directed thrusting at the northern margin of the pluton is accompanied by igneous intrusion into a sediment sequence that includes clasts of medium to coarse granite similar to that in the central part of the Pleasant Hills pluton. This may indicate that there was progressive northward migration of magma pathways during magma emplacement, so that extensional collapse and erosion had started to take place in the southern part of the pluton before magma emplacement was complete in the north.

The pluton is cut by major flat-lying brittle or ductile-brittle shear zones that show S-vergent motion, principally thrusting in the northern part of the plutons and normal faulting in the south. The southward movement was accompanied by a dextral sense of shear associated with the CFZ.

The role of the Rockland Brook splay

The Rockland Brook splay (Fig. 4) is structurally compatible with dominant dextral slip on the CFZ and may have first developed during mid to late Devonian dextral slip on the Cobequid-Chedabucto fault zone noted by Keppie and Dallmeyer (1987). The intense mylonitic deformation in the Rockland Brook fault in the eastern Pleasant Hills pluton probably result from renewed dextral slip in the later Carboniferous on the CFZ. Mineral lineations in the mylonites of the CFZ and of major splays indicate subhorizontal displacement parallel to the fault zones. In places these mylonites have been folded.

Sedimentary basins at the margin of the pluton

The occurrence of sediments with granite clast conglomerates intruded by granitic veins at the northern edge of the Pleasant Hills pluton (Piper, 1994) suggests that magma emplacement moved progressively northward, eventually invading sediments deposited on the northern margin of the emplaced granites. At the northern margin of the Pleasant Hills pluton, purplish and green siltstones, sandstones and conglomerates outcrop in the Economy River. Large rounded pebbles of granite occur in some conglomerates and pebbly sandstones. Other conglomerates contain principally subangular rhyolite clasts. Granule conglomerates consist principally of rhyolitic detritus and vein quartz. Thin sections show that granite clasts are similar to some lithologies in the Pleasant Hills pluton and do not resemble the South Mountain batholith of southern Nova Scotia.

Hornfels and granitic veins show that this sedimentary unit is in igneous contact with a fine-

grained granitic phase of the Pleasant Hills pluton. Both the granite and the sediment unit show northward-directed thrusting. The presence of granite clasts and the cross-cutting granite veins suggest that this unit is essentially synchronous with the Pleasant Hills pluton and therefore of earliest Carboniferous age. It is thus an age equivalent of the type Horton Group.

Northwards, the contact of this Horton unit with the Silurian Wilson Brook Formation can be readily mapped. The Wilson Brook Formation contains parallel and wavy laminated fine sandstones that weather distinctively and fresh surfaces of siltstones show bioturbation. In contrast, the sandstones and siltstones in the Horton unit are massive. In the West Branch Economy River, the Horton unit appears to be thrust over the Wilson Brook Formation.

In the Portapique River, laminated sandstones and bioturbated siltstones of the Wilson Brook Formation can be mapped for about 60 m stratigraphically below the lowest (late Llandovery) fossil occurrence. Below there lies approximately 100 m of massive grey siltstones and sandstones. Southwards, these rocks pass into mylonites of the Rockland Brook fault zone, but a similar lithology is intruded by the Pleasant Hills pluton in the vicinity of Bass River. Although this lithology might be a fine-grained unbioturbated facies of the Wilson Brook Formation, it more closely resembles parts of the Horton unit.

Regional correlation of tectonic events

Radiometric dating and stratigraphically-constrained structural studies show that there was dextral strike-slip motion on the Cobequid-Chedabucto fault zone throughout the late Devonian and Carboniferous. Data is insufficient to determine if the rate or direction of relative motion of the Meguma and Avalon terranes changed significantly during this time. Our data on the plutons show that dextral slip on the CFZ continued during pluton emplacement. Radiometric dating suggests that pluton emplacement took place over a short time interval. The evidence of pegmatites and aplites cross-cutting deformed plutonic rocks in small plutons indicates that much deformation also took place over a short time period.

Was this magma emplacement and deformation event primarily a consequence of tectonic processes on the Cobequid - Chedabucto fault zone, or was it a consequence of a magma supply event? The lack of evidence for a major regional structural change synchronous with magma emplacement and the fact that most of the prominent structures in the plutons are ascribed to magmatic processes suggests that magma supply may have been the triggering process. The A-type magma was formed by melting of lower crust by voluminous mafic magma (Pe-Piper et al. 1991) that is also represented by the major underplated layer beneath the Magdalen basin. The major extensional detachment fault in the Magdalen basin, the Margaree detachment, cross-cuts late Devonian volcanic rocks but does not deform early

Carboniferous sediments in Cape Breton Island (Lynch et al., 1993) and thus immediately precedes magma emplacement. The rapid extension associated with this detachment may have been the trigger for voluminous extensional melting. The widespread unconformity between the Horton and Windsor Groups (Fig. 2), marking a change in structural style in the adjacent basins, follows pluton emplacement by some 8-10 Ma.

PETROGRAPHY

Granitoid rocks

The granitoid rocks of the Pleasant Hills pluton show a variety of colours, textures and grain size distributions. The granites have been classified into: very coarse grained red-orange (vcgrog), coarse grained pink-orange, medium grained pink, fine grained pink (fgpg), fine grained gray-pink (fggpg) and rapakivi (rg) granites (Appendix 1). There are also granodiorites, microgranites, porphyries and various kind of rhyolites and various kinds of mafic rocks (gabbros, diorite, diabases). The majority of the granitoid rocks modally classify as alkali feldspars and some as granites, whereas the intermediate in composition rocks as tonalites and granodiorites (Table 2, Fig. 7). The rocks that classify as granites they may actually be alkali feldspar granites, because most of their counted individual plagioclase crystals may be albite.

The tonalites and granodiorites cannot be distinguished among themselves in hand specimen. Both are lithologies equigranular and medium grained. However, they can be divided into two groups based on the abundance of the most important ferromagnesian minerals hornblende and biotite. These rocks are relatively undeformed, but they do show brittle deformation by the presence of fractures and a few veinlets. They show ductile deformation by the presence of undulose extinction in quartz, plagioclase, microcline and perthite. The biotite tonalites/granodiorites contain subgrains of quartz and plagioclase, and bent albite twinning. The tonalites/granodiorites differ from granites in that they contain more mafic minerals and less K-feldspar. The main minerals are: plagioclase, quartz, perthite, microcline, hornblende and biotite. The accessory minerals include zircon, rutile, opaque minerals, titanite, and allanite. The feldspars alter to epidote, the hornblende to titanite, chlorite and actinolite and the biotite to dusty opaque minerals.

The granites are equigranular; graphic, micrographic and myrmekitic textures are common. The rapakivi textures are only present in the rapakivi granites and rhyolites; antirapakivi textures are also

present. All these granites are either hornblende or biotite granites depending on the dominant ferromagnesian mineral. The presence of fractures and veinlets suggests brittle deformation and ductile deformation is indicated by the presence of undulose extinction in quartz, plagioclase and perthite and quartz subgrains. The main minerals present are: perthite, plagioclase, microcline, quartz, hornblende and biotite. The accessory minerals include opaque minerals, zircon, titanite, rutile, apatite, epidote, hematite, allanite, tourmaline, fluorite and arfvedsonite. The alteration products of these minerals consist of rutile, dusty opaque minerals, muscovite, titanite, actinolite, secondary biotite, chlorite, epidote and sericite.

The felsic volcanic rocks of the Pleasant Hills pluton are fine grained subvolcanic rocks. They show a variety of texture and can be classified as porphyry rhyolite, porphyritic rhyolite, spherulitic rhyolite, perlitic rhyolite, and tuff. Some of them are biotite-rich, whereas others are highly epidotized. The porphyritic rhyolites are the most common type. The porphyry rhyolites contain megacrysts (1-1.5 cm long) of K-feldspar that have an euhedral blocky shape. These volcanic rocks show brittle deformation by the presence of fractures and veinlets. The phenocrysts and microphenocrysts of these rocks consist of quartz, plagioclase and k-feldspar. The groundmass is mostly quartz with some opaque minerals and glass. The accessory minerals include biotite, apatite, zircon, tourmaline, epidote, rutile, opaque minerals, hematite, allanite and hornblende. The alteration products of these minerals consist of epidote, sericite and chlorite.

Hybrid rocks produced by mixing of mafic and felsic magma are common in the Pleasant Hills pluton. Evidence to support this mixing are chilled mafic dykelets and chilled gabbro and diorite clots occurring in the granite. Also, gabbros may contain anhedral to subhedral plagioclase, microcline and quartz megacrysts up to 0.5 cm long. The hybrids contain both rapakivi grains and antirapakivi megacrysts, that are enclosed in diorite or at mafic-felsic boundaries. Quartz crystals with corona reaction rims of hornblende, actinolite and opaque minerals are also present in the hybrids. The common accessory minerals of these rocks include apatite, allanite, zircon and piedmontite (Mn-rich epidote).

Mafic Rocks

Gabbros: The gabbros range in grain size from medium grained to coarse grained. They are inequigranular and can be divided into two groups based on the most common ferromagnesian mineral: clinopyroxene gabbro and hornblende gabbro. Those gabbros that are deformed show brittle deformation by the presence of fractures and veinlets, and ductile deformation by the presence of undulose extinction in quartz and plagioclase.

The main minerals present include hornblende, clinopyroxene, actinolite, plagioclase and quartz. The clinopyroxene is Ti-rich augite. Actinolite is common in both groups, since it is an alteration product of hornblende and clinopyroxene. A noticeable feature is the tabular shape of the plagioclase. The accessory minerals may include apatite, opaque minerals, biotite, and occasionally hematite. Euhedral, bladed apatite is abundant in some gabbros. The secondary minerals may include epidote, dusty opaque minerals, and chlorite. The plagioclase breaks down to produce epidote, whereas chlorite is an alteration product of hornblende.

Diabase: The diabases, based on their grain size, can be divided into fine grained diabase and coarse grained diabase. Some of the fine grained diabase are epidotized. Most of the diabases are relatively undeformed. They show brittle deformation by the presence of fractures and veinlets. Some of the samples are tectonized with aligned lenticular amygdules.

The main minerals include clinopyroxene, hornblende and quartz. The accessory minerals may include calcite, rutile and hematite. The secondary minerals may include chlorite, dusty opaque minerals, actinolite, titanite, epidote and sericite. Chlorite is an alteration product of amphiboles. Plagioclase and clinopyroxene break down to produce epidote.

The most noticeable features of the diabases are tabular plagioclase, abundant dusty opaque minerals and the presence of amygdules. Minerals filling the amygdules may include combinations of chlorite, actinolite, epidote, plagioclase, quartz, calcite and dusty opaque minerals. The epidotized diabases are almost completely altered to epidote. They are equigranular and contain primary titanite which is not found in other diabases. The chilled margin of the diabase contains dusty opaque minerals and anhedral actinolite. They also contain pyrite mineralization and occasionally plagioclase megacrysts.

Hornblende gabbros: The hornblende gabbros (referred to elsewhere as diorites) range in grain size from fine grained to pegmatitic. There is little mineralogical difference in diorites of different grain size. The main minerals include hornblende, actinolite, clinopyroxene, plagioclase and quartz. Actinolite is common in the diorites, because it is an alteration product of hornblende and clinopyroxene. The accessory minerals may include apatite, rutile, biotite, epidote, zircon, arfvedsonite, titanite, calcite, hematite and allanite. Arfvedsonite is associated with hornblende. Titanite and calcite show polysynthetic twinning. Twinned allanite is enclosed in feldspar. The secondary minerals may include epidote, opaque minerals, biotite, titanite, sericite, muscovite, calcite and chlorite. Secondary biotite is an alteration product of hornblende. Sericite is an alteration product of plagioclase.

Rapakivi Granites

The rapakivi granites of the Pleasant Hills pluton are high level or epizonal granites, in fact extrusive equivalents, rapakivi rhyolites, are also present. The rhyolites contain sanidine ovoids with an extensive cellular-textured plagioclase mantle on them, and they look similar to those described by Stimac and Wark (1992) from the silicic lavas of Clear Lake, California. The rapakivi granites in many ways are similar to other rapakivi granites in the literature. Their petrographic characteristics can be summarized as follows: 1) they contain ovoid shapes of perthite megacrysts; 2) they contain more than one generation of plagioclase (phenocrysts, mantles, microphenocrysts, inclusions), K-feldspar (megacrysts, phenocrysts, microphenocrysts, inclusions) and quartz (phenocrysts, microphenocrysts, inclusions); 3) mixtures of mantled and unmantled ovoids may occur in the same sample; 4) both perthite ovoids and plagioclase mantles frequently contain abundant small inclusions of droplet-shaped quartz, hornblende, biotite, oxides; the perthite ovoids may also contain plagioclase inclusions and the plagioclase mantles may contain alkali feldspar inclusions; 5) the unmantled ovoids are resorbed and are in contact with individual K-feldspar crystals; 6) plagioclase crystals are always very altered both in mantles and as individual crystals; 7) both ovoids and mantles are often cut by veinlets and fractures filled with a variety or a combination of the minerals biotite, chlorite, epidote, opaque minerals and quartz; 8) the perthite ovoids may also be broken.

The described petrographic features of the Pleasant Hills pluton rapakivi granites indicate an extended period of alkali feldspar crystallization. In this way, plagioclase could begin to nucleate on perthite when the liquid reached the plagioclase-alkali feldspar cotectic. The existence of mixtures of mantled and unmantled ovoids, and of broken ovoids, is consistent with long distance transport of crystal plus liquid through changing conditions of temperature, pressure, and fluid concentration, possibly augmented by convective circulation. Moreover, the common occurrence of rounded, drop-like, quartz may represent repeated resorption during magma decompression. Shrinkage of the quartz liquidus volume was probably steplike such that quartz alternately crystallized as pressure stabilized, then was partly resorbed for an interval when total pressure decreased or fluid pressure increased again. Veinlets of fluorite and interstitial occurrence of fluorite and tourmaline in some of the fine grained granite phases of this pluton (e.g. the West Economy River section), the relative later age of pegmatite and aplites and the occurrence of miarolitic cavities in some other plutons of similar age and chemistry (e.g. the Cape Chignecto Pluton; Pe-Piper, 1994) are all evidence of late fluid saturation in this pluton.

The granitic magmas that most commonly give rise to rapakivi texture are metaluminous to slightly peraluminous, water undersaturated and emplaced at relatively high temperature (Haapala and

Ramo, 1990; Emslie, 1991). Numerous hypotheses have been forwarded to explain rapakivi granites and they are summarized by Stimac and Wark (1992) as follows: 1) liquid immiscibility; 2) exsolution; 3) metasomatic replacement; 4) changes in pressure or water content caused by magma ascent, fractionation or degassing; 5) magma mixing or assimilation of mafic rocks; 6) accretion of hydrosilicates and thixotropic liquefaction and 7) more complicated scenarios involving general processes. The rapakivi texture has been observed in the granites and in some rhyolites in the Pleasant Hills pluton. Thus, we can assume that this texture for this pluton has a high temperature magmatic origin and we must focus on shifts in magmatic conditions. Such shifts should result in resorption of K-feldspar, whereas plagioclase must be stable after the shift and will mantle the K-feldspar. This could be accomplished by shifts in temperature, pressure, water pressure or magma composition. The rapakivi granites do not show any evidence of hybridization, unlike other rocks in the Pleasant Hills pluton, on the basis of major and trace element chemistry and petrography (e.g. plagioclase zoning). This argues against magma mixing (Hibbard, 1981) as an acceptable explanation for the rapakivi texture in these rocks. Thus, the main petrographic and geochemical features of the Pleasant Hills pluton rapakivi granite that will enable us to explain their origin are as follows: 1)rapakivi granites occur together with non rapakivi granites; 2) rapakivi texture has been found in rhyolites; 3) there is aeromagnetic evidence for underplating of mafic magma (Piper et al., 1993); 4) magacrystic mafic rocks with homogeneous feldspar phenocysts (?equivalent to anorthositic magmas) are common in this and similar other plutons in the area; 5) the hybrid phases of this pluton contain feldspar with complex zoning (sodic cores with calcic rims; plagioclase with perthite rims; 6) the rapakivi granites do not contain reversely zoned plagioclase; 7) the rapakivi granites differ chemically from granodiorites with petrographic evidence of mixing.

We envisage the following process for the formation of the Pleasant Hills pluton rapakivi granites. The rapakivi texture in these rocks must, at least in part, be related to unusually slow rates of cooling during crystallization (e.g. Nekvasil, 1991). Classic rapakivi granite suites are closely associated with and, at least partly, underlain by anorthositic rocks (e.g. Emslie and Stirling, 1993). Residual heat from crystallization and cooling of the anorthositic plutons thus may have played a vital role in sustaining the necessary low rate of heat loss from the granitic magma over a protracted period. Aeromagnetic and field evidence indicate that the Pleasant Hills pluton may be underlain by substantial amount of mafic magma (e.g. Piper et al., 1993) which may have played the same role for the formation of rapakivi texture as an anorthositic magma. For rapakivi granites to form during decompression the change in temperature must be close to adiabatic gradient, this explains why rapakivi granites are found with non-rapakivi granites and other non felsic rocks. If the formation of rapakivi texture requires gradients close to adiabatic then

the country rock through which the magma ascends must have been prewarmed to prevent considerable heat loss during ascent. The large amounts of mafic magma in the Pleasant Hills pluton area may have fulfilled that role (close to Folly Lake diorite). Also, as we go west in the Cobequid Highland the rapakivi granites become extremely rare. This together with the aeromagnetic evidence of smaller mafic underplating in west Cobequid Highlands (Piper et al., 1993) support the idea of hot country rock to create rapakivi texture. The fact that the rapakivi granites occur only locally may be due to a variable rate of decompression during the upward transport in the crust and to a variable rate of heat loss during transport or subsequent crystallization.

GEOCHEMISTRY

A total of 100 samples from the Pleasant Hills pluton have been analyzed for 10 major and minor and 14 trace elements (Table 3). Representative samples (17) also were analyzed for REE by INAA. The analytical methods used are exactly as those described in Pe-Piper and Piper (1989). The norms used in diagrams and various geochemical statements are CIPW (wt%) norms and were calculated assuming all iron as FeO for the granitoid rocks and Fe^{3+}/Fe_{tot}=0.15 for the mafic rocks.

The majority of analyzed granitoid rocks classify as alkali feldspar granites using the chemical nomenclature of Streckeisen and LeMaitre (1979) (Fig. 9); the rest plot in the following fields: syenogranite, monzogranite, quartz syenite, quartz monzonite, granodiorite and tonalite. Plots of elements normalized to abundance in ocean-ridge-granite (ORG) after Pearce and others (1984) have an overall decrease in normalized abundances from Rb to Yb ((strong fractionation for these elements), strong negative Ba anomaly (K-feldspar and biotite fractionation), Rb and Th significantly enriched relative to Nb and Ta (crust dominate pattern), also Ce and Sm enriched relative to their adjacent elements. The overall patterns are close to those of WPG of Pearce et al (1984) in that the values of Hf to Yb are close to the normalizing values and that their trends from Ta to Yb are flatter compared with those of ARC granites.

When compared with well known peraluminous granites (such as the South Mountain Batholith: McKenzie and Clarke, 1975) or island arc granites (such as reviewed by Pearce et al., 1984) they have relatively low amounts of Al_2O_3 and CaO and high total alkalies. The high molar ratio of (Na_2O+K_2O) to Al_2O_3 of these rocks also indicates their alkaline character (Hermes et al., 1978). Many of the rocks contain very small amount of corundum (0-1.6%) in the CIPW norms, distinguishing them from

peraluminous granites. The younger volcanic and subvolcanic rocks have elevated normative corundum values (up to 3%) which is attributed to fractionation and especially to the hornblende fractionation. When compared with alkali granites (such as the Paleozoic alkali granites from the Avalon zone of New England described by Hermes et al. (1978) the Pleasant Hills pluton granitoids plot both in the alkalic and subalkalic fields. Peraluminous granitic rocks owe their high A/CNK values to a combination of source, magmatic and fluid effects. Silicate melt-silicate crystal equilibria generally constrain A/CNK to values of 1.1 to 1.2. Table 3 shows that all the granitoid rocks of the Pleasant Hills pluton have A/CNK less than 1.2, which indicate the slight peraluminous character of some of these granitoids is due to magmatic processes and not source related.

The Pleasant Hills pluton is a bimodal suite and it includes rapakivi granites. In terms of commonly used discriminant diagrams, such as those of Whalen et al. (1987), these granitoids are A types (Fig. 10). Eby (1990, 1992) distinguished two groups of A-type granitoids: group 1 with chemical similarities to oceanic-island basalt and group 2 with similarities to average crust and island-arc basalt. The author concluded that group 1 granitoids were derived from the mantle, whereas group 2 granitoids were the result of melting of lower crust that had been through a cycle of subduction or continent-continent collision. The group 2 also contains granitoids emplaced in a variety of tectonic setting, including post-collisional and what may be true anorogenic. In all element-element plots used by Eby (1992) to discriminate these two groups of A-type granitoids, the Pleasant Hills pluton granitoids plot in the field of group 2 (e.g. Fig. 11). The long-lived Precambrian subduction in this area and the current interpretation of the early Carboniferous magmatism of the Cobequid Highlands as related to the extension of the Magdalen Basin (Pe-Piper et al., 1991 and Piper et al., 1993) both support the characterization of the Pleasant Hills pluton granitoids as group 2, A- type granites.

On the Harker diagrams (Figs. 12A, B, C) as SiO_2 increases there is a decrease of Al_2O_3, TiO_2, FeO_t, CaO, MnO, P_2O_5, MgO, Sr, V; slight decrease in Na_2O; slight increase in Rb and clear increase in K_2O; There is also a general overall linear relationship, with Zr decreasing as SiO_2 increases. This observation is in agreement with successive, more fractionated melts remaining zircon-saturated at continuously decreasing temperatures and Zr concentrations. However, in detail each of the various rock units has its own trend. These trends are: one similar to the general one (main rapakivi, West Economy), almost constant Zr concentrations (main-south, Chain Lake, clasts) or scatter (main-north). There exists no obvious relationship between geochemical trends and the age of the individual rock units. This probably indicates that these rock units evolved under different T control.

The probable fractionation trends in the Pleasant Hills plutons granitoids are inferred from plots of

trace elements such as those used by Tindle and Pearce (1981) and Thompson and Fowler (1986). Using such plots like Ba vs Rb, Ba vs Sr, Zr vs Nb and Ce vs Yb the fractionating phases seem to be K-feldspar, biotite, zircon and plagioclase, although the dominant fractionating phases may be slightly different among the various granitoid groups. On the Y vs Zr plot (Fig. 13A) the individual granitoid groups, despite a scatter, seem to follow two main trends: increase of Y with Zr and b) constant Zr while Y increases. The first trend is well established in the less siliceous granite groups, whereas the second in the more siliceous granite group. Zircon contains both Zr and Y, whereas titanite contains only Y. The observed trends indicate that zircon saturation was attained resulting in zircon fractionation and titanite probably continued to contribute the high amounts of Y. A plot of Zr vs CaO (Fig. 13B) does not produce a single straight line and this is taken to indicate that there was not a closed-system crystal-liquid differentiation in the rock units of the Pleasant Hills pluton.

REE patterns (Fig. 14) show highest REE enrichments (up to 330 x chondrite for La) in the fine-grained granite of West Economy River and Chain Lake Brook, the medium (mgpog) and coarse granites of the main granite phase in the northern half of the pluton and the main rapakivi phases. The REE patterns show decreasing abundance in the very coarse granite (vcgrog) of the main coarse granite at the southern edge of the pluton, the felsic subvolcanic rocks north of the Gamble Lake (which may be one of the oldest igneous phases) and the porphyry that cuts the rapakivi phase. The latter sample has the most depleted REE pattern and its pattern may be attributed to fractionation of accessory minerals. Overall there is no apparent relationship between REE-enrichment and relative age of rock units, e.g. the main coarse granite at the southern edge of the pluton is older that the fine-grained granite of the West Economy River and Chain Lake Brook and is younger than the main rapakivi phase and the main granite phase in the northern half of the pluton. Both the younger (West Economy River-Chain Lake Brook) and the older (Rapakivi-northern edge granites) are more enriched in REE and have stronger negative Eu anomalies. These observations may indicate that there might have been an early separation of magma pockets from the original magma that have followed their own detailed path of fractionation and thus an absolute relationship between fractionation and relative age cannot be seen. The observed REE patterns changes will also indicate that all these magma pockets had reached the saturation point of fractionation of accessory minerals such as titanite, zircon and especially allanite. Allanite is a common accessory mineral in all lithologies (granites, rhyolites and hybrids) and it does contain high concentrations of total REE (up to 25 wt%) and especially light REE (Table 10). The allanites in the Pleasant Hills pluton granitoid rocks show variable composition within individual grains due to metamictization. Some of the earlier plutonic phases (e.g. main granite phase in the northern half of the pluton - sample 42-1-2) also

seem to have high negative Eu anomalies. Strong Eu anomalies in granites are attributed either to plagioclase fractionation or partial melting of lower crust with retention of plagioclase as a residual phase. The occurrence of rapakivi granites and the presence of plagioclase megacrysts and positive Eu anomalies in some mafic rocks from the nearby Folly Lake diorite (Fig. 15) would support the latter (Emslie and Stirling, 1993). REE patterns also suggest that extreme fractionation of these granitoid magmas did not occur (with the exception of the porphyry C4865), probably as a result of higher viscosities in water-undersaturated magmas. Indicated ranges of late-stage temperatures (Table 6) between about 650 ±75 °C are also in accord with crystallization from water-undersaturated magma.

Apatite is a common accessory mineral. A comparison of the plot of P_2O_5 vs SiO_2 (Fig. 12A) with the isotherms for dissolved P_2O_5 contents of apatite-saturated melts after Watson and Harrison (1984) shows that the majority of the analyzed samples plot below the 800 °C isotherm (pressure and dissolved water content are believed to have minor effects only).

Figures 16 and 17 show the regional distribution of the normative anorthite for all analyzed granitoid rocks from the Pleasant Hills pluton. These data may taken to indicate geochemical differentiation of the crystallizing granitic magma to the north and west. This asymmetry may not be well established because the heat was distributed inhomogeneously in the area and therefore the differentiation process of the magma pockets was different in different individual areas.

Summary: In most geochemical plots the various rock units form slightly different clusters. Thus, the fundamental question is: are these clusters due to slight changes in source material i.e. are we dealing with more than one primary magmas or are these clusters due to differentiation of various magma pockets created e.g. by the syn-magmatic tectonism under very different T and fluid conditions? To give an answer to this question we tried to use binary diagrams plotting elements with same incompatibility in order to remove the effect of fractionation. In such diagrams (e.g. Y vs Zr, Ga vs Al_2O_3, Hf/Zr vs Y/Nb) the changes and variability we see can be easily explained by differentiation under different T conditions rather than different source material. In addition, the Sm/Nd data available at present also agree with such an assumption.

Studies elsewhere in the Cobequid Highlands have shown that the oldest gabbros are relatively unevolved olivine tholeiites (Pe-Piper et al., 1989b). Sequences of cross-cutting structures show that younger mafic rocks are progressively enriched in incompatible elements such as Ti, Zr and Nb (Pe-Piper, 1991). Application of this technique (e.g., Fig. 18) shows that the least evolved mafic rocks are the diorite of the Economy Lake shear zone (unit G), some of the diorite sheets in the western part of the

pluton (unit L), some marginal gabbro at the northern rim of the pluton (unit N: sample 4734) and a few dykes in the southern part of the pluton (samples 4854, 7010). These observations are consistent with the inference from structural data that the western part of the pluton is older than the eastern part.

Megacrystic rocks

We call megacrystic rocks those rocks with anomalously large crystals (>1 cm) found in a finer grained rock. The megacrysts in the Pleasant Hills pluton are found in gabbros, diorites and hybrid rocks. The megacrysts are composed of plagioclase and K-feldspar. There are three types of megacrysts in the mafic phases of this pluton:

1) Megacrysts of calcic plagioclase with nearly uniform composition (An_{54}-An_{59}). These crystals must be due to an isothermal crystallization at a nearly constant melt composition in the early stages of a crystallizing mafic magma.

2) Megacrysts with sodic cores (An_3) and calcic rims (An_{15}). These megacrysts formed in a felsic magma with a later addition of a mafic magma.

3) Megacrysts with plagioclase cores and perthite rims.

Additional evidence includes the euhedral shape of the crystals which indicates that they were precipitated from a primary magma. The megacrysts are often found in hybrid samples at the mafic-felsic boundary indicating the mixing of mafic and felsic magmas. Megacrystic mafic rocks have a positive Eu anomaly (samples 4649 and 4778, Fig. 15).

Using all of the above information it is believed that in the studied rocks the megacrysts followed a complex series of events. Mafic magma contaminated by hot residue of plagioclase-pyroxene granulite left by the extraction of large volumes of granitic partial melt from the crust started crystallizing at a constant temperature and melt composition. Some of the mafic melt ascended to the surface in pulses to form gabbros and diorites. At the same time as the crystallization of the mafic magma, a cooler felsic magma was precipitating sodic plagioclase. The hot mafic and cool felsic magma mixed, thus quenching the mafic. The quenching produced a fine grained mafic rock with large calcic megacrysts that crystallized in the mafic magma. The quenching of the mafic magma also caused calcic plagioclase to nucleate on the sodic plagioclase crystals pre-existing in the felsic magma, thus producing calcic plagioclase rims. The disequilibrium caused by the mixing of the mafic and felsic magmas led K-feldspar to nucleate on the pre-existing sodic and calcic plagioclase crystals resulting in megacrysts with sodic or calcic plagioclase cores and K-feldspar rims.

Temperature of formation of the pluton

Metaluminous melts have low Zr solubilities and precipitate zircon early except at high temperatures. Zircon, as an accessory mineral, is found in all granitic phases of the Pleasant Hills pluton. It is usually found as an interstitial mineral, in veinlets that cut perthite crystals, in mafic stringers/clots and it is associated mainly with greenish biotite, opaque minerals and in some samples with amphiboles. As an inclusion it is only found in biotite, opaque minerals and hornblende. The Pleasant Hills pluton granitoids are dominantly metaluminous and their typically high concentrations of Zr contents are consistent with unusually high temperature melts as implied by other data (e.g. rarity of pegmatites, lack of hydrothermal aureole).

Comparison of modal compositions of granites with compositions of minima in the system Ab-Or-Qz-H_2O (Fig. 19) suggests crystallisation under pressure conditions ranging from 10 to 2 kbar and water activity a_{H_2O} of about 0.4 (based on the experimental work of Johannes and Holtz 1990). Rocks suggesting lowest pressure include types C from the NW margin of the pluton and medium granite from the eastern part of the pluton; those indicating highest pressures include the old porphyry from the northeastern margin of the pluton, some rapakivi granite, and types A and B from the NW margin of the pluton. Hornblende granite indicates intermediate pressures.

Fluids in the granitic magma

The presence of fluorite in some of the granitic phases indicate that fluorine must have been an important volatile present in these magmas. However, the mode of occurrence of fluorite (interstitial and veinlets), the rarity of pegmatites and the occurrence of miarolitic cavities in some other plutons of same age and composition elsewhere in the Cobequid Highlands indicate that the granitic magma started as fluid-poor magma and became enriched later, probably through fractionation and/or other processes such as thermogravitational diffusion, diffusion or evolution of a discrete fluorine-rich phase.

If P_f is relatively high, zirconium will be bound into F-containing complexes thus inhibiting the crystallization of zircon (Collins et al., 1982). Crystallization of amphibole would remove fluorine from the melt, releasing Zr to be bound into zircon. The fact that zircon is found in all granites and as inclusions in amphibole indicates that zircon crystallized earlier and amphibole (with about 1% F) later. These observations offer support to the idea that P_f was not high except towards the end stages of the crystallization.

CHEMICAL MINERALOGY

Feldspars

Plagioclase is found in all of the lithologies within the Pleasant Hills pluton, and K-feldspar is only found in the granites, granodiorites and related hybrid lithologies. Detailed plagioclase and K-feldspar compositions and zoning patterns are given in Table 4, whereas the overall compositional range is given in Fig. 20.

Biotite

Biotite is found in all lithologies except the basalts and the diabases. Representative electron microprobe chemical analyses are given in Table 5. The analyzed biotites show a wide range in iron (12 to 22 wt% FeO_t) and both normal and reverse zoning have been observed. The biotite analyses plot in the phlogopite-annite join in an ^{iv}Al vs. $Fe_t/(Fe_t+Mg)$ plot (Fig. 21). In the same diagram they also fall in the field outlined by Clarke (1981) for rocks containing biotite only.

Amphiboles

Amphiboles are present in all lithologies in the Pleasant Hills pluton. Representative microprobe analyses of the amphiboles are given in Table 6. Most of the analyzed amphiboles plot in the fields of edenite, hornblende and actinolitic hornblende of Leake (1978). A few of the diorite samples contain pargasite, pargasitic hornblende and silicic edenite and some of the granite samples contain actinolite. The overall trend seen is that of Si increases as (Na+K) decreases. Using again the terminology of Leake (1978) the amphiboles from the granites are "ferro" amphiboles, whereas the amphiboles from the granodiorites and the diorites are "magnesio" amphiboles. The amphiboles from the granites and few from the diorites are also "alumino" amphiboles (after Leake, 1978). The amphiboles from all lithologies may show both normal and reverse zoning.

Sodic amphiboles in this pluton have been seen only as an accessory mineral overgrowing hornblende or in clots in a variety of mineral combinations such as sphene, zircon, epidote, chlorite actinolite, secondary biotite and always hornblende and opaque minerals and only in the rapakivi granites. Sodic amphiboles are widespread in the nearby Hart Lake-Byers Lake Pluton where it has been identified as arfvedsonite inasmuch as (K+Na) in the A site exceeds 0.5, whereas if it were riebeckite you would anticipate $(K+Na)A < 0.5$. Textural evidence in this pluton also indicates that the sodic amphibole is later than the calcic amphiboles (it overgrows them). Arfvedsonite normally incorporates

ferrous iron and thus the mode of the occurrence of this mineral in this pluton may indicate a decrease in fO_2 in the late-stage of crystallization of the rapakivi granites.

Amphibole analyses can be used for geobarometry and geothermometry. Using a graph of ^{iv}Al vs. Al_{tot} from Hammarstrom and Zen (1986) the analyses of the amphiboles from the Pleasant Hills pluton lithologies cluster along the reference line (Selway, 1991). Pressure estimates based on the method of Schmidt (1992) are reported in Table 6: most range from 1.5 to 3 kbars. Corresponding temperatures based on the method of Blundy and Holland (1990) are estimated as 650 ±75 °C.

Clinopyroxene

Fresh clinopyroxene crystals have been found in gabbros, diorite and hybrid rocks. Representative electron microprobe analyses are given in Table 7. Most of the analyzed clinopyroxenes classify as salites and few as diopsides in the nomenclature of Deer et al (1966). The analyzed clinopyroxene crystals show normal zoning with FeO_t ranging from 7.50 to 9.76, and MgO ranging from 13.77 to 14.79.

Zircon

Zircons were analyzed for one rapakivi granite (C4863A) and one coarse-grained granite (C 4681) and representative analyses are given in Table 8. Zircon commonly is found as inclusions in hornblende and opaque minerals, as interstitial grains often poikilitically enclosed by opaque minerals and in one sample by allanite, in clots together with opaque minerals and/or biotite. All these observations indicate that in these granites zircon was precipitating until the later stages of crystallization which also implies that the temperature in the granite magma was kept high. Zircon also shows complex zoning (Fig. 22) and some of the zoned crystals show reaction rims (Fig. 22A). These observations may indicate that there was also inherited zircon and that may explain the high Zr content of these granites.

Titanite

Titanite is a common accessory mineral in most of the lithologies of the Pleasant Hills pluton. However, titanite crystals studied in detail come only from the rapakivi granites (Table 9). These crystals under reflected light look very patchy, with dark and light colour domains. Several such patches have been analyzed and in general the main chemical difference between light and dark domains seems to be Y (Table 9); the light colour domains contained more Y.

Allanite

Allanite has been found as an accessory mineral in the granites, granodiorites and other hybrid lithologies, the felsic volcanic rocks, and the pegmatitic hornblende diorites. Several electron microprobe analyses were done and two representative analyses are given in Table 10. The FeO_t, MgO and REE content in allanite varies greatly within individual grains. In the granites, the FeO_t content of the allanite ranges from 14.93 to 19.46, and in the hybrid rocks from 15.78 to 19.57. The MgO content in the granites range from 0.07 to 0.61 and in the hybrid rocks from 0.88 to 1.21 wt%. The total REE content in the granites for allanite ranges from 7.91 to 22.91 and in the hybrid rocks from 18.92 to 25.07. Thus the allanites are rich in iron and light REE.

The composition of the plutonic allanites in general varies greatly within individual crystals probably because of hydration, metamictization that occurs during the slow cooling of the pluton, and alteration (Chesner and Ettlinger, 1989). Metamictization is the breakdown of the space lattice by radioactive emanations while still retaining the mineral's original external morphology (Kerr, 1977; Gary et al., 1974). The allanites in the Pleasant Hills pluton show variable composition within the individual crystals probably due to metamictization.

Opaque minerals

The most common opaque minerals in the pluton are hematite and magnetite (Table 11). They are often intergrown indicating the magnetite is breaking down to produce hematite. Hematite and magnetite are associated with hornblende. Another iron-titanium oxide opaque mineral found is ilmenite. The ilmenites we tried to analyze were from the very coarse red orange granite. These ilmenites showed a very wide range of MnO concentrations (1-22 wt% of MnO).

The sulfide opaque minerals found are chalcopyrite and pyrite. These sulfides are rather more common in the mafic rocks than in the felsic rocks. Marcasite is found in the diabase chilled margins.

Chlorite

Chlorite is found almost in all lithologies of the pluton. Representative analyses are given in Table 12. Most of the analyzed chlorites are iron rich and classify as ripidolite and some as brunsvigite in the nomenclature of Hey (1954).

Both normal and reverse zoning has been observed in the analyzed chlorite crystals. In the granites, the FeO_t content of the chlorite ranges from 30.46 to 38.46 wt%, and the MgO content ranges from 5.56 to 9.44 wt %.

ACKNOWLEDGEMENTS

We thank all our students who either through summer employment or through their Honours thesis helped us to produce this report. In particular we thank: J. Selway, M. Feetham, K. Parlee, D. Robichaud and G. Davis. I. Koukouvelas assisted with the structural interpretations. The geochemical work was done at the Saint Mary's University Regional geochemical Centre and the Dalhousie University Regional Electron Microprobe Centre.

References

Bailey, E.H., and Stevens, R.E., 1960. Selective staining of K-feldspar and plagioclase on rock slabs and thin sections. American Mineralogist, 45, 1020-1025.

Blundy, J.D., and Holland, T.J.B., 1990. Calcic amphibole equilibria and a new amphibole-plagioclase geothermometer. Contributions to Mineralogy and Petrology,, 104, 208-224.

Chesner, C.A., and Ettlinger, A.D., 1989. Composition of volcanic allanite from the Toba tuffs, Sumatra, Indonesia. American Mineralogist, 74, 750-758.

Clarke, D.B., 1981. The mineralogy of peraluminous granites: a review. Canadian Mineralogist, 19, 3-17.

Collins, W.J., Beams, S.D., White, A.J.R., and Chappell, B.W.,1982. Nature and origin of A-type granites with particular reference to south-eastern Australia. Contributions to Mineralogy and Petrology, 80, 189-200.

Deer, W.A., Howie, R.A., and Zussman, J., 1966, An introduction to the rock forming minerals. Longman; London.

de la Roche, H., Leterrier, J., Grandclaude, P., and Marchal, M., 1980. A classification of volcanic and plutonic rocks using R1-R2 diagram and major element analyses-It relationships with current nomenclature. Chemical Geology, 29, 183-210.

Doig, R., Murphy, J.B., Pe-Piper, G. and Piper, D.J.W., in press. U-Pb geochronology of late Paleozoic plutons, Cobequid Highlands, Nova Scotia, Canada: evidence for late Devonian emplacement adjacent to the Meguma-Avalon terrane boundary in the Canadian Appalachians. Geological Journal.

Donohoe, H.V., and Wallace, P.I. 1982. Geological map of the Cobequid Highlands, Nova Scotia. Scale

1:50 000. Nova Scotia Department of Mines and Energy.

Donohoe, H.V. Jr. and Wallace, P.I. 1985. Repeated orogeny, faulting and stratigraphy of the Cobequid Highlands, Avalon Terrane of northern Nova Scotia. Geological Association of Canada - Mineralogical Association of Canada Joint Annual Meeting, Guidebook 3, Fredericton, N.B., 77p.

Eby, G.N., 1990. The A-type granitoids: A review of their occurrence and chemical characteristics and speculations on their petrogenesis. Lithos, 26, 115-134.

Eby, G.N., 1992. Chemical subdivision of the A-type granitoids: Petrogenetic and tectonic implications. Geology, 20, 641-644.

Eisbacher, G.H. 1969. Displacement and stress field along part of the Cobequid Fault, Nova Scotia. Canadian Journal of Earth Sciences, 6, 1095-1104.

Eisbacher, G.H. 1970. Deformation mechanisms of mylonitic rocks and fractured granites in the Cobequid Mountains, Nova Scotia, Canada. Geological Society of America Bulletin, 81, 2009-2020.

Emslie, R.F., 1991. Granitoids of rapakivi granite-anorthosite and related associations. Precambrian Research, 51, 173-192.

Emslie, R.F.and Stirling, J.A.R., 1993. Rapakivi and related granitoids of the Nain plutonic suite: Geochemistry, mineral assemblages and fluid equilibria. Canadian Mineralogist, 31, 821-847.

Gary, M., McAfee, R.Jr., and Wolf, C.L., (editors), 1974. Glossary of Geology. American Geological Institute, Washington, D.C. 805 pp.

Haapala, I., and Ramo, O.T., 1990. Petrogenesis of the Proterozoic rapakivi granites of Finland. In: Stein, H.J., and Hannah, J.L. (eds.), Ore-bearing granite systems: Petrogenesis and mineralizing processes. Geological Society of America Special Paper 246, p. 275-286.

Hammarstrom, J.M., and Zen, E., 1986. Aluminium in hornblende: an empirical igneous geobarometer. American Mineralogist, 71, 1297-1313.

Hermes, O.D., Ballard, R.D., and Banks, P.O., 1978. Upper Ordovician peralkalic granites from the Gulf of Maine. Geological Society of America Bulletin, 89, 1761-1774.

Hey, M.H., 1954. A new review of the chlorites. Mineralogical Magazine, 30, 277-292.

Hibbard, M.J. 1980. Indigenous source of late-stage dikes and veins in granitic plutons. Economic Geology, 75, 410-423.

Johannes, W. and Holtz, F. 1990. Formation and composition of H_2O-undersaturated granitic melts. In High temperature metamorphism and crustal anatexis. Edited by J.R. Ashworth and M. Brown. Unwin Hyman, London, UK, p. 87-104.

Karlstrom, K.E., Miller, C.F., Kingsbury, J.A. and Wooden, J.L. 1993. Pluton emplacement along an active ductile fault zone, Piute Mountains, southeastern California: interaction between deformational and solidification processes. Geological Society of America Bulletin, 105, 213-230.

Keen, C.E., Kay, W.A., Keppie, J.D., Marillier, F.J.Y., Pe-Piper, G., & Waldron, J.G.F. 1991. Crustal characteristics of the Canadian Appalachians southwest of Nova Scotia, from deep marine reflection profiling. Canadian Journal of Earth Sciences, 28, 1096-1111.

Keppie, J.D. 1989. Northern Appalachian terranes and their accretionary history. Geol. Soc. Am. Sp. Paper 230, 159-192.

Keppie, J.D. & Dallmeyer, R.D. 1987. Dating transcurrent terrane accretion: an example from the Meguma and Avalon composite terranes in the northern Appalachians. Tectonics, 6, 831-847.

Kerr, P.F., 1977. Optical Mineralogy. McGraw-Hill, Inc., New York, 492p.

Koukouvelas, I., Pe-Piper, G. and Piper, D.J.W., In Press: Pluton emplacement by wall-rock thrusting, hanging-wall translation and extensional collapse: latest Devonian plutons of the Cobequid fault zone, Nova Scotia, Canada. Geological Magazine.

Leake, B.E., 1978, Nomenclature of amphiboles. Mineralogical Magazine, v. 42, p. 533-563.

Lynch, G., Tremblay, C. and Rose, H., 1993. Geological map (1:50,000) of Margaree River area, Cape Breton Island, Nova Scotia (11K6 and west 11K7). Geological Survey of Canada Open File 2612.

Marillier, F., and Verhoef, J. 1989. Crustal thickness under the Gulf of St. Lawrence, northern Appalachians, from gravity and deep seismic data. Canadian Journal of Earth Sciences, 26, 1517-1532.

Marillier, F., and Reid, I. 1990. In: The Potential of Deep Seismic Profiling for Hydrocarbon Exploration. Edited by: B. Pinet and C. Bois. Éditions Technip, Paris, pp. 209-218.

Mawer, C.K. & White, J.C. 1987. Sense of displacement on the Cobequid - Chedabucto fault system, Nova Scotia, Canada. Canadian. Journal of Earth Sciences, 24, 217-223.

McKenzie, C.B., and Clarke, D.B., 1975. Petrology of the South Mountain Batholith, Nova Scotia. Canadian Journal of Earth Sciences, 12, 1209-1218.

Miller, B.V., 1991. Kinematic, structural and tectonic analysis of the Rockland Brook fault, Cobequid Highlands, Nova Scotia. Unpublished M.Sc. thesis, Ohio University, 151 p.

Miller, B.V., Nance, R.D. and Murphy, J.B. 1989. Preliminary kinematic analysis of the Rockland Brook Fault, Cobequid Highlands, Nova Scotia. In: Current Research, Part B, Geological Survey of Canada, Paper 89-1B, pp. 7-14.

Muecke, G.K., Elias, P., & Reynolds, P.H. 1988. Hercynian/Alleghanian overprinting of an Acadian

Terrane: $^{40}Ar/^{39}Ar$ studies in the Meguma Zone, Nova Scotia, Canada. Chemical Geology 73, 153-167.

Nance, R.D. and Murphy, J.B. 1988. Preliminary kinematic analysis of the Bass River Complex, Cobequid Highlands, Nova Scotia. In: Current Research Part B, Geological Survey of Canada Paper 88-1B, p. 227-234.

Nearing, J.D., 1995. Thermochronologic evolution of the Cobequid Highlands, Nova Scotia. Abstract. Atlantic Geoscience Society Annual meeting, Antigonish, February 1995, p.22.

Nekvasil, H., 1991. Ascent of felsic magmas and formation of rapakivi. American Mineralogist, 76, 1279-1290.

Pearce, J.A., Harris, N.B.W. and Tindle, A.G., 1984. Trace element discrimination diagrams for tectonic interpretation of granitic rocks. Journal of Petrology, 25, 952-983.

Pe-Piper, G. 1994. The Carboniferous plutons and associated igneous rocks of the western Cobequid Highlands, Nova Scotia. Open File Report.

Pe-Piper, G., 1991. Granite and associated mafic phases, North River pluton, Cobequid Highlands. Atlantic Geology, 27, 15-28.

Pe-Piper, G., Murphy, J.B. and Turner, D.S., 1989a. Petrology, geochemistry and tectonic setting of some Carboniferous plutons of the Eastern Cobequid Hills. Atlantic Geology, 25, 37-49.

Pe-Piper, G., Cormier, R.F., and Piper, D.J.W. 1989b. The age and significance of Carboniferous plutons of the western Cobequid Hills, Nova Scotia. Canadian Journal of Earth Sciences, 26, 1297-1307.

Pe-Piper, G. and Piper, D.J.W. 1989. The upper Hadrynian Jeffers Group, Cobequid Hills, Avalon Zone of Nova Scotia: a back-arc volcanic complex. Geological Society of America Bulletin, 101, 364-376.

Pe-Piper, G., Piper, D.J.W. and Clerk, S.B., 1991. Persistent mafic igneous activity in an A-type granite pluton, Cobequid Highlands, Nova Scotia. Canadian Journal of Earth Sciences, 28, 1058-1072.

Piper, D.J.W. 1994. Late Devonian - earliest Carboniferous basin formation and relationship to plutonism, Cobequid Highlands, Nova Scotia. In: Current Research, Geological Survey of Canada Paper 94-1

Piper, D.J.W., Pe-Piper, G. and Loncarevic, B.D., 1993. Devonian - Carboniferous igneous intrusions and their deformation, Cobequid Highlands, Nova Scotia. Atlantic Geology, 29, 219-232.

Schmidt, M.W., 1992. Amphibole composition in tonalite as a function of pressure: an experimental calibration of the Al-in-hornblende barometer. Contributions to Mineralogy and Petrology, 110,

304-310.

Selway, J., 1991. The petrology, geochemistry and a detailed map of the Pleasant Hills pluton in the Cobequid Highlands, Nova Scotia. B.Sc. hons. thesis, Department of Geology, Saint Mary's University, Halifax, N.S., 179 pp.

Stimac, J.A., and Wark, D.A., 1992. Plagioclase mantles on sanidine in silicic lavas, Clear Lake, California: Implications for the origin of rapakivi texture. Geological Society of America Bulletin, 104, 728-744.

Streckeisen, A., and LeMaitre, R.M., 1979. A chemical approximation to the modal QAPF classification of the igneous rocks. N. Jb. Miner. Abh., 136, 169-206.

Thompson, R.N. and Fowler, M.B., 1986. Subduction-related shoshonitic and ultrapotassic magmatism: a study of Siluro- Ordovician syenites from the Scottish Caledonides. Contributions to Mineralogy and Petrology, 94, 507-522.

Tindle, A., and Pearce, J.A., 1981. Petrogenetic modelling of in situ fractional crystallization in the zoned Loch Doon pluton, Scotland. Contributions to Mineralogy and Petrology, 78, 196-207.

Waldron, J.G.F., Piper, D.J.W., and Pe-Piper, G. 1989. Deformation of the Cape Chignecto Pluton, Cobequid Highlands, Nova Scotia: thrusting at the Meguma-Avalon boundary. Atlantic Geology, 25, 51-62.

Watson, E.B., and Harrison, T.M., 1984. Accessory minerals and the geochemical evolution of crustal magmatic systems: a summary and prospectus of experimental approaches. Phys. Earth Planet. Inter., 35, 19-30.

Whalen, J.B., Currie, K.L., and Chappell, B.W., 1987. A-type granites; Geochemical characteristics, discrimination, and petrogenesis. Contributions to Mineralogy and Petrology, 95, 407-419.

Wiebe, R.A., 1993. Basaltic injections into floored silicic magma chambers. Eos, 74, 1-3.

Williams, H. 1979. Appalachian orogen in Canada. Canadian Journal of Earth Sciences, 16, 792-807.

Table 1. Relationships of major plutonic phases

Rock type	Occurrence	Relative age	Representative samples
Epidote veins	in mafic lithologies in north of pluton		
Aplite veins	Northern rim	Cut all other phases	
Main diabase dykes	particularly northern pluton	Cut all other phases	5031, 6204
Gabbro sheets	Northwestern pluton, along inferred thrust faults. Some associated dykes.	chilled against fine granite	
Rhyolite bodies, rimmed by diabase	In rapakivi granite in Toad Lake area	Cut rapakivi granite	4865 (rhy) 4866 (db)
Granodiorite, minor diorite bodies	eastern pluton in Gamble Lake area	cut rapakivi granite. Some hybrids have rapakivi texture	4688
Medium and fine granite	margin of eastern pluton		7025, 4692
Porphyritic rhyolite, fine granite, rare medium granite	sheets at northern rim of western pluton	Cut by gabbro. Form a series of sheets.	26-13-6 25-5-8
Medium granite	western margin of pluton		4761
Gabbro/diorite and granodiorite	southern margin of pluton	mylonitically deformed, passes northward to less deformed granodiorite. Mostly chemically evolved, some may be older.	4714, 4779 4702 (gd)
Rapakivi granite	Mostly eastern pluton, some transitional to medium granite		4689, 4670
Fine-medium granite locally rapakivi	North-central pluton, widespread, probably several phases		42-1-2, 6936
Primitive dykes	various southern parts of pluton	cut medium and coarse granite (units B and K')	7011, 4854
Coarse hornblende granite	Widespread in southern part of western pluton	Cut by dykes of finer granite phases	4699, 4700

Coarse and medium granite	Central part of eastern pluton	Intermingled with gabbro	6940, 5039
Coarse and medium granite	Southern part of eastern pluton		4681, 4735
Gabbro/diorite	several sheets in western pluton	Net-veined with lobate contacts and some hybridization by fine-medium granite and tonalite. Cut by dyke of rapakivi granite	7392, 4753
Porphyritic rhyolite	Northeast margin	Deformed, cut by undeformed fine-medium granite. Has diorite enclaves [*CHECK*]	4697, 4728
Gabbro	small bodies at north margin of pluton	deformed prior to intrusion of fine granite	4734
Gabbro/diorite	Economy Lake shear zone		

Table 2: Modal compositions of representative granitoid samples from the Pleasant Hills pluton

Sample No	C4670	C4686	C4689	C4694	C4699	C4700	C4705a	C4705b	C4721	C4736
Plagioclase[1]	4.7	0.3	2.7	2.0	7.1	2.8	4.7	12.2	13.5	0.2
Ab[2]	7.9	9.9	9.9	14.2	5.3	8.0	5.3	4.6	5.6	8.7
K-Feldspar	39.3	49.1	46.1	45.9	26.0	31.8	43.7	34.7	28.7	44.8
Quartz	19.7	27.8	24.6	30.2	33.3	31.7	31.5	39.6	34.8	24.3
Amphibole	16.5	0.7	8.7	-	0.5	0.2	-	-	4.7	-
Biotite	0.1	0.2	2.0	-	10 6	-	-	-	0.6	-
Opaques	1.3	0.9	1.1	1.0	1.6	0.9	1.1	1.4	2.0	1.2
Accessories[3]	-	0.9	-	-	-	-	-	-	-	-
Epidote	1.9	1.1	4.3	3.0	14.2	8.8	2.7	0.7	6.4	4.4
Alteration	1.5	0.4	0.6	-	1.4	1.1	6.2	4.1	3.4	-
Holes	7.0	8.7	-	4.2	-	14.7	4.8	2.7	0.3	16.4
Color Index	21.3	4.2	16.7	4.0	26.9	11.0	10.0	6.2	17.1	5.6
IUGS Nomenclature components										
Plagioclase	6.56	0.34	3.24	2.17	9.90	3.77	5.52	13.39	16.34	0.26
K-feldspar	65.92	67.74	67.23	65.11	43.65	53.57	57.51	43.14	41.53	68.59
Quartz	27.51	31.92	29.53	32.72	46.44	42.66	37.00	43.47	42.13	31.15
IUGS Name[4]	AFG	AFG	AFG	AFG	GR	GR	AFG	GR	GR	AFG

Sample No	C4863	C5039	25-5-1	25-5-6	25-5-8	26-13-1	26-13-2
Plagioclase	18.3	29.1	-	-	-	-	-
Ab	9.3	-	20.8	22.6	12.7	27.7	26.0
K-Feldspar	28.2	1.7	52.4	50.7	52.9	41.7	43.4
Quartz	34.6	43.1	25.3	24.6	32.2	25.3	26.5
Amphibole	2.7	6.7	-	-	-	-	-
Biotite	-	-	-	-	-	-	0.5
Opaques	0.3	0.1	1.5	2.1	2.1	4.8	3.2
Accessories	-	-	-	-	-	0.3	-
Epidote	1.4	10.1	-	-	-	0.3	0.3
Alteration	5.2	1.6	-	-	-	-	-
Holes	-	7.6	-	-	-	-	-
Color Index	9.6	16.9	1.5	2.1	2.1	5.3	4.0
IUGS Nomenclature components							
Plagioclase	20.24	39.38	-	-	-	-	-
K-feldspar	41.48	2.30	74.3	74.9	67.1	73.3	72.37
Quartz	38.27	58.3	25.7	25.1	32.9	26.7	27.63
IUGS Name	GR	TON	AFG	AFG	AFG	AFG	AFG

Notes

1:Plagioclase refers to individual plagioclase grains of which composition is unknown.

2. This includes albite in perthite and albite as individual crystals and it is counted as alkali-feldspar in IUGS calculations.

3. Includes zircon, sphene, apatite.

4: AFG=alkali-feldspar granite; GR=granite; TON=tonalite.

Modes are based on counting 1000 to 1500 points in one or two thin sections (depending on grain size of rock) stained using a modification of the method of Bailey and Stevens (1960).

Table 3. Whole- rock chemical analyses of representative samples

Sample No.	C4601	C4602	C4605	C4669	C4670	C4671	C4672	C4673	C4674	C4677
Major elements by XRF (wt%)										
SiO_2	47.96	45.13	50.97	68.41	72.42	45.23	75.16	55.77	52.65	48.04
TiO_2	1.81	1.58	1.89	0.86	0.45	2.55	0.25	2.09	2.50	2.97
Al_2O_3	17.04	15.19	15.57	13.61	13.14	15.35	12.64	13.88	14.14	14.54
Fe_2O_{3t}	11.85	11.52	10.91	5.17	3.20	13.24	2.42	9.66	11.50	12.94
MnO	0.26	0.23	0.26	0.10	0.05	0.19	0.02	0.19	0.23	0.24
MgO	5.81	8.16	5.47	1.42	1.15	6.64	0.83	4.10	4.45	5.49
CaO	5.42	8.43	9.14	1.89	0.84	10.56	0.26	5.19	6.23	7.55
Na_2O	4.75	2.46	2.52	4.00	3.39	2.65	3.74	3.35	3.23	3.22
K_2O	0.41	0.22	1.02	4.32	5.02	0.58	4.79	2.61	2.36	1.82
P_2O_5	0.23	0.21	0.40	0.17	0.09	0.46	0.04	0.59	0.69	0.88
L.O.I	3.80	8.40	1.60	0.10	0.30	2.80	0.40	0.90	0.90	1.00
Total	99.34	101.53	99.75	100.05	100.05	100.25	100.55	98.33	98.88	98.69
Trace elements by XRF (ppm)										
Ba	277	109	505	247	368	72	186	367	435	463
Rb	14	10	23	188	176	36	211	124	131	82
Sr	316	179	356	94	57	415	26	171	205	279
Y	19	20	28	80	89	38	111	60	59	48
Zr	122	104	219	591	472	212	337	376	357	371
Nb	<5	<5	9	39	46	16	50	40	29	31
Th	<10	<10	<10	15	18	2	23	<10	6	<10
Pb	<10	<10	<10	6	<10	<10	20	<10	25	<10
Ga	17	18	19	25	25	24	25	22	24	21
Zn	120	104	134	86	30	112	22	107	153	150
Cu	45	47	45	<5	<5	57	<5	22	27	52
Ni	127	116	69	11	7	96	10	35	42	62
V	273	255	253	42	17	311	6	199	242	290
Cr	232	207	132	25	24	176	44	74	86	92
REE and selected trace elements by INAA (ppm)										
La	n.d.	n.d.	n.d.	n.d.	80.51	n.d.	109	n.d.	45.47	n.d.
Ce	n.d.	n.d.	n.d.	n.d.	160	n.d.	124	n.d.	107	n.d.
Nd	n.d.	n.d.	n.d.	n.d.	73.93	n.d.	81.94	n.d.	50.02	n.d.
Sm	n.d.	n.d.	n.d.	n.d.	15.40	n.d.	17.18	n.d.	11.02	n.d.
Eu	n.d.	n.d.	n.d.	n.d.	1.49	n.d.	1.49	n.d.	2.99	n.d.
Tb	n.d.	n.d.	n.d.	n.d.	2.94	n.d.	3.51	n.d.	2.04	n.d.
Yb	n.d.	n.d.	n.d.	n.d.	9.95	n.d.	12.02	n.d.	6.07	n.d.
Lu	n.d.	n.d.	n.d.	n.d.	1.37	n.d.	1.62	n.d.	0.84	n.d.
Ba	n.d.	n.d.	n.d.	n.d.	n.d.	n.d.	n.d.	n.d.	n.d.	n.d.
Co	n.d.	n.d.	n.d.	n.d.	2.38	n.d.	0.63	n.d.	30.24	n.d.
Cr	n.d.	n.d.	n.d.	n.d.	n.d.	n.d.	n.d.	n.d.	n.d.	n.d.
Cs	n.d.	n.d.	n.d.	n.d.	2.42	n.d.	2.42	n.d.	6.94	n.d.
Hf	n.d.	n.d.	n.d.	n.d.	14.47	n.d.	12.70	n.d.	8.98	n.d.
Sb	n.d.	n.d.	n.d.	n.d.	n.d.	n.d.	n.d.	n.d.	n.d.	n.d.
Sc	n.d.	n.d.	n.d.	n.d.	4.29	n.d.	2.13	n.d.	25.53	n.d.
Ta	n.d.	n.d.	n.d.	n.d.	4.07	n.d.	5.53	n.d.	2.76	n.d.
Th	n.d.	n.d.	n.d.	n.d.	24.02	n.d.	30.84	n.d.	9.63	n.d.
U	n.d.	n.d.	n.d.	n.d.	2.95	n.d.	4.32	n.d.	1.54	n.d.
A/CNK[1]				0.93	1.05	1.07				

[1]: $A/CNK = molAl_2O_3/molCaO+molNa_2O+molK_2O$

Table 3 (continued)

Sample No.	C4679	C4680	C4681	C4682	C4685	C4686	C4687	C4688	C4689	C4690
Major elements by XRF (wt%)										
SiO_2	44.36	76.29	70.77	50.49	71.02	75.29	59.39	50.31	72.45	73.53
TiO_2	2.83	0.10	0.48	3.14	0.43	0.19	1.76	2.80	0.38	0.23
Al_2O_3	14.57	12.26	13.18	13.64	13.26	12.86	14.03	13.67	13.17	13.22
Fe_2O_{3t}	13.99	1.09	4.09	13.00	3.19	1.95	7.94	12.56	3.23	2.03
MnO	0.25	0.02	0.07	0.28	0.04	0.02	0.17	0.22	0.07	0.03
MgO	6.80	0.87	1.13	4.92	1.20	0.75	3.21	5.00	0.99	1.25
CaO	9.37	0.01	0.91	6.36	0.74	0.29	4.21	6.94	0.65	0.37
Na_2O	2.45	4.47	3.45	3.46	3.87	3.58	4.00	3.12	3.89	3.85
K_2O	1.21	4.32	5.49	1.86	5.61	4.87	3.33	2.28	5.11	5.01
P_2O_5	0.47	0.01	0.09	0.86	0.09	0.03	0.49	0.81	0.07	0.04
L.O.I	2.80	0.10	0.20	1.30	0.60	0.30	1.00	0.70	0.30	0.30
Total	99.10	99.54	99.86	99.31	100.05	100.13	99.53	98.41	100.31	99.86
Trace elements by XRF (ppm)										
Ba	278	24	360	374	343	180	343	462	223	161
Rb	84	265	206	148	196	213	151	154	262	257
Sr	324	<5	51	241	57	45	142	249	27	24
Y	38	64	78	60	82	60	62	58	88	74
Zr	202	57	831	391	572	228	361	346	361	262
Nb	12	47	37	30	49	43	42	29	48	48
Th	<10	<10	17	3	<10	25	15	<10	21	<10
Pb	<10	<10	3	17	<10	14	14	<10	45	<10
Ga	24	29	25	29	24	22	22	25	24	25
Zn	127	22	55	208	31	20	123	154	80	24
Cu	64	6	<5	48	11	<5	25	55	<5	7
Ni	99	5	12	43	7	6	23	25	9	6
V	321	<5	10	279	20	<5	166	290	9	<5
Cr	127	11	37	47	13	33	44	49	29	13
REE and selected trace elements by INAA (ppm)										
La	n.d.	n.d.	91.18	47.80	n.d.	63.41	n.d.	n.d.	77.76	n.d.
Ce	n.d.	n.d.	213	108	n.d.	115	n.d.	n.d.	169	n.d.
Nd	n.d.	n.d.	86.73	53.35	n.d.	45.71	n.d.	n.d.	68.45	n.d.
Sm	n.d.	n.d.	17.18	11.56	n.d.	8.90	n.d.	n.d.	13.67	n.d.
Eu	n.d.	n.d.	1.72	3.36	n.d.	0.59	n.d.	n.d.	1.12	n.d.
Tb	n.d.	n.d.	2.95	1.97	n.d.	1.69	n.d.	n.d.	2.62	n.d.
Yb	n.d.	n.d.	8.86	5.93	n.d.	7.09	n.d.	n.d.	9.30	n.d.
Lu	n.d.	n.d.	1.27	0.86	n.d.	0.99	n.d.	n.d.	1.32	n.d.
Ba	n.d.	n.d.	n.d.	n.d.	n.d.	n.d.	n.d.	n.d.	n.d.	n.d.
Co	n.d.	n.d.	3.21	35.42	n.d.	0.84	n.d.	n.d.	3.30	n.d.
Cr	n.d.	n.d.	n.d.	n.d.	n.d.	n.d.	n.d.	n.d.	n.d.	n.d.
Cs	n.d.	n.d.	3.15	10.43	n.d.	1.65	n.d.	n.d.	3.08	n.d.
Hf	n.d.	n.d.	22.42	9.52	n.d.	8.91	n.d.	n.d.	12.60	n.d.
Sb	n.d.	n.d.	n.d.	n.d.	n.d.	n.d.	n.d.	n.d.	n.d.	n.d.
Sc	n.d.	n.d.	4.15	27.51	n.d.	2.16	n.d.	n.d.	3.68	n.d.
Ta	n.d.	n.d.	3.87	2.83	n.d.	4.40	n.d.	n.d.	5.05	n.d.
Th	n.d.	n.d.	24.73	8.12	n.d.	27.55	n.d.	n.d.	26.02	n.d.
U	n.d.	n.d.	3.60	2.23	n.d.	4.78	n.d.	n.d.	4.22	n.d.
A/CNK		1.02	0.99		0.96	1.10	0.79		1.01	1.06

Table 3 (continued)

Sample No.	C4691	C4692	C4694	C4697	C4699	C4700	C4701	C4702	C4703	C4704
Major elements by XRF (wt%)										
SiO_2	61.55	72.90	73.59	69.48	71.69	71.94	71.47	60.95	48.95	72.83
TiO_2	1.25	0.30	0.24	0.37	0.37	0.34	0.39	1.80	2.80	0.32
Al_2O_3	14.12	12.85	13.16	15.48	13.98	14.16	14.28	13.70	12.76	12.76
Fe_2O_{3t}	6.72	1.94	2.45	2.64	2.71	2.67	2.93	11.35	15.28	4.11
MnO	0.09	0.04	0.02	0.05	0.03	0.03	0.04	0.05	0.33	0.07
MgO	3.26	1.76	0.88	1.41	1.21	1.01	1.22	2.53	4.10	1.23
CaO	5.40	1.25	0.54	1.68	1.02	1.21	1.03	1.29	6.37	3.47
Na_2O	2.86	3.44	3.85	3.84	3.51	3.70	3.57	4.67	4.71	4.12
K_2O	3.67	4.76	5.04	4.47	4.89	4.78	5.07	2.52	2.52	0.68
P_2O_5	0.21	0.05	0.05	0.11	0.09	0.08	0.09	0.37	1.91	0.09
L.O.I	1.20	0.50	0.70	0.90	0.60	0.10	0.40	0.70	0.20	0.50
Total	100.33	99.79	100.52	100.43	100.10	100.02	100.49	99.93	99.93	100.18
Trace elements by XRF (ppm)										
Ba	495	558	188	852	578	518	636	158	792	106
Rb	391	223	298	173	193	190	179	106	152	53
Sr	284	135	34	210	103	108	117	150	222	198
Y	77	78	84	26	40	39	40	35	103	34
Zr	350	597	301	185	186	177	205	385	840	158
Nb	44	71	42	12	14	11	14	34	55	11
Th	<10	<10	22	<10	14	16	13	<10	<10	10
Pb	<10	<10	13	16	9	<10	24	<10	<10	<10
Ga	25	24	23	14	17	15	17	22	24	16
Zn	31	33	22	43	20	22	19	22	177	49
Cu	12	5	<5	<5	<5	<5	<5	<5	31	<5
Ni	25	9	9	5	7	8	8	34	6	10
V	98	13	6	28	24	20	30	169	71	32
Cr	99	15	44	31	34	35	30	33	9	35
REE and selected trace elements by INAA (ppm)										
La	n.d.	n.d.	n.d.	23.71	34.55	36.11	n.d.	n.d.	n.d.	n.d.
Ce	n.d.	n.d.	n.d.	50.84	54.10	63.08	n.d.	n.d.	n.d.	n.d.
Nd	n.d.	n.d.	n.d.	17.86	30.96	33.09	n.d.	n.d.	n.d.	n.d.
Sm	n.d.	n.d.	n.d.	3.83	6.19	6.35	n.d.	n.d.	n.d.	n.d.
Eu	n.d.	n.d.	n.d.	0.86	1.14	1.08	n.d.	n.d.	n.d.	n.d.
Tb	n.d.	n.d.	n.d.	0.60	1.06	1.16	n.d.	n.d.	n.d.	n.d.
Yb	n.d.	n.d.	n.d.	2.09	3.75	3.72	n.d.	n.d.	n.d.	n.d.
Lu	n.d.	n.d.	n.d.	0.32	0.54	0.54	n.d.	n.d.	n.d.	n.d.
Ba	n.d.	n.d.	n.d.	n.d.	n.d.	n.d.	n.d.	n.d.	n.d.	n.d.
Co	n.d.	n.d.	n.d.	3.98	2.27	3.32	n.d.	n.d.	n.d.	n.d.
Cr	n.d.	n.d.	n.d.	n.d.	n.d.	n.d.	n.d.	n.d.	n.d.	n.d.
Cs	n.d.	n.d.	n.d.	3.76	4.39	3.92	n.d.	n.d.	n.d.	n.d.
Hf	n.d.	n.d.	n.d.	5.08	6.44	6.00	n.d.	n.d.	n.d.	n.d.
Sb	n.d.	n.d.	n.d.	n.d.	n.d.	n.d.	n.d.	n.d.	n.d.	n.d.
Sc	n.d.	n.d.	n.d.	4.97	4.93	4.82	n.d.	n.d.	n.d.	n.d.
Ta	n.d.	n.d.	n.d.	0.91	1.90	1.72	n.d.	n.d.	n.d.	n.d.
Th	n.d.	n.d.	n.d.	10.67	17.13	22.81	n.d.	n.d.	n.d.	n.d.
U	n.d.	n.d.	n.d.	2.09	2.46	2.90	n.d.	n.d.	n.d.	n.d.
A/CNK	0.76	0.98	1.04	1.09	1.08	1.05	1.08	1.07		0.92

Table 3 (continued)

Sample No.	C4705	C4706	C4707	C4713	C4714	C4721	C4728	C4734	C4735	C4736
Major elements by XRF (wt %)										
SiO_2	75.62	71.70	72.41	59.22	46.55	71.54	71.00	47.49	74.34	72.91
TiO_2	0.05	0.39	0.36	0.83	1.61	0.41	0.36	1.53	0.23	0.24
Al_2O_3	13.05	14.03	14.04	16.87	16.03	13.85	14.03	15.32	12.85	13.45
Fe_2O_{3t}	0.49	2.69	2.71	6.02	11.58	2.73	2.59	10.88	2.10	2.13
MnO	0.02	0.03	0.04	0.08	0.18	0.04	0.04	0.19	0.04	0.03
MgO	0.93	1.21	1.26	3.50	8.50	1.44	1.85	6.76	1.02	1.12
CaO	0.38	1.61	1.50	4.49	10.24	1.86	0.95	10.37	0.18	0.29
Na_2O	3.31	3.48	3.35	4.17	2.18	3.55	3.82	3.91	4.12	4.09
K_2O	6.00	3.67	4.08	3.04	1.14	3.32	3.91	0.59	5.02	5.18
P_2O_5	0.01	0.09	0.08	0.21	0.22	0.10	0.08	0.20	0.04	0.05
L.O.I	0.10	0.20	0.20	0.50	0.80	0.40	0.70	3.30	0.30	0.50
Total	99.96	99.10	100.03	98.93	99.03	99.24	99.33	100.54	100.23	99.99
Trace elements by XRF (ppm)										
Ba	53	597	515	787	184	358	528	185	219	220
Rb	214	127	178	114	59	148	105	29	158	176
Sr	18	161	133	415	342	144	136	430	43	47
Y	18	42	29	24	27	33	24	19	49	57
Zr	26	200	174	166	160	199	177	107	331	334
Nb	<5	15	13	9	10	13	12	<5	45	49
Th	<10	15	12	<10	<10	<10	<10	<10	<10	<10
Pb	11	<10	<10	<10	<10	<10	<10	<10	<10	<10
Ga	12	14	15	18	19	16	16	18	20	20
Zn	17	17	21	72	99	24	24	106	24	23
Cu	10	<5	<5	57	43	7	10	61	6	7
Ni	<5	11	6	16	170	7	15	101	8	5
V	<5	26	30	147	256	36	41	248	<5	<5
Cr	14	30	39	32	334	13	32	162	167	16
REE and selected trace elements by INAA (ppm)										
La	n.d.	n.d.	n.d.	n.d.	n.d.	n.d.	n.d.	n.d.	n.d.	n.d.
Ce	n.d.	n.d.	n.d.	n.d.	n.d.	n.d.	n.d.	n.d.	n.d.	n.d.
Nd	n.d.	n.d.	n.d.	n.d.	n.d.	n.d.	n.d.	n.d.	n.d.	n.d.
Sm	n.d.	n.d.	n.d.	n.d.	n.d.	n.d.	n.d.	n.d.	n.d.	n.d.
Eu	n.d.	n.d.	n.d.	n.d.	n.d.	n.d.	n.d.	n.d.	n.d.	n.d.
Tb	n.d.	n.d.	n.d.	n.d.	n.d.	n.d.	n.d.	n.d.	n.d.	n.d.
Yb	n.d.	n.d.	n.d.	n.d.	n.d.	n.d.	n.d.	n.d.	n.d.	n.d.
Lu	n.d.	n.d.	n.d.	n.d.	n.d.	n.d.	n.d.	n.d.	n.d.	n.d.
Ba	n.d.	n.d.	n.d.	n.d.	n.d.	n.d.	n.d.	n.d.	n.d.	n.d.
Co	n.d.	n.d.	n.d.	n.d.	n.d.	n.d.	n.d.	n.d.	n.d.	n.d.
Cr	n.d.	n.d.	n.d.	n.d.	n.d.	n.d.	n.d.	n.d.	n.d.	n.d.
Cs	n.d.	n.d.	n.d.	n.d.	n.d.	n.d.	n.d.	n.d.	n.d.	n.d.
Hf	n.d.	n.d.	n.d.	n.d.	n.d.	n.d.	n.d.	n.d.	n.d.	n.d.
Sb	n.d.	n.d.	n.d.	n.d.	n.d.	n.d.	n.d.	n.d.	n.d.	n.d.
Sc	n.d.	n.d.	n.d.	n.d.	n.d.	n.d.	n.d.	n.d.	n.d.	n.d.
Ta	n.d.	n.d.	n.d.	n.d.	n.d.	n.d.	n.d.	n.d.	n.d.	n.d.
Th	n.d.	n.d.	n.d.	n.d.	n.d.	n.d.	n.d.	n.d.	n.d.	n.d.
U	n.d.	n.d.	n.d.	n.d.	n.d.	n.d.	n.d.	n.d.	n.d.	n.d.
A/CNK	1.03	1.11	1.11	0.92		1.08	1.15			1.05

Table 3 (continued)

Sample No.	C4737	C4739	C4748	C4749	C4750	C4753	C4754	C4755	C4758	C4761
Major elements by XRF (wt%)										
SiO_2	72.84	75.25	75.16	46.38	47.58	53.66	48.11	46.46	77.62	76.29
TiO_2	0.33	0.12	0.24	3.78	3.84	1.40	1.50	2.12	0.12	0.12
Al_2O_3	13.62	13.90	13.22	12.72	12.87	14.03	15.56	15.60	11.85	12.24
Fe_2O_{3t}	2.47	1.56	1.25	14.52	14.08	8.51	11.61	12.06	2.49	2.46
MnO	0.04	0.02	0.03	0.23	0.25	0.13	0.20	0.18	0.01	0.02
MgO	1.09	0.92	1.23	6.39	6.10	4.94	7.25	7.49	0.72	0.74
CaO	0.48	0.13	0.58	9.83	9.22	11.43	10.08	10.31	0.00	0.13
Na_2O	3.85	2.35	5.50	2.87	4.08	3.84	2.38	2.25	4.58	4.53
K_2O	4.76	6.16	2.41	0.39	0.49	0.35	0.90	0.72	3.24	4.29
P_2O_5	0.06	0.02	0.06	0.16	0.30	0.23	0.19	0.49	0.01	0.02
L.O.I	0.20	0.60	0.60	0.70	0.70	0.80	1.40	1.60	0.00	0.10
Total	99.74	101.03	100.28	97.97	99.51	99.32	99.18	99.28	100.64	100.94
Trace elements by XRF (ppm)										
Ba	304	255	779	216	423	34	216	228	29	28
Rb	142	232	53	24	19	9	31	31	113	187
Sr	77	65	118	342	360	445	315	380	7	14
Y	49	73	12	24	33	54	30	32	79	102
Zr	351	166	125	139	141	243	136	134	467	441
Nb	47	41	5	9	9	29	9	13	72	60
Th	<10	12	<10	<10	<10	<10	<10	<10	22	11
Pb	<10	<10	<10	<10	<10	<10	<10	<10	<10	<10
Ga	22	20	10	23	21	23	18	20	25	26
Zn	25	22	15	98	121	73	108	77	31	25
Cu	9	<5	6	69	59	<5	66	53	<5	<5
Ni	5	9	<5	69	62	54	106	100	10	6
V	11	7	15	652	485	151	278	274	<5	<5
Cr	18	29	15	86	50	188	168	194	41	44
REE and selected trace elements by INAA (ppm)										
La	n.d.	n.d.	n.d.	n.d.	n.d.	n.d.	n.d.	n.d.	n.d.	n.d.
Ce	n.d.	n.d.	n.d.	n.d.	n.d.	n.d.	n.d.	n.d.	n.d.	n.d.
Nd	n.d.	n.d.	n.d.	n.d.	n.d.	n.d.	n.d.	n.d.	n.d.	n.d.
Sm	n.d.	n.d.	n.d.	n.d.	n.d.	n.d.	n.d.	n.d.	n.d.	n.d.
Eu	n.d.	n.d.	n.d.	n.d.	n.d.	n.d.	n.d.	n.d.	n.d.	n.d.
Tb	n.d.	n.d.	n.d.	n.d.	n.d.	n.d.	n.d.	n.d.	n.d.	n.d.
Yb	n.d.	n.d.	n.d.	n.d.	n.d.	n.d.	n.d.	n.d.	n.d.	n.d.
Lu	n.d.	n.d.	n.d.	n.d.	n.d.	n.d.	n.d.	n.d.	n.d.	n.d.
Ba	n.d.	n.d.	n.d.	n.d.	n.d.	n.d.	n.d.	n.d.	n.d.	n.d.
Co	n.d.	n.d.	n.d.	n.d.	n.d.	n.d.	n.d.	n.d.	n.d.	n.d.
Cr	n.d.	n.d.	n.d.	n.d.	n.d.	n.d.	n.d.	n.d.	n.d.	n.d.
Cs	n.d.	n.d.	n.d.	n.d.	n.d.	n.d.	n.d.	n.d.	n.d.	n.d.
Hf	n.d.	n.d.	n.d.	n.d.	n.d.	n.d.	n.d.	n.d.	n.d.	n.d.
Sb	n.d.	n.d.	n.d.	n.d.	n.d.	n.d.	n.d.	n.d.	n.d.	n.d.
Sc	n.d.	n.d.	n.d.	n.d.	n.d.	n.d.	n.d.	n.d.	n.d.	n.d.
Ta	n.d.	n.d.	n.d.	n.d.	n.d.	n.d.	n.d.	n.d.	n.d.	n.d.
Th	n.d.	n.d.	n.d.	n.d.	n.d.	n.d.	n.d.	n.d.	n.d.	n.d.
U	n.d.	n.d.	n.d.	n.d.	n.d.	n.d.	n.d.	n.d.	n.d.	n.d.
A/CNK	1.10	1.29	1.04						1.07	0.99

Table 3 (continued)

Sample No	C4774	C4778	C4779	C4801	C4854	C4865	C4866	C4867 1	25-5- 1A	25-5-
Major elements by XRF (wt%)										
SiO_2	48.70	56.66	48.67	63.03	48.16	76.35	45.95	47.18	75.21	76.33
TiO_2	2.31	1.39	2.34	1.16	1.64	0.07	2.44	3.41	0.17	0.18
Al_2O_3	14.06	15.81	15.65	15.98	14.90	13.14	15.15	12.51	12.62	12.88
Fe_2O3_t	2.61	9.32	12.80	6.64	11.45	0.94	13.15	15.46	1.76	1.81
MnO	0.37	0.10	0.18	0.04	0.24	0.03	0.23	0.24	0.02	0.02
MgO	6.48	4.73	5.86	1.44	7.91	0.35	7.06	3.81	0.90	0.84
CaO	10.39	4.82	7.49	2.97	7.99	0.40	9.63	8.90	0.27	0.23
Na_2O	2.83	3.39	3.70	4.23	2.85	3.51	1.90	2.12	3.49	3.50
K_2O	0.68	1.87	1.23	3.19	0.93	4.45	1.16	1.78	5.13	5.02
P_2O_5	0.28	0.15	0.42	0.20	0.21	0.02	0.42	1.85	0.02	0.02
L.O.I	0.40	1.10	0.50	0.30	3.90	0.60	2.10	1.00	0.20	0.00
Total	99.11	99.34	98.84	99.18	100.18	99.86	99.19	98.26	99.79	100.83
Trace elements by XRF (ppm)										
Ba	177	324	289	472	85	131	280	612	196	186
Rb	22	73	35	67	81	292	96	105	211	205
Sr	294	430	468	257	249	72	271	238	23	21
Y	22	13	26	56	23	95	28	85	83	92
Zr	141	106	214	356	115	98	203	656	247	237
Nb	11	7	19	44	<5	53	12	49	32	31
Th	<10	<10	<10	<10	<10	<10	<10	<10	20	21
Pb	65	11	19	13	<10	11	31	<10	12	11
Ga	23	17	19	27	18	28	25	23	21	19
Zn	151	53	98	15	121	33	204	219	38	35
Cu	132	15	31	23	66	21	51	31	5	8
Ni	65	59	69	12	88	8	104	17	<5	5
V	338	143	243	91	256	<5	261	118	<5	<5
Cr	209	34	42	11	108	20	103	6	18	23
REE and selected trace elements by INAA (ppm)										
La	n.d.	13.37	n.d.	49.88	n.d.	9.50	n.d.	n.d.	75.30	n.d.
Ce	n.d.	32.37	n.d.	127	n.d.	25.57	n.d.	n.d.	175	n.d.
Nd	n.d.	13.25	n.d.	69.18	n.d.	25.93	n.d.	n.d.	72.60	n.d.
Sm	n.d.	2.82	n.d.	16.32	n.d.	10.48	n.d.	n.d.	14.40	n.d.
Eu	n.d.	1.05	n.d.	2.05	n.d.	0.05	n.d.	n.d.	0.49	n.d.
Tb	n.d.	0.50	n.d.	2.82	n.d.	3.01	n.d.	n.d.	2.61	n.d.
Yb	n.d.	1.17	n.d.	7.27	n.d.	11.35	n.d.	n.d.	8.65	n.d.
Lu	n.d.	0.18	n.d.	0.91	n.d.	1.51	n.d.	n.d.	1.30	n.d.
Ba	n.d.	n.d.	n.d.	n.d.	n.d.	n.d.	n.d.	n.d.	n.d.	n.d.
Co	n.d.	49.87	n.d.	37.89	n.d.	42.30	n.d.	n.d.	0.98	n.d.
Cr	n.d.	n.d.	n.d.	n.d.	n.d.	n.d.	n.d.	n.d.	25.00	n.d.
Cs	n.d.	2.28	n.d.	0.96	n.d.	4.00	n.d.	n.d.	n.d.	n.d.
Hf	n.d.	2.86	n.d.	13.27	n.d.	6.35	n.d.	n.d.	9.37	n.d.
Sb	n.d.	n.d.	n.d.	n.d.	n.d.	n.d.	n.d.	n.d.	n.d.	n.d.
Sc	n.d.	13.93	n.d.	10.15	n.d.	2.33	n.d.	n.d.	3.21	n.d.
Ta	n.d.	1.19	n.d.	2.71	n.d.	5.03	n.d.	n.d.	2.83	n.d.
Th	n.d.	4.98	n.d.	5.42	n.d.	32.32	n.d.	n.d.	29.20	n.d.
U	n.d.	0.86	n.d.	0.94	n.d.	6.67	n.d.	n.d.	n.d.	n.d.
A/CNK				1.01		1.16			1.07	1.11

Table 3 (continued)

Sample No.	25-5-2	25-5-3	25-5-4	25-5-5	25-5-6	25-5-7	25-5-8	26-13-1	26-13-2	26-13-3
Major elements by XRF (wt%)										
SiO_2	74.34	75.69	74.73	73.76	73.20	75.52	73.10	71.31	71.94	70.36
TiO_2	0.18	0.18	0.20	0.20	0.24	0.20	0.20	0.39	0.28	0.27
Al_2O_3	13.02	12.62	13.13	13.05	13.52	13.16	13.02	13.80	13.78	13.27
Fe_2O_{3t}	1.89	1.53	1.82	1.72	2.11	1.68	1.86	3.74	3.20	3.21
MnO	0.02	0.03	0.02	0.02	0.01	0.02	0.02	0.05	0.06	0.05
MgO	0.75	0.79	0.78	0.86	0.79	0.78	0.85	0.95	0.73	0.88
CaO	0.50	0.61	0.22	0.18	0.07	0.28	0.17	0.78	0.85	0.86
Na_2O	3.63	3.62	3.60	3.84	3.80	3.44	4.00	4.35	4.90	4.56
K_2O	5.27	4.85	5.30	5.21	5.17	5.44	5.25	4.51	5.12	4.97
P_2O_5	0.03	0.03	0.03	0.04	0.04	0.03	0.03	0.06	0.04	0.04
L.O.I	0.30	0.00	0.00	0.30	0.20	0.10	0.30	0.10	0.00	0.60
Total	99.93	99.95	99.83	99.18	99.15	100.65	98.80	100.04	100.90	99.07
Trace elements by XRF (ppm)										
Ba	281	325	215	223	438	192	255	630	627	597
Rb	188	178	204	230	198	236	210	180	203	200
Sr	59	69	30	28	31	24	35	54	42	47
Y	89	64	75	78	71	81	64	72	83	87
Zr	257	242	247	241	308	245	256	464	554	577
Nb	30	29	30	28	28	30	19	27	32	36
Th	16	14	17	17	14	16	13	12	13	12
Pb	18	<10	28	28	29	17	27	<10	12	10
Ga	22	18	19	17	20	22	20	20	21	19
Zn	16	17	33	33	19	30	40	31	49	44
Cu	7	0	6	4	7	4	7	6	6	7
Ni	<5	6	8	5	7	8	7	<5	5	8
V	6	<5	<5	<5	<5	<5	6	14	<5	<5
Cr	28	32	41	23	39	22	37	26	24	28
REE and selected trace elements by INAA (ppm)										
La	n.d.	n.d.	n.d.	n.d.	n.d.	n.d.	49.90	n.d.	n.d.	n.d.
Ce	n.d.	n.d.	n.d.	n.d.	n.d.	n.d.	121	n.d.	n.d.	n.d.
Nd	n.d.	n.d.	n.d.	n.d.	n.d.	n.d.	51.70	n.d.	n.d.	n.d.
Sm	n.d.	n.d.	n.d.	n.d.	n.d.	n.d.	9.95	n.d.	n.d.	n.d.
Eu	n.d.	n.d.	n.d.	n.d.	n.d.	n.d.	0.52	n.d.	n.d.	n.d.
Tb	n.d.	n.d.	n.d.	n.d.	n.d.	n.d.	1.66	n.d.	n.d.	n.d.
Yb	n.d.	n.d.	n.d.	n.d.	n.d.	n.d.	6.10	n.d.	n.d.	n.d.
Lu	n.d.	n.d.	n.d.	n.d.	n.d.	n.d.	0.94	n.d.	n.d.	n.d.
Ba	n.d.	n.d.	n.d.	n.d.	n.d.	n.d.	n.d.	n.d.	n.d.	n.d.
Co	n.d.	n.d.	n.d.	n.d.	n.d.	n.d.	1.40	n.d.	n.d.	n.d.
Cr	n.d.	n.d.	n.d.	n.d.	n.d.	n.d.	33.00	n.d.	n.d.	n.d.
Cs	n.d.	n.d.	n.d.	n.d.	n.d.	n.d.	n.d.	n.d.	n.d.	n.d.
Hf	n.d.	n.d.	n.d.	n.d.	n.d.	n.d.	9.10	n.d.	n.d.	n.d.
Sb	n.d.	n.d.	n.d.	n.d.	n.d.	n.d.	n.d.	n.d.	n.d.	n.d.
Sc	n.d.	n.d.	n.d.	n.d.	n.d.	n.d.	2.96	n.d.	n.d.	n.d.
Ta	n.d.	n.d.	n.d.	n.d.	n.d.	n.d.	1.59	n.d.	n.d.	n.d.
Th	n.d.	n.d.	n.d.	n.d.	n.d.	n.d.	19.20	n.d.	n.d.	n.d.
U	n.d.	n.d.	n.d.	n.d.	n.d.	n.d.	n.d.	n.d.	n.d.	n.d.
A/CNK	1.03	1.02	1.09	1.06	1.13	1.09	1.04	1.03	0.91	0.90

Table 3 (continued)

Sample No.	26-13 -4	26-13 -5	26-13 -6	42-1-2	C5031	C5037	C5039	C6102	C6194	C6203
Major elements by XRF (wt%)										
SiO_2	71.46	71.05	70.37	70.75	45.58	74.03	72.31	68.10	77.70	75.10
TiO_2	0.27	0.43	0.40	0.30	2.71	0.28	0.39	0.82	0.06	0.17
Al_2O_3	13.34	14.08	13.94	13.87	14.88	13.41	14.67	12.90	11.70	12.80
Fe_2O_{3t}	3.19	3.27	3.64	2.61	15.11	1.80	2.11	5.55	1.46	1.68
MnO	0.05	0.05	0.05	0.05	0.44	0.03	0.04	0.10	0.03	0.03
MgO	0.85	1.00	0.95	0.85	7.24	0.24	0.68	1.05	0.10	0.19
CaO	0.78	0.80	0.79	0.91	8.90	0.77	1.93	2.34	0.71	0.44
Na_2O	4.09	4.37	4.65	4.45	2.46	3.52	4.63	3.92	7.07	4.39
K_2O	4.87	4.34	4.33	5.00	1.12	5.18	2.41	4.53	0.38	4.34
P_2O_5	0.03	0.07	0.07	0.05	0.46	0.05	0.12	0.18	0.04	0.04
L.O.I	0.50	0.20	0.30	0.20	1.30	0.30	0.30	0.55	0.85	0.75
Total	99.43	99.66	99.49	99.04	100.20	99.61	99.59	100.04	100.10	99.93
Trace elements by XRF (ppm)										
Ba	583	647	578	482	305	452	845	245	45	506
Rb	197	176	164	143	76	174	53	119	10	109
Sr	38	68	45	79	288	72	232	83	101	45
Y	82	64	73	53	35	38	21	104	46	56
Zr	566	409	498	385	197	200	183	716	252	244
Nb	35	22	28	23	13	26	10	54	103	32
Th	14	12	15	20	<10	19	<10	20	29	24
Pb	16	<10	<10	<10	11	22	11	13	10	<10
Ga	23	20	17	20	22	19	13	26	20	17
Zn	41	40	28	29	92	15	13	62	8	13
Cu	<5	7	6	<5	61	7	<5	8	43	<5
Ni	5	7	<5	<5	121	<5	<5	10	<5	<5
V	<5	22	16	9	338	17	28	55	26	5
Cr	30	38	39	27	142	7	10	14	15	<5
REE and selected trace elements by INAA (ppm)										
La	n.d.	n.d.	52.70	55.98	n.d.	n.d.	n.d.	n.d.	n.d.	n.d.
Ce	n.d.	n.d.	123	119	n.d.	n.d.	n.d.	n.d.	n.d.	n.d.
Nd	n.d.	n.d.	53.40	48.41	n.d.	n.d.	n.d.	n.d.	n.d.	n.d.
Sm	n.d.	n.d.	11.10	10.90	n.d.	n.d.	n.d.	n.d.	n.d.	n.d.
Eu	n.d.	n.d.	1.70	1.00	n.d.	n.d.	n.d.	n.d.	n.d.	n.d.
Tb	n.d.	n.d.	1.96	1.70	n.d.	n.d.	n.d.	n.d.	n.d.	n.d.
Yb	n.d.	n.d.	7.20	5.90	n.d.	n.d.	n.d.	n.d.	n.d.	n.d.
Lu	n.d.	n.d.	1.11	0.86	n.d.	n.d.	n.d.	n.d.	n.d.	n.d.
Ba	n.d.	n.d.	n.d.	n.d.	n.d.	n.d.	n.d.	n.d.	n.d.	n.d.
Co	n.d.	n.d.	2.00	2.01	n.d.	n.d.	n.d.	n.d.	n.d.	n.d.
Cr	n.d.	n.d.	36.00	n.d.	n.d.	n.d.	n.d.	n.d.	n.d.	n.d.
Cs	n.d.	n.d.	n.d.	n.d.	n.d.	n.d.	n.d.	n.d.	n.d.	n.d.
Hf	n.d.	n.d.	13.70	11.43	n.d.	n.d.	n.d.	n.d.	n.d.	n.d.
Sb	n.d.	n.d.	n.d.	n.d.	n.d.	n.d.	n.d.	n.d.	n.d.	n.d.
Sc	n.d.	n.d.	6.52	4.94	n.d.	n.d.	n.d.	n.d.	n.d.	n.d.
Ta	n.d.	n.d.	2.17	1.77	n.d.	n.d.	n.d.	n.d.	n.d.	n.d.
Th	n.d.	n.d.	18.60	19.32	n.d.	n.d.	n.d.	n.d.	n.d.	n.d.
U	n.d.	n.d.	n.d.	3.31	n.d.	n.d.	n.d.	n.d.	n.d.	n.d.
A/CNK	0.99	1.06	1.01	0.97		1.05	1.07	0.83	0.88	1.01

Table 3 (continued)

Sample No.	C6204	C6206	C6208	C6258	C6260	C6261	C6262	C6263	C6932	C6936
Major elements by XRF (wt%)										
SiO_2	45.00	45.50	77.50	78.20	70.30	71.40	71.20	75.90	73.72	73.27
TiO_2	2.61	2.53	0.08	0.06	0.25	0.38	0.41	0.11	0.23	0.27
Al_2O_3	14.10	15.40	11.80	12.00	13.30	13.50	13.20	10.70	13.29	13.61
Fe_2O_{3t}	15.70	14.80	1.26	1.10	3.06	2.87	2.79	2.23	1.90	2.19
MnO	0.16	0.22	0.03	0.04	0.09	0.07	0.07	0.03	0.02	0.03
MgO	6.66	7.01	0.18	0.19	0.15	0.36	0.38	0.07	0.02	0.21
CaO	7.44	7.49	0.94	0.83	0.81	1.34	1.40	0.31	0.17	0.25
Na_2O	1.86	2.50	6.94	6.99	4.84	5.36	4.91	2.59	3.81	3.80
K_2O	0.63	1.08	0.22	0.20	4.82	3.90	4.60	6.10	5.22	4.92
P_2O_5	0.56	0.40	0.04	0.04	0.04	0.08	0.08	0.02	0.03	0.05
L.O.I	5.55	3.40	1.20	0.55	0.35	0.40	0.85	0.30	0.70	0.50
Total	100.27	100.33	100.19	100.20	98.01	99.66	99.89	98.36	99.11	99.10
Trace elements by XRF (ppm)										
Ba	50	293	46	114	655	465	582	249	280	399
Rb	33	64	5	7	177	142	185	259	194	175
Sr	210	291	96	191	50	62	48	25	28	58
Y	46	40	36	40	101	62	50	111	64	59
Zr	279	211	232	243	585	367	372	660	300	219
Nb	21	14	102	111	42	28	25	64	33	33
Th	<10	<10	21	30	20	17	21	29	24	24
Pb	<10	<10	<10	14	14	<10	<10	25	13	11
Ga	19	23	14	16	25	20	16	21	21	19
Zn	37	69	10	15	116	22	36	18	21	11
Cu	6	33	130	37	6	<5	<5	<5	<5	<5
Ni	99	82	<5	<5	<5	<5	<5	<5	<5	5
V	303	293	26	25	<5	23	22	<5	6	17
Cr	182	90	11	18	10	14	13	<5	10	8
REE and selected trace elements by INAA (ppm)										
La	n.d.	n.d.	n.d.	n.d.	n.d.	n.d.	n.d.	n.d.	n.d.	n.d.
Ce	n.d.	n.d.	n.d.	n.d.	n.d.	n.d.	n.d.	n.d.	n.d.	n.d.
Nd	n.d.	n.d.	n.d.	n.d.	n.d.	n.d.	n.d.	n.d.	n.d.	n.d.
Sm	n.d.	n.d.	n.d.	n.d.	n.d.	n.d.	n.d.	n.d.	n.d.	n.d.
Eu	n.d.	n.d.	n.d.	n.d.	n.d.	n.d.	n.d.	n.d.	n.d.	n.d.
Tb	n.d.	n.d.	n.d.	n.d.	n.d.	n.d.	n.d.	n.d.	n.d.	n.d.
Yb	n.d.	n.d.	n.d.	n.d.	n.d.	n.d.	n.d.	n.d.	n.d.	n.d.
Lu	n.d.	n.d.	n.d.	n.d.	n.d.	n.d.	n.d.	n.d.	n.d.	n.d.
Ba	n.d.	n.d.	n.d.	n.d.	n.d.	n.d.	n.d.	n.d.	n.d.	n.d.
Co	n.d.	n.d.	n.d.	n.d.	n.d.	n.d.	n.d.	n.d.	n.d.	n.d.
Cr	n.d.	n.d.	n.d.	n.d.	n.d.	n.d.	n.d.	n.d.	n.d.	n.d.
Cs	n.d.	n.d.	n.d.	n.d.	n.d.	n.d.	n.d.	n.d.	n.d.	n.d.
Hf	n.d.	n.d.	n.d.	n.d.	n.d.	n.d.	n.d.	n.d.	n.d.	n.d.
Sb	n.d.	n.d.	n.d.	n.d.	n.d.	n.d.	n.d.	n.d.	n.d.	n.d.
Sc	n.d.	n.d.	n.d.	n.d.	n.d.	n.d.	n.d.	n.d.	n.d.	n.d.
Ta	n.d.	n.d.	n.d.	n.d.	n.d.	n.d.	n.d.	n.d.	n.d.	n.d.
Th	n.d.	n.d.	n.d.	n.d.	n.d.	n.d.	n.d.	n.d.	n.d.	n.d.
U	n.d.	n.d.	n.d.	n.d.	n.d.	n.d.	n.d.	n.d.	n.d.	n.d.
A/CNK			0.88	0.91	0.91	0.87	0.85	0.94	1.09	1.13

Table 3 (continued)

Sample No.	C6937	C6938	C6940	C7008	C7009A	C7010	C7011	C7017	C7019	C7021
Major elements by XRF (wt%)										
SiO_2	73.42	54.19	71.97	50.70	47.30	47.60	46.00	74.30	45.70	72.20
TiO_2	0.29	2.26	0.38	1.13	1.40	1.44	2.21	0.27	2.10	0.28
Al_2O_3	13.08	14.69	14.86	15.30	16.40	16.40	14.10	12.60	15.10	13.30
Fe_2O_{3t}	1.80	10.16	2.00	10.80	12.70	10.90	15.40	2.02	14.20	2.15
MnO	0.03	0.18	0.04	0.22	0.23	0.30	0.35	0.04	0.22	0.05
MgO	0.12	2.73	0.57	7.28	8.03	8.84	7.49	0.34	7.03	0.48
CaO	0.83	5.90	1.73	8.47	8.97	9.39	9.09	0.69	9.80	0.72
Na_2O	3.66	4.42	4.69	2.75	2.48	2.12	2.23	4.37	2.37	3.98
K_2O	4.97	1.88	2.83	1.99	1.28	1.18	1.14	4.47	0.31	5.26
P_2O_5	0.05	0.93	0.11	0.11	0.18	0.19	0.26	0.07	0.26	0.07
L.O.I	0.90	0.90	0.50	1.00	1.35	2.10	1.10	0.90	2.85	0.60
Total	99.15	98.24	99.68	99.75	100.32	100.46	99.37	100.07	99.94	99.09
Trace elements by XRF (ppm)										
Ba	333	972	852	226	218	329	188	288	214	305
Rb	198	54	61	122	60	62	65	157	14	162
Sr	56	405	215	223	301	229	218	52	302	91
Y	51	65	22	21	26	29	35	91	32	38
Zr	215	308	179	88	106	111	137	202	132	211
Nb	30	26	10	5	6	7	7	32	6	29
Th	24	<10	<10	<10	< 10	<10	<10	21	<10	21
Pb	21	13	12	14	45	58	10	<10	13	13
Ga	19	21	14	17	20	18	20	19	20	18
Zn	23	57	8	92	142	139	116	12	116	17
Cu	0	15	5	53	70	55	29	16	54	9
Ni	<5	<5	<5	117	114	159	126	5	80	<5
V	16	126	26	217	208	220	356	19	267	16
Cr	5	<5	8	270	75	209	198	12	82	<5
REE and selected trace elements (ppm)										
La	n.d.	n.d.	n.d.	n.d.	n.d.	n.d.	n.d.	n.d.	n.d.	n.d.
Ce	n.d.	n.d.	n.d.	n.d.	n.d.	n.d.	n.d.	n.d.	n.d.	n.d.
Nd	n.d.	n.d.	n.d.	n.d.	n.d.	n.d.	n.d.	n.d.	n.d.	n.d.
Sm	n.d.	n.d.	n.d.	n.d.	n.d.	n.d.	n.d.	n.d.	n.d.	n.d.
Eu	n.d.	n.d.	n.d.	n.d.	n.d.	n.d.	n.d.	n.d.	n.d.	n.d.
Tb	n.d.	n.d.	n.d.	n.d.	n.d.	n.d.	n.d.	n.d.	n.d.	n.d.
Yb	n.d.	n.d.	n.d.	n.d.	n.d.	n.d.	n.d.	n.d.	n.d.	n.d.
Lu	n.d.	n.d.	n.d.	n.d.	n.d.	n.d.	n.d.	n.d.	n.d.	n.d.
Ba	n.d.	n.d.	n.d.	n.d.	n.d.	n.d.	n.d.	n.d.	n.d.	n.d.
Co	n.d.	n.d.	n.d.	n.d.	n.d.	n.d.	n.d.	n.d.	n.d.	n.d.
Cr	n.d.	n.d.	n.d.	n.d.	n.d.	n.d.	n.d.	n.d.	n.d.	n.d.
Cs	n.d.	n.d.	n.d.	n.d.	n.d.	n.d.	n.d.	n.d.	n.d.	n.d.
Hf	n.d.	n.d.	n.d.	n.d.	n.d.	n.d.	n.d.	n.d.	n.d.	n.d.
Sb	n.d.	n.d.	n.d.	n.d.	n.d.	n.d.	n.d.	n.d.	n.d.	n.d.
Sc	n.d.	n.d.	n.d.	n.d.	n.d.	n.d.	n.d.	n.d.	n.d.	n.d.
Ta	n.d.	n.d.	n.d.	n.d.	n.d.	n.d.	n.d.	n.d.	n.d.	n.d.
Th	n.d.	n.d.	n.d.	n.d.	n.d.	n.d.	n.d.	n.d.	n.d.	n.d.
U	n.d.	n.d.	n.d.	n.d.	n.d.	n.d.	n.d.	n.d.	n.d.	n.d.
A/CNK	1.01		1.07					0.95		0.98

Table 3 (continued)

Sample No.	C7025	C7321	C7327	C7377	C7378	C7382	C7383	C7385	C7389	C7391
Major elements by XRF (wt%)										
SiO_2	75.70	68.25	69.58	71.79	72.05	74.86	74.03	70.11	67.72	70.96
TiO_2	0.28	0.55	0.60	0.28	0.28	0.17	0.20	0.39	0.67	0.54
Al_2O_3	11.30	15.26	14.29	13.67	13.39	12.41	12.59	14.09	15.35	14.16
Fe_2O_{3t}	3.54	2.76	4.03	3.05	3.26	2.78	3.00	2.98	3.98	3.10
MnO	0.08	0.05	0.04	0.04	0.03	0.01	0.02	0.04	0.05	0.03
MgO	0.34	1.20	0.61	0.08	0.00	0.00	0.00	0.40	0.65	0.33
CaO	0.36	1.42	1.15	0.94	0.44	0.19	0.62	1.45	1.13	1.47
Na_2O	1.89	2.76	4.29	4.29	4.57	4.08	3.76	3.78	4.68	4.61
K_2O	5.57	5.90	4.29	5.25	4.84	4.54	4.91	4.77	4.84	4.60
P_2O_5	0.04	0.12	0.19	0.05	0.02	0.01	0.01	0.07	0.13	0.09
L.O.I	1.20	1.00	0.80	0.50	0.20	0.10	0.50	0.30	0.40	0.30
Total	100.30	99.27	99.87	99.94	99.08	99.15	99.64	98.38	99.60	100.19
Trace elements by XRF (ppm)										
Ba	212	1160	711	591	567	94	160	723	803	702
Rb	186	239	155	202	142	141	188	175	169	110
Sr	66	169	137	42	45	16	59	103	118	124
Y	135	24	59	89	92	95	105	46	46	54
Zr	853	256	296	583	582	680	820	318	469	521
Nb	64	14	27	40	41	51	53	24	25	28
Th	19	22	16	19	18	23	25	17	16	20
Pb	<10	10	<10	<10	19	12	<10	17	24	<10
Ga	30	15	17	23	24	25	26	19	19	17
Zn	18	22	21	41	74	12	11	14	18	7
Cu	<5	<5	<5	<5	15	<5	<5	<5	7	5
Ni	8	7	7	<5	<5	<5	7	6	6	7
V	13	61	36	<5	<5	6	<5	22	31	20
Cr	21	12	<5	<5	5	<5	5	14	8	8
REE and selected trace elements by INAA (ppm)										
La	n.d.	n.d.	n.d.	n.d.	n.d.	n.d.	n.d.	n.d.	n.d.	n.d.
Ce	n.d.	n.d.	n.d.	n.d.	n.d.	n.d.	n.d.	n.d.	n.d.	n.d.
Nd	n.d.	n.d.	n.d.	n.d.	n.d.	n.d.	n.d.	n.d.	n.d.	n.d.
Sm	n.d.	n.d.	n.d.	n.d.	n.d.	n.d.	n.d.	n.d.	n.d.	n.d.
Eu	n.d.	n.d.	n.d.	n.d.	n.d.	n.d.	n.d.	n.d.	n.d.	n.d.
Tb	n.d.	n.d.	n.d.	n.d.	n.d.	n.d.	n.d.	n.d.	n.d.	n.d.
Yb	n.d.	n.d.	n.d.	n.d.	n.d.	n.d.	n.d.	n.d.	n.d.	n.d.
Lu	n.d.	n.d.	n.d.	n.d.	n.d.	n.d.	n.d.	n.d.	n.d.	n.d.
Ba	n.d.	n.d.	n.d.	n.d.	n.d.	n.d.	n.d.	n.d.	n.d.	n.d.
Co	n.d.	n.d.	n.d.	n.d.	n.d.	n.d.	n.d.	n.d.	n.d.	n.d.
Cr	n.d.	n.d.	n.d.	n.d.	n.d.	n.d.	n.d.	n.d.	n.d.	n.d.
Cs	n.d.	n.d.	n.d.	n.d.	n.d.	n.d.	n.d.	n.d.	n.d.	n.d.
Hf	n.d.	n.d.	n.d.	n.d.	n.d.	n.d.	n.d.	n.d.	n.d.	n.d.
Sb	n.d.	n.d.	n.d.	n.d.	n.d.	n.d.	n.d.	n.d.	n.d.	n.d.
Sc	n.d.	n.d.	n.d.	n.d.	n.d.	n.d.	n.d.	n.d.	n.d.	n.d.
Ta	n.d.	n.d.	n.d.	n.d.	n.d.	n.d.	n.d.	n.d.	n.d.	n.d.
Th	n.d.	n.d.	n.d.	n.d.	n.d.	n.d.	n.d.	n.d.	n.d.	n.d.
U	n.d.	n.d.	n.d.	n.d.	n.d.	n.d.	n.d.	n.d.	n.d.	n.d.
A/CNK	1.15	1.13	1.04	0.95	0.99	1.04	1.00	1.01	1.02	0.93

Table 3 (continued)

Sample No.	C7392	C7393	C7394	C7395	C7397	C6679	42-1-1
Major elements by XRF (wt%)							
SiO_2	48.01	72.72	70.68	74.11	74.45	46.91	48.12
TiO_2	1.52	0.32	0.37	0.20	0.25	3.69	1.95
Al_2O_3	15.79	13.88	14.27	13.22	13.15	12.86	15.18
Fe_2O_{3t}	11.17	2.63	2.19	1.64	2.07	16.30	10.98
MnO	0.20	0.03	0.04	0.02	0.01	0.35	0.20
MgO	7.77	0.20	0.47	0.03	0.05	4.81	6.63
CaO	10.19	0.70	1.73	0.54	0.53	9.31	8.65
Na_2O	2.48	4.62	4.43	3.27	3.85	3.39	2.70
K_2O	1.53	5.02	4.52	5.85	5.03	1.21	2.10
P_2O_5	0.22	0.05	0.06	0.03	0.04	0.92	0.45
L.O.I	1.50	0.10	0.40	0.10	0.80	0.60	1.40
Total	100.38	100.27	99.16	99.01	100.23	100.35	98.36
Trace elements by XRF (ppm)							
Ba	326	496	411	192	265	585	573
Rb	96	174	71	164	147	21	115
Sr	301	47	106	33	47	334	370
Y	25	59	58	44	44	52	35
Zr	126	392	326	261	269	211	195
Nb	9	30	26	27	35	21	14
Th	<10	20	17	22	16	<10	<10
Pb	10	13	<10	15	16	<10	<10
Ga	17	21	18	20	19	24	20
Zn	100	16	21	39	16	126	133
Cu	60	5	17	<5	<5	36	52
Ni	122	<5	7	<5	6	30	95
V	239	6	22	8	11	298	257
Cr	212	13	13	5	6	48	177
REE and selected trace elements by INAA (ppm)							
La	n.d.	n.d.	n.d.	n.d.	n.d.	n.d.	n.d.
Ce	n.d.	n.d.	n.d.	n.d.	n.d.	n.d.	n.d.
Nd	n.d.	n.d.	n.d.	n.d.	n.d.	n.d.	n.d.
Sm	n.d.	n.d.	n.d.	n.d.	n.d.	n.d.	n.d.
Eu	n.d.	n.d.	n.d.	n.d.	n.d.	n.d.	n.d.
Tb	n.d.	n.d.	n.d.	n.d.	n.d.	n.d.	n.d.
Yb	n.d.	n.d.	n.d.	n.d.	n.d.	n.d.	n.d.
Lu	n.d.	n.d.	n.d.	n.d.	n.d.	n.d.	n.d.
Ba	n.d.	n.d.	n.d.	n.d.	n.d.	n.d.	n.d.
Co	n.d.	n.d.	n.d.	n.d.	n.d.	n.d.	n.d.
Cr	n.d.	n.d.	n.d.	n.d.	n.d.	n.d.	n.d.
Cs	n.d.	n.d.	n.d.	n.d.	n.d.	n.d.	n.d.
Hf	n.d.	n.d.	n.d.	n.d.	n.d.	n.d.	n.d.
Sb	n.d.	n.d.	n.d.	n.d.	n.d.	n.d.	n.d.
Sc	n.d.	n.d.	n.d.	n.d.	n.d.	n.d.	n.d.
Ta	n.d.	n.d.	n.d.	n.d.	n.d.	n.d.	n.d.
Th	n.d.	n.d.	n.d.	n.d.	n.d.	n.d.	n.d.
U	n.d.	n.d.	n.d.	n.d.	n.d.	n.d.	n.d.
A/CNK		0.97	0.93	1.04	1.03		

Table 4: Representative electron microprobe analyses of feldspars

Sample	Rock[1]	Crystal[2]	Pos'n	Mineral[3]	An	Ab	Or
C4672	mgpg	ph	rim	Ab	1.8	97.1	1.1
		mph1		Ab	0.9	90.0	9.1
		mph2		Ab	3.9	95.6	0.5
		mph3		Ab	0.7	98.8	0.5
C4674	megdi	meg1	core	Lab	55.97.	43.24	0.78
		meg1	core	Lab	57.92	41.34	0.73
		meg1	rim	Lab	53.84	44.89	1.27
C4678	megdi			Kf	0	15.8	84.2
(hybr)		over-plg		Kf	0	6.3	93.7
		ph1	core	Olig	13.0	87.0	0
		ph1	rim	Kf	0	5.1	94.9
		ph2	core	Olig	21.0	79	0
		ph2	rim	Olig	13.4	86.6	0
		meg1	core	Kf	5.1	74.8	20.1
		meg1	rim	Kf	4.0	63.1	32.9
		meg2	core	Lab	55.15	43.16	1.69
		meg2	rim	Kf	0.32	8.39	91.29
	gr	lph1	core	Ab	4.8	90.5	4.7
		lph1	int	Kf	0	6.1	93.9
		lph1	int	Kf	0	6.6	93.4
		lph1	rim	Kf	0	21.3	78.7
		incl		Ab	3.7	96.3	0
		ph2		Kf	0	8.3	91.7
		ph3	core	Olig	10.8	42.9	46.4
C4681	cgpog	ph1	rim	Ab	3.1	95.9	1.0
		ph2	rim	Ab	2.9	97.1	0
		ph2	int	Ab	0.9	99.1	0
		ph3	rim	Ab	0.9	95.6	3.5
		ph4	core	Ab	3.6	96.4	0
		ph5	core	Kf	0	3.5	96.5
		ph6	rim	Kf	0	7.7	92.3
		ph7	rim	Kf	0	6.4	93.6
		ph8	core	Kf	0	10.13	89.87
C4685	cgpog	ph1	rim	Ab	1.6	98.4	0
		ph1	core	Ab	1.6	98.4	0
		ph2	rim	Ab	1.9	98.1	0
		ph3	int	Ab	2.0	97.3	0.7
		ph3	rim	Ab	2.8	97.2	0
		ph4	rim	Ab	2.6	96.3	1.1
		ph5	rim	Ab	4.1	95.9	0
		ph6	rim	Kf	0	8.5	91.5
		ph7	core	Kf	0	7.7	92.3
		ph8	rim	Kf	0	13.1	86.9
C4689	rg	ph1	core	Ab	2.2	97.8	0
		ph2	core	Ab	1.9	97.4	0.7
		ph3	core	Ab	0.8	93.2	6.0
		ph4	core	Ab	1.8	98.2	0
		sph	core	Ab	1.3	98.7	0
		ph5	rim	Ab	0	100	0
		pph	core	Kf	0	11.4	88.6
		pph	core	Kf	0	28.8	71.2
		pph	core	Kf	0	20.8	79.2
		ph6	core	Kf	0	2.5	97.5
		ph7	rim	Kf	0	18.3	81.7

		ph8	rim	Kf	0	9.0	91.0
		meg1	core	Kf	0.36	7.53	92.10
		meg1	core	Kf	0.86	49.07	50.07
		meg1	rim	Kf	0.00	5.16	94.84
		rap1	core	Kf	0.5	26.8	72.7
		rap1		Olig	10.8	87.5	1.7
		rap1		Kf	0	23.1	76.9
		rap1		Ab	0	100	0
		rap1		Ab	10	86.6	3.3
		rap1	rim	Kf	0	7.6	92.4
C4697	felvol	mph1		Olig	28.6	68.9	2.5
		over		Kf	0.5	19.5	80.0
		mph2		Olig	28.4	68.8	2.7
		g		Olig	28.3	70.1	1.6
		mph3	core	Olig	27.0	69.9	3.1
		mph3	int	Olig	27.5	70.1	2.5
		mph3	rim	Andes	35.1	72.6	2.3
C4699	vcgrog	ph1	rim	Olig	13.9	85.4	0.7
		ph1	core	Olig	15.3	84.7	0
		ph1	core	Ab	8.8	91.2	0
		ph2	core	Olig	19.4	80.6	0
		ph2	int	Olig	18.6	81.4	0
		ph2	rim	Olig	18.0	82.0	0
		ph3	core	Ab	8.2	91.8	0
		ph3	rim	Ab	2.7	97.3	0
		ph4	core	Olig	15.4	84.6	0
		ph4	rim	Olig	16.4	82.9	0.7
		ph5	core	Kf	0	11.8	88.2
		ph5	rim	Kf	0	11.3	88.7
		ph6	core	Kf	0	4.9	95.1
		ph6	rim	Kf	0	4.9	95.1
C4701	vcgrog	ph1	rim	Olig	14.9	84.7	0.4
		ph1	core	Olig	20.9	78.4	0.7
		ph2	rim	Olig	16.0	84.0	0
		ph2	core	Olig	18.5	80.5	0.9
		ph3	core	Kf	0	8.1	91.9
		ph3	rim	Kf	0	5.9	94.1
		sph1	core	Olig	18.7	81.3	0
		sph1	rim	Olig	17.0	73.8	9.1
		ph4	core	Olig	17.3	82.0	0.7
		ph4	core	Olig	16.8	82.7	0.5
		ph4	rim	Olig	13.0	81.1	5.8
		ph5	core	Olig	20.2	78.0	1.8
		ph5	rim	Olig	17.6	81.8	0.6
		unh	core	Olig	11.4	88.1	0.5
		sph2		Kf	0	4.8	95.2
		ph6	core	Kf	0	5.9	94.1
		ph6	rim		0	4.3	95.7
C4717	megm	ph1	core	andes	33.26	66.50	0.24
		ph1	rim	andes	32.21	67.66	0.13
		ph2	core	Lab	55.91	43.80	0.28
		ph2	rim	Lab	54.68	44.74	0.58
		ph3	core	Andes	46.83	53.17	0.00
		ph3	rim	Andes	37.02	62.98	0.00
C4728	porprhy	ph1	core	Ab	0.4	99.6	0
	(meg)	mph1		Kf	0	11.1	88.9
		mph2		Ab	1.8	95.3	3.0

		mph3		Ab	5.4	92.6	2.0
		ph2	core	Ab	1.3	97.5	1.2
		mph4		Ab	2.5	83.7	13.8
		mph5		Kf	0	5.7	94.3
		mph6		Ab	2.4	96.9	0.6
C4737	rrhy	rap1	core	Kf	0.00	3.47	96.53
		rap1	rim	Ab	1.15	98.85	0.00
		rap2	core	Kf	0.00	4.91	95.09
		rap2	core	Olig	12.16	86.90	0.95
		rap2	rim	Kf	1.55	52.57	45.89
C4863A	rg	ph1	core	Ab	0.9	98.0	1.1
		ph2	rim	Ab	1.0	98.5	0.5
		ph3	core	Ab	0.8	74.2	25.0
		ph4	rim	Ab	1.7	98.3	0
		ph5	int	Kf	0	3.6	96.4
		ph6	core	Ab	2.96	97.04	0.00
		ph6	rim	Ab	1.37	98.27	0.36
		rap1	core	Kf	0.54	47.55	51.91
		rap1		Ab	2.82	96.94	0.24
		rap1		Kf	0.26	9.19	90.54
		rap1	rim	Olig	15.24	84.41	0.35

NOTES

1. The abbreviations for rock types in this Table are as in Appendix 1.
2. ph=phenocryst; mph=microphenocryst; g=groundmass; unh=unhedral; l=large; s=small; pph=perthite; rap=crystal with rapakivi texture; over=overgrowth; meg=megacryst.
3. Ab=albite; Kf=K-feldspar; Olig=Oligoclase; Andes=andesine; Lab=Labradorite.

Table 5. Representative electron microprobe analyses of biotite

Sample	C4678	C4681		C4689		C4697				
Lithol.	di	cgpog	rg		felvol					
Pos.	inc in hb	phc	phr in hb	over r	clot	mph	mph	gr	mph	gr
SiO_2	36.30	37.01	34.55	35.10	36.52	36.37	36.70	36.30	36.40	36.59
TiO_2	1.23	1.60	0.67	0.78	1.01	4.38	4.30	4.22	4.70	4.50
Al_2O_3	15.51	12.29	14.11	14.31	14.44	14.69	14.62	14.67	14.67	14.80
FeO_t	23.07	26.24	26.94	27.60	26.41	18.33	19.30	19.57	17.74	17.64
MnO	0.00	0.38	0.42	0.33	0.31	0.22	0.26	0.33	0.27	0.26
MgO	8.88	8.10	7.32	7.01	6.66	11.28	10.83	10.87	11.92	12.10
CaO	0.00	0.69	0.33	0.58	0.00	0.00	0.00	0.00	0.00	0.00
Na_2O	0.16	0.36	0.35	0.00	0.00	0.43	0.30	0.36	0.36	0.40
K_2O	9.19	8.67	5.82	8.24	8.94	9.47	9.50	9.30	9.18	9.36
Total	94.34	95.34	90.51	93.95	94.29	95.17	95.81	95.62	95.24	95.65
Atomic Formulae (Number of oxygen 22)										
Si	5.687	5.853	5.704	5.663	5.819	5.553	5.585	5.545	5.529	5.533
Ti	0.145	0.190	0.083	0.095	0.121	0.503	0.492	0.485	0.537	0.512
Al	2.865	2.291	2.746	2.722	2.712	2.644	2.623	2.642	2.627	2.638
Fe''	3.023	3.470	3.720	3.724	3.519	2.341	2.456	2.500	2.253	2.231
Mn	0.000	0.051	0.059	0.045	0.042	0.028	0.034	0.043	0.035	0.033
Mg	2.073	1.909	1.801	1.685	1.582	2.567	2.456	2.475	2.698	2.727
Ca	0.000	0.117	0.058	0.100	0.000	0.000	0.000	0.000	0.000	0.000
Na	0.049	0.110	0.112	0.000	0.000	0.127	0.089	0.107	0.106	0.117
K	1.837	1.749	1.226	1.696	1.817	1.845	1.844	1.812	1.779	1.806

Sample	C4697			C4699						
Lithol.	felvol			vcgrog						
Pos.	gr	mphc	mphr	phlc	phli	phlr	phlr	phlr	lath	lath
									stringer	
SiO_2	36.59	36.63	36.17	39.56	36.14	36.81	36.78	36.36	37.07	37.30
TiO_2	4.11	4.55	4.36	2.05	2.21	1.90	1.73	2.26	2.30	2.10
Al_2O_3	14.66	14.50	14.37	21.16	16.48	16.58	17.32	15.97	16.45	17.20
FeO_t	19.07	18.32	18.87	15.96	21.56	20.96	20.51	22.71	21.60	20.72
MnO	0.44	0.34	0.23	0.00	0.00	0.00	0.00	0.00	0.00	0.00
MgO	10.77	11.39	11.02	5.54	7.69	8.13	7.70	7.63	8.06	8.36
CaO	0.00	0.00	0.00	0.00	0.00	0.00	0.23	0.00	0.00	0.00
Na_2O	0.32	0.37	0.36	0.00	0.00	0.27	0.26	0.00	0.00	0.26
K_2O	9.55	9.59	9.71	7.45	8.63	8.44	7.79	8.95	9.47	9.61
Total	95.51	95.69	95.09	91.72	92.71	93.09	92.32	93.88	94.95	95.55
Atomic formulae (Number of oxygen 22)										
Si	5.588	5.565	5.555	5.962	5.690	5.740	5.743	5.696	5.711	5.685
Ti	0.472	0.520	0.504	0.232	0.262	0.223	0.203	0.266	0.266	0.241
Al	2.639	2.597	2.602	3.760	3.059	3.048	3.189	2.949	2.988	3.091
Fe''	2.436	2.328	2.424	2.012	2.839	2.733	2.679	2.975	2.783	2.641
Mn	0.057	0.044	0.030	0.000	0.000	0.000	0.000	0.000	0.000	0.000
Mg	2.451	2.579	2.522	1.244	1.804	1.889	1.792	1.781	1.851	1.899
Ca	0.000	0.000	0.000	0.000	0.000	0.000	0.038	0.000	0.000	0.000
Na	0.095	0.109	0.107	0.000	0.000	0.082	0.079	0.000	0.000	0.077
K	1.861	1.859	1.902	1.432	1.733	1.679	1.552	1.789	1.861	1.869

Table 5 (continued)

Sample	C4699							C4701		
Lithol.	vcgrog							vcgrog		
Pos.	lath	lath	grain	ph2c	ph2r	ph2r	ph2c	ph1r	ph1c	ph2c
		stringer								
SiO_2	36.78	36.35	36.30	36.35	36.34	37.03	36.83	36.90	35.89	36.59
TiO_2	2.47	2.68	2.44	2.70	2.40	2.50	3.18	2.80	1.62	3.04
Al_2O_3	15.60	15.84	16.37	14.99	16.11	15.77	15.38	14.85	16.56	15.00
FeO_t	23.20	22.21	21.84	23.73	22.54	22.62	22.86	22.13	22.36	22.71
MnO	0.00	0.00	0.00	0.00	0.00	0.00	0.00	0.00	0.00	0.00
MgO	8.08	7.74	7.72	7.42	7.71	8.01	7.88	8.62	9.03	8.10
CaO	0.00	0.00	0.00	0.00	0.00	0.00	0.00	0.00	0.00	0.00
Na_2O	0.00	0.00	0.00	0.00	0.00	0.00	0.00	0.26	0.00	0.00
K_2O	9.28	9.08	9.21	9.48	9.53	9.45	9.58	9.37	9.45	9.58
Total	95.41	93.90	93.88	94.67	94.63	95.38	95.71	94.93	94.91	95.02
Atomic Formulae (Number of oxygen 22)										
Si	5.689	5.686	5.669	5.703	5.662	5.713	5.681	5.723	5.573	5.691
Ti	0.287	0.315	0.287	0.319	0.281	0.290	0.369	0.327	0.189	0.356
Al	2.845	2.921	3.014	2.773	2.959	2.868	2.797	2.715	3.031	2.750
Fe''	3.001	2.906	2.853	3.114	2.937	2.919	2.949	2.870	2.904	2.954
Mn	0.000	0.000	0.000	0.000	0.000	0.000	0.000	0.000	0.000	0.000
Mg	1.863	1.804	1.797	1.735	1.790	1.842	1.812	1.992	2.090	1.877
Ca	0.000	0.000	0.000	0.000	0.000	0.000	0.000	0.000	0.000	0.000
Na	0.000	0.000	0.000	0.000	0.000	0.000	0.000	0.078	0.000	0.000
K	1.831	1.812	1.835	1.898	1.894	1.860	1.885	1.854	1.872	1.901

Sample	C4701									
Lithol.	vcgrog									
	ph2r	lath	lath	lath	ph3r	ph3r	ph3c	lath	lath	c
		stringer					str	str	str	
SiO_2	36.91	37.50	37.24	36.51	36.47	37.43	37.37	52.91	38.71	36.94
TiO_2	2.79	1.63	1.96	2.03	2.11	2.40	2.88	1.11	1.85	2.37
Al_2O_3	15.31	19.75	18.71	16.91	17.17	17.02	16.04	12.42	16.88	16.06
FeO_t	21.53	17.81	18.02	18.76	20.39	19.70	20.72	16.12	19.04	20.90
MnO	0.00	0.00	0.00	0.00	0.18	0.00	0.00	0.00	0.00	0.00
MgO	9.12	8.23	8.79	8.95	9.35	9.03	9.17	6.13	9.00	9.22
CaO	0.00	0.00	0.00	0.00	0.00	0.00	0.00	0.00	0.00	0.00
Na_2O	0.00	0.22	0.00	0.26	0.19	0.00	0.26	0.00	0.00	0.00
K_2O	9.78	8.96	9.15	8.22	8.90	9.57	9.67	5.84	9.52	9.34
Total	95.44	94.10	93.87	91.64	94.76	95.15	96.11	94.53	95.00	94.83
Atomic Formulae (Number of oxygen 22)										
Si	5.681	5.671	5.669	5.717	5.592	5.695	5.676	7.471	5.855	5.682
Ti	0.323	0.185	0.224	0.239	0.243	0.275	0.329	0.118	0.210	0.274
Al	2.778	3.521	3.358	3.122	3.104	3.053	2.872	2.068	3.010	2.912
Fe''	2.772	2.253	2.294	2.457	2.615	2.507	2.632	1.904	2.408	2.689
Mn	0.000	0.000	0.000	0.000	0.023	0.000	0.000	0.000	0.000	0.000
Mg	2.092	1.855	1.994	2.089	2.137	2.047	2.076	1.290	2.029	2.114
Ca	0.000	0.000	0.000	0.000	0.000	0.000	0.000	0.000	0.000	0.000
Na	0.000	0.065	0.000	0.079	0.056	0.000	0.077	0.000	0.000	0.000
K	1.921	1.729	1.777	1.642	1.741	1.858	1.874	1.052	1.837	1.833

Table 5 (continued)

Sample	C4701			C4863A			
Lithol.	vcgrog			rg			
Pos.	r	c	r	over	over	phc	mphc
	str	stringer		on feld			
SiO_2	36.76	37.35	36.71	33.32	33.87	37.90	36.06
TiO_2	2.17	1.23	1.46	2.65	1.11	0.92	0.89
Al_2O_3	17.10	16.85	17.23	14.72	16.21	15.95	16.28
FeO_t	19.74	19.75	20.63	24.87	25.01	21.00	22.27
MnO	0.00	0.00	0.00	0.00	0.00	0.00	0.00
MgO	8.73	9.77	9.16	8.13	9.06	9.35	9.40
CaO	0.00	0.00	0.00	1.95	0.00	0.00	0.00
Na_2O	0.00	0.00	0.00	0.20	0.22	0.23	0.22
K_2O	8.92	9.10	9.24	5.04	5.42	8.69	8.38
Total	93.42	94.05	94.43	90.88	90.90	94.04	93.50
Atomic Formulae (Number of oxygen 22)							
Si	5.686	5.737	5.652	5.427	5.472	5.845	5.649
Ti	0.252	0.142	0.169	0.325	0.135	0.107	0.105
Al	3.118	3.051	3.128	2.827	3.088	2.900	3.007
Fe''	2.554	2.537	2.657	3.388	3.379	2.709	2.918
Mn	0.000	0.000	0.000	0.000	0.000	0.000	0.000
Mg	2.012	2.236	2.102	1.973	2.182	2.149	2.195
Ca	0.000	0.000	0.000	0.340	0.000	0.000	0.000
Na	0.000	0.000	0.000	0.063	0.069	0.069	0.067
K	1.760	1.783	1.815	1.047	1.117	1.710	1.675

Abreviations for this and all subsequent mineral chemical analyses tables are as follows: inc=inclusion; ph=phenocryst; mph=microphenocryst; gr=groundmass; c=core; r=rim; i=intermediate; over=overgrowth; str=stringer; s=small; hb=hornblende

Table 6. Representative electron microprobe analyses of amphiboles

Sample	C4678									
Lithol.	di									
Pos.	ph1c	ph1r	sph2c	sph2r	mph1c	mph1r	ph3c	ph3r	sph4c	sph4r
SiO_2	46.65	46.05	46.54	46.91	46.41	46.93	47.83	46.21	46.18	47.16
TiO_2	1.10	1.32	1.50	1.53	1.22	1.33	1.18	1.49	1.53	1.45
Al_2O_3	5.49	5.75	5.99	5.86	6.34	5.95	5.21	6.09	5.96	5.72
FeO_t	18.94	18.34	19.28	19.41	18.78	18.71	18.61	19.04	19.25	18.94
MnO	0.40	0.37	0.46	0.45	0.34	0.49	0.39	0.26	0.40	0.48
MgO	11.16	11.15	10.82	11.94	10.69	10.90	10.95	10.87	10.53	11.14
CaO	10.53	10.49	10.56	10.64	10.88	10.59	11.13	10.86	10.73	10.55
Na_2O	1.73	1.85	1.64	1.70	1.59	1.64	1.41	1.71	1.76	1.67
K_2O	0.68	0.59	0.63	0.72	0.66	0.65	0.55	0.68	0.68	0.65
Total	96.68	95.91	97.42	99.16	96.91	97.19	97.26	97.21	97.02	97.76
Atomic Formulae (Number of oxygen 23)										
Si	7.112	7.064	7.048	6.988	7.050	7.099	7.213	7.015	7.035	7.099
Ti	0.126	0.152	0.171	0.171	0.139	0.151	0.134	0.170	0.175	0.164
Al	0.987	1.040	1.069	1.029	1.135	1.061	0.926	1.090	1.070	1.015
Fe''	2.415	2.353	2.442	2.418	2.386	2.367	2.347	2.417	2.453	2.384
Mn	0.052	0.048	0.059	0.057	0.044	0.063	0.050	0.033	0.052	0.061
Mg	2.536	2.549	2.442	2.651	2.420	2.457	2.461	2.459	2.391	2.499
Ca	1.720	1.724	1.714	1.698	1.771	1.717	1.799	1.767	1.752	1.702
Na	0.511	0.550	0.482	0.491	0.468	0.481	0.412	0.503	0.520	0.487
K	0.132	0.115	0.122	0.137	0.128	0.125	0.106	0.132	0.132	0.125
P^1(kb)	1.69	1.94	2.08	1.89	2.39	2.04	1.40	2.18	2.08	1.82

Sample	C4678						C4678			
Lithol.	di						gr			
Pos.	sph4r	ph5c	ph5r	ph5r	mph2c	mph2r	ph1c	ph1r	mph	ph1i
SiO_2	46.51	46.62	45.27	46.25	47.14	47.10	47.21	46.76	52.59	49.71
TiO_2	1.48	1.48	2.39	1.58	1.40	1.09	0.77	1.37	0.00	0.90
Al_2O_3	5.83	5.91	5.27	6.20	5.72	5.75	6.21	6.00	2.17	3.83
FeO_t	18.15	19.08	18.69	19.11	19.15	19.19	18.20	19.30	18.95	17.62
MnO	0.49	0.50	0.62	0.48	0.46	0.39	0.33	0.39	0.34	0.53
MgO	11.49	10.90	10.70	10.84	11.42	11.06	10.13	10.43	11.06	12.42
CaO	10.54	10.86	10.52	10.81	10.60	10.70	9.97	10.94	12.52	10.83
Na_2O	1.78	1.66	1.46	1.79	1.68	1.43	1.03	1.59	0.24	1.19
K_2O	0.61	0.57	0.56	0.71	0.70	0.72	0.44	0.66	0.30	0.38
Total	96.88	97.58	95.48	97.77	98.27	97.43	94.29	97.44	98.17	97.41
Atomic Formulae (Number of oxygen 23)										
Si	7.052	7.047	7.007	6.991	7.070	7.118	7.282	7.081	7.780	7.413
Ti	0.169	0.168	0.278	0.180	0.158	0.124	0.089	0.156	0.000	0.101
Al	1.042	1.053	0.962	1.105	1.011	1.025	1.129	1.071	0.378	0.673
Fe''	2.302	2.412	2.419	2.416	2.402	2.426	2.348	2.444	2.344	2.197
Mn	0.063	0.064	0.081	0.061	0.058	0.050	0.043	0.050	0.043	0.067
Mg	2.597	2.456	2.468	2.442	2.553	2.491	2.329	2.354	2.438	2.760
Ca	1.712	1.759	1.745	1.751	1.703	1.733	1.648	1.775	1.985	1.730
Na	0.523	0.487	0.438	0.525	0.489	0.419	0.308	0.467	0.069	0.344
K	0.118	0.110	0.111	0.137	0.134	0.139	0.087	0.128	0.057	0.072
P(kb)	1.95	2.00	1.57	2.25	1.80	1.87	2.36	2.09	-	0.19

[1] Pressure estimates using method of Schmidt (1992)

Table 6 (continued)

Sample	C4678		C4681						C4685	
Lithol.	gr		cgpog						rg	
Pos.	ph2c	ph2r	ph1c	ph1c	ph1r	ph2c	ph2r	ph3r	ph1c	ph1r
SiO_2	46.39	45.99	44.23	43.17	42.99	44.61	44.31	43.80	45.61	45.55
TiO_2	1.35	1.66	1.15	0.40	1.42	1.61	1.42	1.53	1.34	1.49
Al_2O_3	6.24	6.08	6.28	7.33	6.83	6.39	6.35	6.73	6.18	6.39
FeO_t	19.01	19.30	26.37	27.95	26.04	25.13	24.35	24.83	20.56	20.57
MnO	0.41	0.52	0.66	0.70	0.66	0.63	0.69	0.71	0.41	0.50
MgO	10.57	10.63	5.29	4.25	5.15	6.39	6.56	6.36	9.60	9.78
CaO	10.94	10.71	10.64	11.18	10.75	10.56	10.26	10.55	10.86	10.67
Na_2O	1.42	1.75	1.66	1.22	2.25	1.79	2.04	2.27	1.71	2.05
K_2O	0.70	0.70	0.86	0.93	0.98	0.82	0.82	0.93	0.78	0.75
Total	97.03	97.34	97.14	97.13	97.07	97.93	96.80	97.71	97.05	97.75
Number of oxygen 23										
Si	7.048	6.993	6.999	6.897	6.841	6.952	6.971	6.865	7.003	6.950
Ti	0.154	0.190	0.137	0.048	0.170	0.189	0.168	0.180	0.155	0.171
Al	1.118	1.090	1.172	1.381	1.281	1.174	1.178	1.244	1.119	1.149
Fe''	2.415	2.454	3.490	3.735	3.466	3.275	3.204	3.255	2.640	2.625
Mn	0.053	0.067	0.088	0.095	0.089	0.083	0.092	0.094	0.053	0.065
Mg	2.393	2.409	1.248	1.012	1.221	1.484	1.538	1.486	2.197	2.224
Ca	1.781	1.745	1.804	1.914	1.833	1.763	1.729	1.772	1.787	1.744
Na	0.418	0.516	0.509	0.378	0.694	0.541	0.622	0.690	0.509	0.606
K	0.136	0.136	0.174	0.190	0.199	0.163	0.165	0.186	0.153	0.146
P(kb)	2.31	2.18	2.57	3.56	3.09	2.58	2.60	2.91	2.32	2.46

Sample	C4685									
Lithol.	rg									
Pos.	ph2c	ph2r	ph3c	ph3r	ph3r	ph4c	ph4r	ph5c	ph5r	ph5r
SiO_2	45.24	45.59	45.99	45.61	45.42	40.64	46.29	46.13	45.60	46.57
TiO_2	1.56	1.33	1.42	1.50	1.41	0.00	1.09	1.29	1.58	1.14
Al_2O_3	6.42	6.19	5.91	6.31	6.63	10.89	5.56	6.17	6.22	4.76
FeO_t	20.84	20.57	21.19	20.65	20.76	26.79	20.54	21.15	20.66	22.45
MnO	0.59	0.50	0.54	0.54	0.44	0.32	0.46	0.50	0.49	0.47
MgO	9.61	9.90	9.28	10.04	9.73	4.21	10.23	9.41	9.72	9.70
CaO	10.74	10.78	10.53	10.79	10.45	11.73	10.56	10.26	10.60	10.91
Na_2O	1.92	1.93	1.54	2.09	1.71	1.27	2.05	1.43	2.01	1.35
K_2O	0.85	0.85	0.86	0.75	0.82	1.35	0.70	0.73	0.81	0.63
Total	97.77	97.64	97.26	98.28	97.37	97.20	97.48	97.07	97.69	97.98
Atomic Formulae (Number of oxygen 23)										
Si	6.921	6.969	7.056	6.929	6.951	6.484	7.069	7.069	6.965	7.126
Ti	0.179	0.153	0.164	0.171	0.162	0.000	0.125	0.149	0.181	0.131
Al	1.158	1.115	1.069	1.130	1.196	2.048	1.001	1.115	1.120	0.859
Fe''	2.666	2.630	2.719	2.624	2.657	3.575	2.623	2.711	2.639	2.873
Mn	0.076	0.065	0.070	0.069	0.057	0.043	0.060	0.065	0.063	0.061
Mg	2.191	2.255	2.122	2.273	2.219	1.001	2.328	2.149	2.213	2.212
Ca	1.761	1.766	1.731	1.756	1.713	2.005	1.728	1.685	1.735	1.789
Na	0.570	0.572	0.458	0.616	0.507	0.393	0.607	0.425	0.595	0.401
K	0.166	0.166	0.168	0.145	0.160	0.275	0.136	0.143	0.158	0.123
P(kb)	2.50	2.30	2.08	2.37	2.68	6.74	1.75	2.30	2.32	1.08

Table 6 (continued)

Sample	C4685					C4689				
Lithol.	rg					rg				
Pos.	ph6r	ph7r	ph7i	ph7c		ph1r	ph1c	ph1r	ph1r	clotr
SiO_2	45.65	45.24	44.83	45.67	45.69	43.17	42.78	41.79	43.55	43.54
TiO_2	1.38	1.41	1.47	1.35	1.54	1.39	1.13	1.24	1.63	1.38
Al_2O_3	6.35	6.16	6.10	6.64	6.03	6.83	6.77	7.03	6.78	6.47
FeO_t	20.70	21.09	21.19	21.89	20.70	25.18	25.28	25.37	25.02	24.72
MnO	0.48	0.73	0.52	0.42	0.53	0.66	0.62	0.57	0.57	0.68
MgO	9.37	9.59	9.35	9.34	9.79	6.17	5.95	5.89	6.10	6.68
CaO	10.90	10.27	10.42	10.52	10.62	10.49	10.37	10.55	10.44	10.52
Na_2O	1.85	1.93	1.89	2.05	1.92	2.41	2.44	2.35	2.55	2.44
K_2O	0.83	0.81	0.83	0.81	0.84	0.99	1.14	1.14	0.99	1.07
Total	97.51	97.23	96.60	98.69	97.66	97.29	96.48	95.93	97.63	97.50
Atomic Formulae (Number of oxygen 23)										
Si	6.986	6.963	6.954	6.935	6.983	6.823	6.834	6.737	6.845	6.853
Ti	0.159	0.163	0.171	0.154	0.177	0.165	0.136	0.150	0.193	0.163
Al	1.146	1.118	1.115	1.189	1.087	1.273	1.275	1.336	1.256	1.201
Fe''	2.649	2.715	2.749	2.780	2.646	3.328	3.378	3.421	3.289	3.254
Mn	0.062	0.095	0.068	0.054	0.069	0.088	0.084	0.078	0.076	0.091
Mg	2.137	2.200	2.161	2.114	2.230	1.453	1.417	1.415	1.429	1.567
Ca	1.787	1.694	1.732	1.712	1.739	1.776	1.775	1.822	1.758	1.774
Na	0.549	0.576	0.568	0.604	0.569	0.739	0.756	0.735	0.777	0.745
K	0.162	0.159	0.164	0.157	0.164	0.200	0.232	0.234	0.199	0.215
P(kb)	2.44	2.31	2.30	2.65	2.16	3.05	3.06	3.35	2.97	2.71

Sample	C4689						
Lithol.	rg						
Pos.	ph2c	ph2r	mph	ph2c	sph3c	sph3r	ph2r
SiO_2	44.84	44.27	44.35	44.92	44.17	43.59	43.66
TiO_2	1.37	1.73	1.36	1.27	0.00	1.66	1.46
Al_2O_3	5.94	6.22	6.16	5.98	6.81	6.27	6.45
FeO_t	22.27	23.56	23.73	23.06	26.64	24.79	24.36
MnO	0.62	0.71	0.56	0.41	0.77	0.51	0.55
MgO	8.52	7.02	6.97	7.96	5.09	6.44	6.21
CaO	10.20	10.42	10.50	10.33	11.54	10.47	10.60
Na_2O	2.52	2.67	2.63	2.49	1.16	2.20	2.43
K_2O	0.81	0.82	0.86	0.83	0.95	0.90	0.95
Total	97.09	97.42	97.12	97.25	97.13	96.83	96.67
Atomic Formulae (Number of oxygen 23)							
Si	6.969	6.918	6.953	6.989	7.006	6.893	6.909
Ti	0.160	0.203	0.160	0.149	0.000	0.197	0.174
Al	1.088	1.146	1.139	1.097	1.274	1.169	1.203
Fe''	2.895	3.079	3.112	3.000	3.534	3.278	3.224
Mn	0.082	0.094	0.074	0.054	0.103	0.068	0.074
Mg	1.974	1.635	1.629	1.846	1.203	1.518	1.465
Ca	1.699	1.745	1.764	1.722	1.961	1.774	1.797
Na	0.759	0.809	0.800	0.751	0.357	0.675	0.746
K	0.161	0.163	0.172	0.165	0.192	0.182	0.192
P(kb)	2.17	2.44	2.41	2.21	3.05	2.55	2.72

Table 6 (continued)

Sample	C4674					C4717				
Lithol.	megm					megm				
Pos.	c	c	r	c	r	c	r	c	c	r
SiO_2	49.19	47.63	44.77	48.09	48.05	48.43	45.71	51.07	50.06	50.29
TiO_2	0.87	1.38	0.95	1.22	1.24	0.60	0.66	0.19	0.42	0.46
Al_2O_3	4.17	5.22	10.71	4.60	4.40	6.30	8.72	2.89	5.49	4.93
Cr_2O_3	0.05	0.03	0.05	0.04	0.03	0.02	0.02	0.02	0.00	0.00
FeO_t	18.30	18.79	17.40	18.81	19.17	15.81	17.95	23.02	14.78	14.32
MnO	0.28	0.20	0.22	0.22	0.28	0.17	0.17	0.23	0.25	0.26
MgO	12.22	11.92	7.30	11.66	11.49	12.54	10.55	8.50	13.68	14.10
CaO	11.42	11.02	14.37	10.80	10.97	12.38	12.14	6.89	12.31	12.26
Na_2O	0.95	1.30	0.79	1.13	1.09	0.73	0.97	3.49	0.65	0.65
K_2O	0.34	0.49	0.33	0.37	0.37	0.20	0.56	0.13	0.22	0.18
Total	97.79	97.98	96.89	96.94	97.09	97.18	97.45	96.43	97.86	97.45
Atomic Formulae (Number of oxygen 23)										
Si	7.335	7.131	6.776	7.258	7.260	7.183	6.870	7.803	7.316	7.363
Ti	0.098	0.155	0.108	0.138	0.141	0.067	0.075	0.022	0.046	0.051
Al	0.733	0.921	1.911	0.818	0.784	1.102	1.545	0.521	0.946	0.851
Cr	0.006	0.004	0.006	0.005	0.004	0.002	0.002	0.002	0.000	0.000
Fe''	2.282	2.353	2.203	2.374	2.422	1.961	2.256	2.942	1.806	1.754
Mn	0.035	0.025	0.028	0.028	0.036	0.021	0.022	0.030	0.031	0.032
Mg	2.716	2.660	1.647	2.623	2.587	2.772	2.363	1.936	2.979	3.077
Ca	1.825	1.768	2.331	1.747	1.776	1.967	1.955	1.128	1.928	1.923
Na	0.275	0.377	0.232	0.331	0.319	0.210	0.283	1.034	0.184	0.185
K	0.065	0.094	0.064	0.071	0.071	0.038	0.107	0.025	0.041	0.034
P(kb)	0.48	1.37	6.09	0.88	0.72	2.24	4.34	-	1.49	1.04

Sample	C4717				C4751			C4810		
Lithol.	megm				cd			gd		
Pos.	c	c	c	r	c	r	c	c	r	c
SiO_2	49.95	49.38	46.89	48.71	41.47	44.64	52.70	47.58	47.87	48.65
TiO_2	0.14	0.77	0.95	0.73	4.53	2.98	0.44	1.14	1.25	0.76
Al_2O_3	5.85	5.72	7.39	6.30	11.46	10.45	2.26	5.00	5.18	5.02
Cr_2O_3	0.00	0.00	0.04	0.00	0.28	0.23	0.24	0.00	0.00	0.00
FeO_t	15.27	15.06	16.34	15.56	12.56	12.07	10.17	19.58	19.37	18.68
MnO	0.19	0.24	0.22	0.19	0.11	0.10	0.20	0.27	0.25	0.30
MgO	13.37	13.42	12.61	12.80	12.84	13.87	15.14	11.06	11.20	11.61
CaO	12.60	12.40	9.42	12.37	11.72	11.96	18.33	11.01	11.09	11.44
Na_2O	0.67	0.80	0.83	0.73	2.65	1.79	0.28	1.35	1.38	0.99
K_2O	0.18	0.31	2.37	0.31	0.38	0.37	0.00	0.45	0.48	0.47
Total	98.22	98.10	97.06	97.70	98.00	98.46	99.76	97.44	98.07	97.92
Atomic Formulae (Number of oxygen 23)										
Si	7.291	7.230	7.031	7.178	6.136	6.492	7.506	7.190	7.177	7.265
Ti	0.015	0.085	0.107	0.081	0.504	0.326	0.047	0.130	0.141	0.085
Al	1.007	0.987	1.306	1.095	1.999	1.792	0.379	0.891	0.916	0.884
Cr	0.000	0.000	0.005	0.000	0.033	0.026	0.027	0.000	0.000	0.000
Fe''	1.864	1.844	2.049	1.918	1.554	1.468	1.211	2.475	2.429	2.333
Mn	0.023	0.030	0.028	0.024	0.014	0.012	0.024	0.035	0.032	0.038
Mg	2.908	2.928	2.818	2.811	2.831	3.006	3.214	2.491	2.502	2.584
Ca	1.971	1.945	1.514	1.953	1.858	1.864	2.797	1.783	1.782	1.831
Na	0.190	0.227	0.241	0.209	0.760	0.505	0.077	0.396	0.401	0.287
K	0.034	0.058	0.453	0.058	0.072	0.069	0.000	0.087	0.092	0.090
P(kb)	1.78	1.69	3.21	2.20	6.50	5.52	-	1.23	1.35	1.20

Table 6 (continued)

Sample	C4810	
Lithol.	gd	
Pos.	c	r
SiO_2	47.82	47.93
TiO_2	1.40	1.44
Al_2O_3	5.34	5.79
Cr_2O_3	0.00	0.00
FeO	19.26	18.88
MnO	0.27	0.29
MgO	11.08	11.34
CaO	11.33	10.95
Na_2O	1.40	1.36
K_2O	0.54	0.63
Total	98.44	98.61

Atomic Formulae (Number of oxygen 23)

Si	7.148	7.128
Ti	0.157	0.161
Al	0.941	1.015
Cr	0.000	0.000
Fe''	2.408	2.348
Mn	0.034	0.037
Mg	2.468	2.513
Ca	1.815	1.745
Na	0.406	0.392
K	0.103	0.120
P(kb)	1.47	1.82

Table 7: Representative electron microprobe analyses of clinopyroxene

Sample	C4751			C4752	
Lithol.	cd			cd	
Position	gr1c	gr1r	gr2r	gr1c	gr1r
SiO_2	52.53	52.33	51.69	51.91	51.65
TiO_2	0.63	0.65	0.72	0.80	0.61
Al_2O_3	1.56	1.54	2.46	1.98	2.05
FeO_t	9.55	9.76	7.53	8.43	8.51
MnO	0.25	0.30	0.18	0.26	0.20
MgO	14.66	14.35	14.79	14.17	14.60
CaO	21.87	21.75	22.81	22.64	22.09
Na_2O	0.38	0.44	0.31	0.36	0.35
Total	101.44	101.12	100.57	100.56	100.08

Note:
gr=grain; c=core; r=rim

Table 8. Representative electron microprobe analyses of zircons

Sample	C4681				C4863A	
Lithol.		cgpog				rg
	1	2	3	4	5	6
SiO_2	32.25	32.64	32.84	31.66	32.46	31.76
Al_2O_3	0.88	0.30	-	-	-	-
FeO_t	2.58	o.64	-	0.32	-	0.58
MgO	0.30	0.18	-	0.15	-	-
ZrO_2	64.45	66.37	67.78	64.57	67.44	64.56
Y_2O_3	-	-	-	1.63	-	1.12
Total	100.46	100.13	100.62	99.33	99.90	98.04

NOTE
1,2,3: Dark zones (in reflected light); 4= light zone (in reflected light); 5= core (dark); 6= rim (light).

Table 9. Representative electron microprobe analyses of titanite

Sample	C4689						C4863A		C4681	
Lithol.		rg						rg		cgpog
	1	2	3	4	5	6	7	8	9	
SiO_2	31.44	31.37	30.95	30.52	30.52	30.60	30.16	29.94	32.81	
TiO_2	29.14	28.71	28.94	26.44	27.10	26.26	27.94	28.70	26.79	
Al_2O_3	5.01	5.34	5.03	5.30	4.73	5.43	3.57	3.25	4.57	
FeO_t	1.97	1.89	1.86	2.49	2.88	2.89	3.28	3.20	4.74	
MgO	-	-	0.24	0.18	0.24	0.20	0.50	0.35	0.49	
CaO	29.56	29.52	28.63	27.13	27.89	27.42	26.41	26.54	26.65	
F	1.70	1.86	1.74	1.45	1.49	1.94	1.34	1.19	n.d.	
Y_2O_3	1.08	1.33	1.88	3.91	2.24	3.28	2.64	2.65	n.d.	
Ce_2O_3	-	-	-	-	-	-	0.22	0.21	n.d.	
BaO	-	0.71	-	-	0.80	-	-	0.72	n.d.	
Total	99.90	100.73	99.27	97.42	97.89	98.02	96.06	96.75	96.05	

Table 10. Representative electron microprobe analyses of allanite

Sample	C4678	C4701
Litho.	meggd	vcgrog
SiO_2	30.76	31.28
TiO_2	1.98	2.61
Al_2O_3	11.83	11.96
FeO_t	15.78	16.11
MnO	0.13	0.24
MgO	1.20	0.61
CaO	10.08	8.19
ThO_2	0.25	0.94
Y_2O_3	0.29	0.12
La_2O_3	6.40	5.48
Ce_2O_3	13.62	12.37
Pr_2O_3	1.02	0.81
Nd_2O_3	3.44	3.31
Total	96.77	94.02

Table 11. Representative electron microprobe analyses of Fe-Ti oxides

Sample	C4697		
Lithol.	felvol		
	1	2	3
SiO_2	0.23	0.30	0.42
TiO_2	44.40	2.07	0.48
FeO_t	41.58	87.14	88.84
MnO	6.79	0.36	0.21
MgO	0.13	0.22	-
CaO	0.11	-	-
Total	93.24	90.09	89.95

Table 12. Representative electron microprobe analyses of chlorites

Sample	C4672			C4689	C4863A	
Lithol.	mgpg			rg	rg	
SiO_2	24.21	24.11	23.53	25.99	28.78	31.76
TiO_2	0.00	0.00	0.00	0.00	0.27	0.38
Al_2O_3	19.55	19.64	20.47	18.19	16.47	16.89
FeO_t	36.56	37.01	36.78	35.35	31.05	26.76
MnO	0.18	0.00	0.19	0.91	0.36	0.20
MgO	6.22	4.54	6.50	6.67	9.60	8.21
Na_2O	0.25	0.26	0.28	0.29	0.26	0.18
K_2O	0.00	0.08	0.00	0.14	0.59	3.02
Total	86.97	85.64	87.75	87.54	87.38	87.40
Atomic Formulae (Number of oxygen 28)						
Si	5.501	5.580	5.307	5.831	6.281	6.796
Ti	0.000	0.000	0.000	0.000	0.044	0.061
Al	5.237	5.359	5.443	4.812	4.238	4.261
Fe''	6.947	7.164	6.938	6.633	5.667	4.789
Mn	0.035	0.000	0.036	0.173	0.067	0.036
Mg	2.106	1.566	2.185	2.230	3.122	2.618
Na	0.110	0.117	0.122	0.126	0.110	0.075
K	0.000	0.024	0.000	0.040	0.164	0.824

Appendix 1. Catalogue of hand specimens

Sample	Name	Geochemical Analysis	Thin Section	Probe Section
4600	sprhy			+
4601	fgm	+	+	
4602	pm	+		+
4603	felvol			
4604	felvol		+	
4605	fgm	+	+	
4606	pm		+	
4607	felvol			
4608	gd		+	
4666	cgpog			
4667	gd			
4668	fgm			
4669	gd(m)	+	+	
4670*	rg	+	+	
4671	megm	+	+	
4672	mgpg	+	+	+
4673	gd	+	+	
4674	megdi	+	+	+
4675	meggd			
4676	gd			
4677	megm	+	+	
4678	meggd(contact bet. g+di)			+
4679	fgm	+	+	
4680	fgpg	+	+	
4681	cgpog	+	+	+
4682	m-cgm	+	+	
4683	rg			
4684	rg			
4685	rg	+	+	+
4686*	mgpg	+	+	
4687	gd	+	+	
4688	di	+	+	
4689*	rg	+	+	+
4690	rg	+	+	
4691	felvol	+	+	
4692	g	+	+	
4693	mgpg			
4694	rg	+	+	
4695	fgpg			
4696	cgpog			
4697	felvol	+	+	+
4698	myl(l)		+	
4699*	vcgrog	+	+	+
4700*	vcgrog	+	+	
4701	vcgrog	+	+	+
4702	gd	+	+	
4703	fgm	+	+	
4704	ggn	+	+	
4705**	fgpg	+	+	
4706	megggn	+	+	+
4707	vcgrog	+	+	
4708	vcgrog			
4709	fgm			
4710	gd		+	

4711	wggn			
4712	cgpog			
4713	gd	+	+	
4714	fgm	+	+	
4715	fgm			
4716	myl(d)		+	
4717	megm			+
4718	cd			
4719	megm			
4720	fgm			
4721+	vcgrog	+	+	
4728	megporrhy	+	+	+
4729	felvol			
4730	fgm			
4731	fgpg			
4732	fgm			
4733	fgm		+	
4734	fgm	+	+	
4735	cgpog	+	+	+
4736+	cgpog	+	+	
4737	rrhy	+	+	+
4738	fgpg(aplite)			
4739	porhrhy	+	+	
4740	cgpog			
4741	felvol			
4742	gd			
4743	felvol			
4744	felvol			
4745	felvol			
4746	gd			
4747	felvol			
4748	felvol	+	+	+
4749	m-cgm	+	+	
4750	cd	+	+	
4751	cd			+
4752	cd			+
4753	pm	+	+	
4754	m-cgm	+	+	
4755	megm	+	+	
4756	megm			
4757	megm			
4758	mgpg	+	+	
4759	fgm			
4760	felvol			
4761	mgpg	+	+	
4765	cd			
4766	gd			
4767	felvol			
4768	felvol		+	
4769	fgm			
4770	fgm		+	
4771	fgm		+	
4772	fgm			
4773	fgm			+
4774	fgm	+		+
4775	gd(min)?		+	
4776	myl(d)		+	
4777	fgm			
4778	myl(d)	+		+
4779	myldi	+		+
4780	porphrhy			
4781	felvol			

4782	felvol		+	
4783	felvol		+	
4784	felvol			
4785	felvol			
4786	fgm			
4787	rfelvol		+	
4788	porphyrhy(m)		+	
4789	rrhy?			
4790	gd			
4791	felvol		+	
4792	pm		+	
4793	myl(d)		+	
4794	fgpg			
4795	rg			
4796	mgpg			
4797	rg			
4798	fgm			
4799	fgm			
4800	fgm(m)		+	
4801	myl(d)	+	+	
4802	folgd			
4803	myl(d)			+
4804	fgm			
4805	myl(l)		+	
4806	m-cgm		+	
4807	cgpog			
4808	vcgpog(m)			
4809	gd			
4810	gd			+
4811	felvol		+	
4812	felvol		+	
4813	qrtzit			
4814	qrtzit		+	
4815	fgpg			
4848	fgm			+
4849	cgpog(m)			
4850	cgpog			+
4852	fgm			+
4853	cgpopg(m)			
4854	fgm	+	+	+
4855	cgpog			
4856	felvol			
4857	cgpog			
4858	qrtzit			
4859	aplite cut by mv			
4860	gd			+
4861	cgpog			
4862	cgpog			+
4863+	rg			+
4864	fgm		+	
4865	sprhy	+	+	+
4866	fgm	+		+
4867	fgm	+	+	+
4868	cgpog			
4869	fgpg			+
4870	mgpg			
5023	fgm			
5024	pm			
5025	fgpg			
5026	fgm			
5027	fmg			

5028	fgm			
5029	gd			
5030	mgg			
5031	fgm			
5032	cgpog			
5033	rg			
5034	fgm			
5035	cgpog			
5036	cgpog			
5037	rg			
5038	mgpg			
5039*	mgpg			
5040	pm			
5041	mgpg			
5042	(m)			
5043	cgpog			
5044	m-cgm			
5045	gd			
5046	cgpog			
5047	cgpog			
5092	m-cgm			
25-5-1*	fgpg	+	+	
25-5-1a	fgpg	+		
25-5-2	fgpg	+	+	
25-5-3	fgpg	+	+	
25-5-4	fgpg	+	+	+
25--5	fgpg	+	+	
25-5-6*	fgpg	+	+	
25-5-7	fgpg	+	+	
25-5-8*	fgpg	+	+	
26-13-1	fgpg	+	+	
26-13-2	fgpg	+	+	
26-13-3	fgpg	+	+	
26-13-4	fgpg	+	+	
26-13-5	fgpg	+	+	
26-13-6	fgpg	+	+	
42-1-2	cgpg	+	+	
6096	gd			
6097	di			
6098	myl(l)			
6099	di			
6100	amplibolite			
6101	mylgd			
6102	gd	+		+
6103	mgm			
6104	porphyrhy			
6105	porphyrhy			
6106	porphrhy			
6101	mly(d) (gd)			
6191	congl			
6192	congl			
6193	slst			
6194	congl(g clast)	+	+	
6195	congl(g clast)			+
6196	congl			
6197	congl			
6198	congl		+	
6199	sst			
6200	slst			
6201	shale			
6202	sed			
6203	fggg	+	+	

6204	mgm(cleaved)	+		+
6205	myl(l)			
6206	gabbro	+		+
6207	mgm(spots)			+
6208	fgpgg(clast)	+	+	
6232	mafic			
6254	sst			
6255	slst			
6256	congl		+	
6257	congl			
6258(contact)	sst/grnt(clast)	+	+	+
6259	microgrnt		+	
6260	fgpgg	+	+	
6261	microgrnt	+		+
6262	microgrnt	+	+	
6263	microgrnt	+		+
6264	microgrnt			
6265	slst		+	
6266	sst			
6584	mgpg			
6679	f-mgdi		+	
6931	microgrnt			
6932	fgg/fgm	+	+	
6933	fgdi/gb			
6934	cgpog			
6935	m-cgggd			
6936	cgpg	+	+	
6937	cggd	+	+	
6938	cgpgg	+	+	
6939	cgpg			
6940	mgpgg	+		
6941	gb			
7000	fgpg			
7001	fgm			
7002	mgpog(large cubic cubes)			
7003	mgpog			+
7004	cgpog			
7005	cgpog			
7006	fgpg			
7007	fgm			
7008	fgm(min)	+		+
7009A	mgm	+		+
7009	fgm(min)			
7010	mgm	+		+
7010N	mgm			
7011	fgm-mgm	+		+
7012	qrtzit			
7013*	qrtzit			+
7014	myl(d)			
7015	myl(d)			
7016	sst			
7017	g	+	+	+
7018	gd			
7019	mgm	+	+	
7020	rg			
7021	rg	+	+	
7022	gd or rg			
7023	fgm or sed			
7024	fgpg			
7025	microgrnt	+	+	
7026	fgpgg			
7027	mgpog			

7028	aplite		
7029	rhy		
7030	alteredg		
7033 (spots)	mgm		
7034	mgpog		
7035	qrtzit		
7036	limestone		
7037	limestone		
7038	cong		
7039	cong		
7040	myl (d) (gd)		
7041	mgm		
7042	mgm		
7043	mgm		
7044	fgpgg		+
7045	cong		
7047	fmg		+
7049A	mgpog		
7050 (maf & gd)	gd		
7051	fgm		
7052	qrtzit		
7053A	fggpg		
7075A	fgpg (contact)		
7076A	slst		
7321	fgpgg	+	+
7322	fggg		
7323	fgpg		
7324	fgporpg		
7325	mv		
7326	mgrg		
7327	fgporpg	+	+
7328	mgporg		
7376	fgporpg		
7377	fgporpg	+	+
7378	f-mgporvpgg	+	+
7379	fgporpg		
7380	fgpg		
7381	f-mgpg		
7382	f-mgpg	+	+
7383	mgvpg	+	+
7384	mgrg		
7385	mgrg	+	+
7386	mgpgg		
7387	mgpgg		
7388	f-mgpg		
7389	mgpg	+	+
7390	mgpg		
7391	fgg	+	+
7392	gb	+	+
7393	mgrpg	+	+
7394	mgpg	+	+
7395	rhy	+	+
7396	ton		
7397	m-cgrg	+	+
7535	f-mgpg		
7536	f-mgpg		
7537	fmgpg		
7542	mgdi		
7543	di		
7544	mgdi		
7545	porrhy		
7546	mgdi		

7547	pordi/gb
7549	mgdi
7550	myl?sed?
7551	mgpog
7552	cgpog +
7553	myl(d)
7554	myl(d)?sed?
7555	sed(min)
7569	mggd
7570	mgpg +
7571	cggd
7572	folf-cgg
7574	folf-mgpgg
7577	fgg
7578	?db
7579	mgpgg
7580	f-mgdi/f-mgpg
7581	mgdi
7582	m-cgpg(myl)
7585	mgpgd
7586	f-mgpgd
7587	myl(l)/leucogrnt
7588	m-cgpg

* May contain inclusions of feldspar megacrysts
+ Samples with modal analyses

Legend
Granite:g
Very coarse grained red-orange granite: vcgrog
Coarse grained pink-orange granite: cgpog
Medium grained pink granite: mgpg
Fine grained pink granite: fgpg
Fine grained granite: fgg
Porphyritic granite: porpg
Red granite: rdg
Gray granite: gg
Pink gray granite: pgg
Vuggy granite: vg
Microgranite: microgrnt
Rapakivi granite: rg
Granodiorite: gd
Mylonite(dark): myl(d)
Mylonite(light):myl(l)
Fine grained mafic: fgm
Medium-coarse grained mafic: m-cgm
Porphyritic mafic: pm
Megacrystic mafic: megm
Coarse grained diorite with plag: cd
Spherulitic rhyolite: sprhy
Red rhyolite: rrhy
Rhyolite: rhy
Tonalite: ton
Foliated: fol
Mafic veinlet: mv
Sediment: sed
Quartzite: qrtzit
Conglomerate: cong
Siltstone: slst
Felsic volcanic: felvol
Porphyritic rhyolite: porrhy

Amphibolite: amph
Leucogranite: leucogrnt
Diorite: di
Fine diorite: fgdi
Medium diorite: mgdi
Coarse diorite: cgdi
Diabase: db
Gabbro: gb
Granitic gneiss: ggn
Megacrystic: meg
Rapakivi: r
Porphyritic: por
White: w

Appendix 2. Inventory of analytical samples

(a) **Felsic rocks**

1. GRANITIC CLASTS IN SEDIMENTS

6194	6-555	Chain Lake Brook
6258	6-572	West Economy River
6208	6-559	East B. Economy River

2. VARIOUS LATE FINE GRAINED PHASES

porphyry associated with gabbro that cuts the rapakivi phase

4865* [REE]	4-742	sprhy	W. of Bass River	(4866, 4867 are associated gabbro)

aplite cutting main coarse grained granite in south of pluton

4705	4-602	fgpg	"aplite"

rapakivi rhyolite cutting main granite phase

4737	4-609	rrhyol	dyke 2m wide	Bass River

medium grained granite cutting major gabbro sheet

7391	6-773	Med pnk granite dyke cutting diorite
7395	6-777	W of Economy River. Cuts net-veined gabbro

3. FGPG AT NORTHWESTERN EDGE OF PLUTON: TYPE A

West Economy River

26-13-2	3-253	West Economy River
26-13-3	3-254	
26-13-4	3-255	
26-13-6 [REE]	3-257	
6260	6-573	main fine-grained granite phase 30 m from contact
7377	6-767	fn porphy granite *like 6260*
7378	6-768	vuggy fn porphy granite *like 6260*

18. FGPG AT NORTHWESTERN EDGE OF PLUTON: TYPE B

26-13-1	3-252	West Economy River
26-13-5	3-256	
6262	6-575	main fine-grained granite phase 100 m from contact
6261	6-574	porphyritic mgr., shear-bounded small body

17. FGPG AT NORTHWESTERN EDGE OF PLUTON: TYPE C

Chain Lake Brook and E. branch Economy river

25-5-1 [REE]	3-243	
	3-244	
	3-245	
	3-246	
	3-247	
	3-248	
	3-249	
	3-250	
25-5-8* [REE]	3-251	
6203	6-556	1.6m granite dyke fgpgg cutting sediment
6932	6-755	fn pk gr

4. FINE-MEDIUM GRAINED GRANITE NEAR NW RIM OF PLUTON

6263	6-576	porphyritic mgr., shear-bounded small body
7382	6-769	fn-med granite, ?another sheet, S of previous
7383	6-770	med vuggy granite. ?different phase

5. MAIN GRANITE PHASE IN NORTHERNWESTERN HALF OF PLUTON

regular granite

42-1-2*[REE]	3-451	middle part of Economy River [like group 18]
6936	6-805	N. of Newton Lake. crs pnk granite [like group 17]
6937	6-797	NW of Newton lake. foliated crs granodiorite. Relationship to rapakivi phase unclear. [like group 17]

medium granite cutting main gabbro bodies

7394	6-776	Net-veining granite in gabbro. Affinities unclear. [like group 18]

15. MED. GRAINED GRANITE IN NORTHWESTERN HALF OF PLUTON, GEOCHEMICALLY DISTINCT

6940	6-794	near 5037. Med pnk granite. may or may not be associated with rapakivi phase
5039	4-712	W. of Economy Lake (nearby - intermingled with mafic)

14. MAIN GRANITE PHASE AT WESTERN MARGIN OF PLUTON

4758	4-22	mgpg	S end Gerrish Mtn Road
4761*	4-23	mgpg	N end Gerrish Mtn Road

7. MAIN COARSE GRAINED HORNBLENDE GRANITE AT SOUTHERN EDGE OF WESTERN PLUTON

4699[REE]	4-24	vcgrog	S. of Economy Lake
4700*[REE]	4-12	vcgrog	S. of Economy Lake
4701	4-13	vcgrog	S. of Economy Lake
4707	4-17	vcgrog	SE of Economy Lake
4721	4-604	vcgrog	SE of Economy Lake

these granites tend to be little deformed, associated with more deformed hybrids, cut by common aplite. Found only south of Economy Lake

4706	4-16	gd, SE of Economy Lake, deformed, intercalated with vcg
4704	4-15	gd, SE of Economy Lake, deformed, intercalated with vcg

8. MAIN COARSE GRAINED GRANITE AT SOUTHERN EDGE OF EASTERN PLUTON

4681*[REE]	4-6	cgpog	W. of Gamble Lake

9. MAIN RAPAKIVI PHASES, WESTERN PLUTON

West of Economy Lake and northern Economy River

5037	4-711	W of Economy Lake "mafic rapakivi"
7385	6-771	W Economy river: med rapakivi
7389	6-772	W Economy river: Med pnk granite, ?rare rap patches.
7393	6-775	Slightly rapakivi pnk granite
7397	6-778	Road W of Economy River. med crs rap. granite. This is near southern edge of the main central diorite bodies.

10. MAIN RAPAKIVI PHASES, EASTERN PLUTON

W of Bass River

7021	6-592	rg	[KP1, 37] West of Bass River

Gamble Lake area

4685	4-595	rp	W. of Gamble Lake
4689*[REE]	4-9	rg	W. of Gamble Lake
4690	4-598	rg	W. of Gamble Lake (in this area, rapakivi associated with granodiorites and hybrids)
4694	4-10	?rp ?mgpg	W. of Gamble Lake

4670[REE] 4-2 rg NW of Gamble Lake

11. MEDIUM GRAINED GRANITE IN THE EASTERN PART OF THE PLUTON

Bass River

4735	4-607	cgpog	Bass River, 40p. S of contact
4736	4-608	cgpog	Bass River, 40p. S of contact
4748	4-610	"felsvol"	?mylonite Bass River
7017	6-590	granite	SW of Bass River

Gamble Lake area

4672[REE]	4-4	mgpg	S. of Gamble Lake
4680	4-594	fgpg	W. of Gamble Lake [might be dyke]
4686[REE]	4-8	mgpg	W. of Gamble Lake

16. FINE GRAINED MARGINAL GRANITE IN NORTHEASTERN PART OF PLUTON

7025	6-593	fine granite W of Bass River [MF1, 4-15]
4692	4-600	N of Gamble Lake
7327	6-766	Toad Lake. Cuts rapakivi granite (not demonstrably cross cutting).

12. EARLY FELSIC VOLCANICS/SUBVOLCANICS

cut by all sorts of other high level rocks. Have high An.

4691	4-599	N. of Gamble Lake, ?cut by gd
4697*[REE]	4-11	N. of Gamble Lake. In this region, cut by pegmatite, mafic dyke, and aplitic veins. In this region, lithic tuff and spheroidal rhyolite observed.
7321	6-765	E. of Gamble Lake. Fn granite transitional to rhyolite, cut by fn pk granite
4728*	4-605	E. of Bass River. megacrystic porph. rhy.

13. FELSIC VOLCANIC/SUBVOLCANIC INCLUSION IN COARSE GRANITE

relative age depends on age of coarse granite than includes it.

4739	4-19	porphy. rhyolite inclusion in coarse granite (i.e. volcanics are older) in northern part of Bass River

(b) **Mafic rocks**

1,3 Gamble Lake area north of the RBF

Diorite

4673	4-591	S. of Gamble Lake
4674[REE]	4-5	S. of Gamble Lake
4688	4-597	W. of Gamble Lake

Granodiorite

4669	4-1	SW of Gamble Lake
4687	4-596	W of Gamble Lake
6102	6-538	SW of Gamble Lake

2,5,7 Diorite along the Rockland Brook fault

S. of Gamble Lake

4801	4-746	myl(d) foliated diorite, S. of Gamble Lake (S of RBF)
6679	6-752	f-mgdi, in Portapique River

SW of Bass River

7017	6-590	SW of Bass River [KP1, p.36] 75% SiO_2

in Bass River

4774	4-745	fgm, mylonitic diorite, S Bass River
4778[REE]	4-749	myl(d), S Bass River
4779	4-615, 4-747	fgm, mylonitic diorite, S Bass River

4,6,8 South of Economy Lake at margin of pluton

Granodiorite

4702	4-14	S of Economy Lake: extreme south of pluton
4713	4-603	SE of Economy Lake: extreme south of pluton

Diorite

4714	4-18	fgm, field term diorite. SE of Economy Lake. Relationship to granodiorite unclear.

South of Newton Lake

7019	6-591	mgm diorite. S. of Newton Lake [KP1, p. 37]

9. Oblique mafic wrench fault, Economy Lake to W. Bass River

Mostly diorite

7009A	6-587	mgm diorite, near Economy Lake. [KP1, p. 19]
7008	6-586	fgm mylonitized diorite, near Economy Lake [KP1, p. 20]

10. Diorite/gabbro in large sheets at western end of pluton

6938	6-756	Granodiorite NW of Newton Lake. Associated with crs granite
7392	6-774	gb Economy river. Cut by granite
4750	4-612	cd E. of Gerrish Mtn road
4749	4-611	m-cgm E. of Gerrish Mtn road
4753	4-20	Granodiorite pm E. of Gerrish Mtn road
4754	4-21	m-cgm E. of Gerrish Mtn road
4755	4-25	m-cgm E. of Gerrish Mtn road

11. Highly evolved gabbro cutting early phase

4703	4-601	fgm foliated mafic dyke cutting 4704, crs hbl granite. both associated with undeformed crs granite. SE of Economy Lake

12. Dykes

6204	6-557	mgm Chain Lake Brook. deformed db dyke cuts sst and fine granite
4720	n.a.	dyke cutting undeformed granodiorite, SE of Economy Lake
5031	4-710	md db cuts med gr E of Economy Lake
6206	6-558	mgm Chain Lake Brook. gb ?older than granite, but ?fines to granite. chemically is evolved.

13. Gabbro associated with porphyry cutting rapakivi granite

4682[REE]	4-7	gabbro cutting rapakivi granite W. of Gamble Lake

4866	4-740	fgm fine gabbro, ?large dyke, associated with porph. rhy. 4865
4867	4-735	fgm fine margin of 4866. Lamprophyric

14 Uncertain whether dyke or gabbro body: chemistry looks like dyke

42-1-1	3-450	Economy river

15. Old gabbro bodies along N margin of pluton

4734	4-606	fgm W of Bass River

16. Dykes with primitive chemistry cutting S part of pluton

7011	6-589	mgm dyke cutting medium granite, S of Newton Lake [KP1, p.15]
4854	4-744	fgm mafic dyke cuts crs granite, SW of Bass River

17. Either xenolith or early primitive dyke

7010	6-588	mgm granite with mafic xenoliths cut by mafic dyke. [KP1, p.18]. Probably a dyke

Appendix 3. Microstructural Observations of Representative Samples

Sample: C4601 (fine-grained mafic)
Amphiboles very fine grained;they occur in "lenses" larger than some of the plagioclase phenocrysts; sphene porphyroblasts in amphibole matrix form lenses within plagioclase bounded domains;large plagioclase phenocrysts are broken by microfractures. This may be a deformed mafic with trachytic texture, which would explain the pattern of amphiboles surrounded by feldspars. Undulose extinction in quartz and numerous subgrains in quartz and amphibole rich veins indicate that the quartz veins crystallized prior to the ductile deformation. The veins do not cross-cut the weak grain scale c-s fabric defined by the quartz-amphibole "domains" and the feldspar "domains".

Sample : C4602 (porphyritic mafic)
Sample : C4605 (fine-grained mafic)
Undulose extinction in quartz; some of the euhedral grains appear to be partially recrystallized (note subgrains); poorly formed open spherulites of plagioclase?; biotite? coronas around (quenched crystals?)

Sample: C4669 (granodiorite)
Dis-equilibrium textures between plagioclase and quartz; Plagioclase phenocrysts show strange deformation twins--polydeformed?; small K-feldspar crystals show deformed perthitic texture; quartz phenocrysts are associated with bent and broken (microboudinage) apatite; apatites cross grain boundaries from parent quartz to subgrains with slight bending; intracrystalline subgrain boundaries in quartz visible only when parent is close to extinction; amphibole phenocrysts show curved (deformed) cleavage surfaces and some show development of apparent new grains. Fractures in plagioclase and K-feldspar filled with quartz and some amphibole+quartz show some evidence of recrystallization; fine-grained amphibole filled microfaults with displacements of 7 microns cross-cut feldspar and quartz phenocrysts; oxides appear to be formed in relation to these fractures, but some euhedral oxides are fractured as well

Sample: C4670 (rapakivi granite)
Sample: C4671 (porphyritic mafic)
It looks like clinopyroxene altering to amphibole with the plagioclase being broken up by the reaction; there is little quartz, but lots of acicular and tabular apatite

Sample: C4672 (medium-grained porphyritic granite)
Quartz is rounded, but there does not appear to be any recrystallization-undulose extinction is not ribbon-like; K-feldspars are perthitic; no evidence of deformation twinning in feldspars; dis-equilibrium texture in some plagioclase; quartz veins in feldspars show no evidence of recrystallization

Sample: C4673 (granodiorite)
Long (60 micron) apatite needles cross quartz crystal boundaries- some are kinked by the rotation at these boundaries- note that there is no uniform sense of rotation direction; broken needles show very small displacements at grain boundaries (<1 micron)

Sample: C4674 (granodiorite)
Amphibole veinlet- shows no lateral movement across fracture; apatite inclusions in quartz and amphiboles mostly undeformed- some show very small breaks; some plagioclase. show slight deformation twins; most structures in feldspars obscured by sericitization

Sample: C4677 (medium-coarse grained mafic)
Twinning in plagioclase looks primary; undulose extinction in quartz not well developed; apatites are stubby- very few are acicular; apatite phenocrysts cross grain boundaries with very little distortion; oxide mineralization forms large, sub-parallel crystals that cross-cut most types of grains.

Sample: C4679 (fine grained mafic)
No apatite present; amphibole? phenocryst surrounded by corona of chlorite in turn surrounded by corona of plagioclase? and small euhedral oxides; coronal porphyroblasts show increasingly euhedral form outwards.

Sample: C4688 (fine grained pink granite)
Quartz-plagioclase granophyres; feldspars anhedral, perthites; some deformation twins in plagioclase; no apatite.

Sample: C4681 (coarse grained pink orange granite
Fractures in feldspars filled with amphibole; larger feldspar phenocrysts contain inclusion of quartz implying dis-equilibrium crystallization; albite twins in plagioclase are deformed slightly in some crystals; no apatite

Sample: C4685 (coarse grained pink orange granite)
Strained plagioclase show deformed albite twins; quartz filled fractures in plagioclase are sub-parallel; small amounts of graphic texture; amphibole-rich veinlets contain some disequilibrated quartz; no apatite

Sample: C4686 (medium grained pink granite
Sample: C4687 (granodiorite)
Interstitial quartz shows disequilibrium texture with plagioclase; long needles of apatite cross grain boundaries undeformed, most apatites appear unbroken-a very few are fractured slightly

Sample: C4688 (granodiorite)
Sample: C4689 (rapakivi granite)
Sample: C4690 (rapakivi granite)
Deformed albite twins in plagioclase-quartz granophyres; amphibole rich vein cuts across crystals producing lateral motions of up to 10-15 microns with a dextral sense of movement.

Sample: C4691 (felsic volcanic)
Rounded and fragmented quartz some feldspars within a fine-grained crystalline matrix; v.fine grain size may be caused by cataclasis? or recrystallization; texture seems to indicate on set of fractures produced, filled and crystallized followed by a second set of similar fractures-both formed at progressively later stages of crystallization

Sample: C4692 (granodiorite)
Some large quartz crystals are fractured; other quartz crystals show ribbon textures indicating recrystallization

Sample: C4694 (medium grained pink granite)
Sample: C4697 (felsic volcanic)
Some quartz subgrains, other small euhedral quartz grains; feldspar porphyroblasts very intact peripherally-they contain crystals of albite; porphyroblasts, inclusions, and quartz cross-cut by undeformed quartz veins; biotite with well developed bird's eye extinction found as randomly oriented phenocrysts within fine grained quartz matrix. A few quartz crystals have trails of new grains extending away from them that show rotation of the extinction angle 90° away from the parent 40 microns away from a 40 micron diameter parent. This implies a lack of preferred orientation in the quartz.

Sample: C4699 (very coarse grained red orange granite
Sample: C4700 (very coarse grained red orange granite)
Sample: C4701 (very coarse red orange granite)
Plagioclase with deformed albite twins and fanning extinction; undulose extinction in quartz ribbons with aspect ratios of 3:1 to 8:1; quartz domains incorporate porphyroblasts of sericitized feldspar, biotite, and oxides; quartz veins, some with tension gash type appearance, cross-cut both quartz and biotite domains; perthitic texture peripherally deformed in some feldspars; biotite

porphyroblast has sinusoidal shape and contains oxides-shape appears to indicate sinistral shear; rapakivi feldspar porphyroblast seems to have pressure shadow effect on adjacent feldspars

Sample: C4702 (granodiorite)
Some differentiation of quartz and biotite domains; oxide mineralization has affinity to develop in biotite domains; both domains contain deformed feldspar porphyroblasts; quartz domains contain some well developed quartz ribbons; c-s fabric not well defined at grain scale (transitional between grain scale and macroscopic c-s fabric?); hints of c-s exist in form of quadrangle shaped biotite bounded quartz domains; oxide filled fracture lies within quartz and biotite domains, and is cross-cut by an amphibole and (epidote?)- rich vein; do oxides act as a catalyst for deformation partitioning or is it circumstantial to their relationship with biotite?; large euhedral oxide porphyroblast shows pressure shadow effects which indicate a dextral sense of shear

Sample: C4703 (fine grained mafic)
Some development of grain-scale c-s fabric defined by quartz/plagioclase domains and biotite/amphibole/oxide domains--gives dextral sense of movement--fabric is nearly homogeneous; apatite inclusions appear to be strung out in one orientation, broadened in another at 90°. Are they actually strung out or do they form a pattern defined by the lattice of the host mineral?

Sample: C4704 (granodiorite)
Sample: C4705 (fine grained pink granite)
Sample: C4706 (granodiorite)
Deformed granodiorite; porphyroblasts include: anhedral perthitic K-feldspar with inclusions of quartz, euhedral epidote, acicular + tabular apatite which is altered; perthitic K-feldspar cross-cut by quartz veinlets-quartz veins truncated by quartz domains composed of new grains. Quartz veins also cross-cut by biotite- and quartz-rich veinlets which are cross-cut by quartz domains (there are porphyroblasts of biotite and quartz rich material). Quartz new grains are concentrated in ribbons that are approximately parallel; quartz domains wander between large feldspar porphyroblasts sinuously-- this pattern may indicate ductile deformation of rock after emplacement of quartz vein.

Micro boudinages of albite with deformation twins and visible cleavage trace; needles of apatite grow within cleavage trace and at 90° to it in the slide z-axis direction-elongation of boudins shows sinistral shear, with maximum extension sub-parallel to poorly developed LPO in quartz newgrains. However!-- adjacent boudinage, composed of fragments of the same crystal grain suggests dextral sense of shear-- several other examples suggest dextral shear, but it may be that feldspar micro boudins are unreliable on a local scale for determining sense of lateral movement.

Formation of quartz domains has been facilitated pertly through breakup of randomly oriented biotite microphenocrysts (from bt+qz veinlets) into the biotite zones. This indicates that the minerals are still warm and their components are highly mobile.

An oxide and biotite filled vein cuts directly across the qtz domains, bt domains, and the porphyroblasts of all sizes. There are two such veins visible on the edge of the slide which may be extensions of the same vein (their textures are very similar).

Some of the smaller deformed feldspars contain deformed apatite crystals which have sinuous shapes that match the deformation of cleavage planes and albite twins in the feldspars.

Some porphyroblasts of less deformed plagioclase are "zoned": they have an inner zone which contains a high concentration of fluid inclusions and accessory minerals, and an outer zone which contains markedly fewer inclusions of all types. Some of these have carlsbad twins which penetrate through both "zones" showing that the zones represent a change in the environment of crystallization of the crystals.

There are two feldspar megacrysts which seem to be acting as

porphyroblasts. There is a well developed quartz LPO between the two feldspars, which gives an impression of greater deformation than that which is suggested by the two large porphyroblasts. fragments of both porphyroblasts remain in close proximity and orientation to their parent.

Feldspar Mega-porphyroblast A:
The porphyroblast has dis-equilibrated intergrown components of albite and perthitic K-feldspar. The perthitic texture is overprinted by deformation twins, and is deformed at the edges of the porphyroblast and in fragments derived from it. The feldspar is cross-cut by a biotite-rich veinlet. The biotite seems in places to be fibrous and grown parallel to the direction of separation on either side of the fracture. The textures and cleavage traces in the porphyroblast are deformed into arcuate shapes.

Feldspar Mega-porphyroblast B:
Perthite textured K-feldspar with deformation twins overprinting the perthitic texture. Phenocryst is greatly fractured, with many of the fragments showing variations in orientation of perthite texture, and deformation twins. Deformation twins seem to be partitioned away from cross-cutting quartz veins or large inclusions.

Some of the peripheral fragments are acting as porphyroblasts, with the amount of rotation being greater towards the centre zone between the two- some of the small porphyroblasts in this area are identifiable as having come from A or B.

The centre zone also contains several intensely deformed albite? porphyroblasts which show folded inclusion trails. The shape of these folds indicates a significant amount of shortening in the crystal without it losing cohesion and breaking. This may indicate that the porphyroblast had warmed up after cooling from crystallization temperature until it had almost reached its original crystallization temperature.

Sample: C4707 (very coarse grained red orange granite)
Sample: C4713 (granodiorite)
Slight development of fanning undulose extinction in perimeter of quartz phenocrysts; small amounts of apatite in quartz have 2 well defined orientations that cross at 75°; quartz filled fractures in plagioclase show small offsets; inclusions of amphibole and biotite in anhedral perthitic K-feldspar with biotite forming around edges of porphyroblast; poorly defined domains of quartz/feldspar and oxide/biotite.

Sample: C4714 (fine grained mafic)
Sample: C4721 (very coarse grained red orange granite)
Sample: C4728 (pink orange rhyolite)
Sample: C4734 (fine grained mafic)
Sample: C4735 (coarse grained pink orange granite)
Sample: C4736 (coarse grained pink orange granite)
Sample: C4737 (rapakivi granite)
Sample: C4739 (pink orange granite)
Sample: C4748 (felsic volcanic)
Sample: C4749 (medium-coarse grained mafic)
Sample: C4750 (coarse grained diorite)
2 amphibole and biotite-rich veinlets cross-cut each other in the middle of an amphibole phenocryst which shows signs of having been "wedged" apart by the veins and subsequently being altered. Texture may indicate formation of new grains.

Sample: C4753 (porphyritic mafic)
Sample: C4754 (medium-coarse grained mafic)
Sample: C4755 (medium-coarse grained mafic)
Sample: C4758 (medium grained pink granite)
Well developed fanning extinction in feldspars; interstitial quartz in feldspar fractures is recrystallized; quartz phenocrysts breaking into subgrains and new

grains peripherally and centrally-there are no well developed quartz ribbons. Interstitial quartz crystallizing, then recrystallizing as plagioclase phenocrysts approach condition of grain size reductions due to cataclasis.

sample: C4761 (medium grained pink granite)
Feldspars very fragmented, and have fanning extinction; undulose extinction, tension gashes in quartz crystals, so that it appears that feldspar and quartz phenocrysts are being pulled apart, and falling into a "debris' cumulate of crystal fragments with temperature conditions still appropriate for quartz and feldspar to form. Interstitial material shows cuneiform texture; some subgrains have formed in the middle of quartz phenocrysts, there are few peripheral phenocrysts-higher surface area seems to have made the quartz phenocrysts susceptible to melting and thus peripheral subgrains have been reabsorbed by the melt, or may have served as nucleation points for formation of cuneiform textures in a cumulate which has been deformed, then the deformation relaxes. There are a few fragments of very fine grained amphibole rich material, some apatites in the quartz phenocrysts, and some quartz grains with well developed undulose extinction that approaches fanning.

Sample: C4774 (fine grained mafic)
Mylonite; fanning extinction in feldspar porphyroblasts

Sample: C4788 (mylonite dark)
Sample: C4779 (fine grained mafic)
Sample: C4801 (mylonite dark)
Sample: C4854 (fine grained mafic)
Very fine grained mafic enclaves (amphiboles?); plagioclase is sericitized; albite twins in plagioclase, some small fragments shoe deformation twins--some feldspars are stretched ad deformed slightly (micro boudinages)

Sample: C4865 (spherulitic rhyolite)
30 micron diameter spherulites; quenched appearing plagioclase crystals; some spherulites appear to be quartz; some of the quenched crystals are broken, possible by the force of the growth of the spherulites.

Sample: C4866 (fine grained mafic)
Sample: C4867 (fine grained mafic)
Sample: 25-5-2- (fine grained pink granite)
Coronal micro-graphic texture of quartz around oxides and plagioclase

Sample: 25-5-1a (fine grained pink granite)
sample: 25-5-2 (fine grained pink granite)
Micrographic texture of quartz and plagioclase is cross cut by veinlets rich in amphiboles and quartz veinlets (2 distinct veinlet types)

Sample: 25-5-3 (fine grained pink granite)
Micrographic texture of quartz and plagioclase cross-cut by 2 veinlet types; all textures cross-cut by micro-faults and mylonitized shear zones with a variety of porphyroblasts indicating both sinistral and dextral shear

Sample: 25-5-4 (fine grained pink granite)
Sample: 25-5-5 (fine grained pink granite)
Micrographic textures of quartz and plagioclase which has slightly recrystallized and lost its "cuneiform" sharp edged appearance. There is evidence of grain size reductions, but no evidence of rotation or obvious porphyroblasts.

Sample: 25-5-6 (fine grained pink granite)
Micrographic texture uncommon, some amphibole veinlets

Sample: 25-5-7 (fine grained pink granite)

Micrographic texture of quartz recrystallizing into new grains, away from the simultaneous extinction of the intergrown crystals. Large plagioclase phenocrysts appear largely unaffected by changes to quartz. Amphibole and epidote rich veinlets are associated with opaques; plagioclase is sericitized, quartz shows undulose extinction.

Sample: 25-5-8 (fine grained pink granite)
Micrographic intergrowth of plagioclase and K-feldspar. Oxides are present in veinlets and associated minerals show red staining.

Sample: 26-13-1 (fine grained pink granite)
Sample: 26-13-2 (fine grained pink granite)
Sample: 26-13-3- (fine grained pink granite)
Sample: 26-13-4 (fine grained pink granite)
Sample: 26-13-5 (fine grained pink granite)
Sample: 26-16-6 (fine grained pink granite)
Sample: C6102 (granodiorite)
Sample: C6194 (clastic)
Some recrystallization of quartz, some fractures in feldspars- grain boundaries appear to be primary igneous texture with fragmentation due to small movements or recrystallization. Recrystallization appears to be disequilibrated. Oxides are randomly dispersed, but there are more in the "chewed up" zones.

Sample: C6203 (fine grained grey granite)
Quartz partially recrystallized (due to strain?): spherulites of plagioclase centred on quenched plagioclase crystals are partially recrystallized into large rounded crystals and rotated away from their position of formation. Large feldspars (not from spherulites-older?) show broken twinning pattern (patchy deformation twins) which is in some places bent. Some feldspars show evidence of being wedged apart by recrystallizing quartz.

Sample: C6204 (medium grained mafic)
Sample: C6206 (gabbro)
Veins of chlorite with actinolite and epidote
Sample: C6208 (fine grained pink-grey granite)
Sample: C6258 (granite contact in sandstone)
Quartz and feldspar beginning to separate into smaller grains-subgrains are mostly large one quarter to one third of grain in quartz. Deformation twins and perthite in albite. Many subgrains distinguished only extinction differences- grain boundaries not visible in plain polarised light. Intergrowth texture of quartz and feldspar indicating disequilibrium. This texture is less common in areas which are recrystallizing- system is stabilizing in solid state while being deformed.

Sample: C6260 (fine grained pink-grey granite)
Graphic intergrowth of quartz and plagioclase; bent twins in sericitized plagioclase. Epidote and hornblende associated with oxides. Some bending and breaking of apatite tablets across grain boundaries between quartz and feldspars.

Sample: C6261 (fine grained pink-grey granite)
Sample: C6262 (fine grained pink-grey granite)
Intergrowths of slightly equilibrated quartz and feldspar. Strings of angular new grains. Lamellar twins in feldspars radiate from a central point as though they were originally part of an open spherulite structure. Quartz ribbons appear to parallel the radiating structure. Apatites are acicular and not very broken up.

Sample: C6263 (microgranite)
Sample: C7008 (fine grained mafic)
Sample: C7009A (medium grained mafic)

Sample: C7010 (medium grained mafic)
Apatites are short, stubby tablets which are not very broken up and appear to be randomly oriented within the feldspars. The texture of the feldspars appears to be a poorly formed semblance of an open spherulite with amphibole, oxides and some biotite forming later in the open spaces. High content of mafic components - fractures are filled with very fine grained amphiboles and show little, if any, lateral displacement.

Sample: C7011 (fine-medium grained mafic)
Apatites are short, stubby tablets which are not very broken up and appear to be randomly oriented within the feldspars. The texture of the feldspars appears to be a poorly formed semblance of an open spherulite with amphibole, oxides and some bt forming later in the open spaces. High content of mafic components - fractures are filled with very fine grained amphiboles and show little, if any, lateral displacement.

sample: C7017 (granodiorite)
Sample: C7019 (medium grained mafic)
Sample: C7021 (rapakivi granite)
Sample: C7025 (microgranite)
Subhedral quartz phenocrysts in a very fine grained groundmass.

Figure Captions

Fig. 1. Geological map of Magdalen Basin showing location of the Cobequid Highlands (from Piper et al. 1993).

Fig. 2. Chronologic summary of late Devonian - early Carboniferous events in the Cobequid Highlands and adjacent areas (from Piper et al. 1993).

Fig. 3. Map of Carboniferous plutons and Cobequid Fault Zone of the western Cobequid Highlands, showing location of Pleasant Hills pluton in relationship to major faults and other plutons.

Fig. 4. Map of Pleasant Hills pluton showing main petrologic phases.

Fig. 5. Stereonets of structural observations in the Pleasant Hills pluton.

Fig. 6. Structural observations in the Pleasant Hills pluton. (A) Duplex structures. A roof thrust (t_1) and a floor thrust (t_2) define a partly exposed duplex with three splays (s_{1-3}) offsetting the floor of the hanging wall. A smaller, fully exposed duplex is observed in the centre of the photograph. Outcrop is 3.5 m wide. (B) Dextral transpressional contact between granite and diorite, deformed under solid-state conditions. The diorite (d) has acted as a barrier to southward motion of the granite (+ symbol). (C) Cross section of alternating sheets of gabbro (+), in places mylonitic, and metasediment (Z pattern) with late intrusion of granite wedge (TIP indicated). The granite has intruded along a pre-existing contact between gabbro and metasediment at the northern margin of the pluton.

Fig. 7. I.U.G.S. classification of the granitoid rocks, Pleasant Hills pluton, based on modal compositions. For detailed analyses, see Table 2. Field names after Streickeisen, 1973.

Fig. 8. Major element variation in the igneous rocks of the Pleasant Hills pluton illustrated using the parameters of de la Roche et al. (1980).

Fig. 9. Normative Q'-ANOR diagram for the Pleasant Hills pluton felsic igneous lithologies. Numbered classification fields after Streckeisen and Le Maitre (1979). Q'=100xQ/(Q+Or+Ab+An); ANOR=100xAn/(Or+An). Symbols as in Fig. 8. 2 = alkali-feldspar granite; 3a = syenogranite; 3b = adamellite-monzogranite; 4 = granodiorite; 5b = tonalite; 7 = quartz syenite; 8 = quartz monzonite.

Fig.10. Zr vs. Ga/Al discriminant diagram for recognition of A-type granite (Whalen and others, 1987). A = field for A-type granites; I+S = field for I- and S- type granites. Symbols as in Fig. 8.

Fig.11. Ce/Nb vs. Y/Nb discriminant diagram for recognition of groups of A-type granitoids. The fields for OIB (oceanic-island basalt) and IAB (island-arc basalt) are after Eby (1992). Symbols as in Fig. 8.

Fig. 12. Major and trace elements variations in Pleasant Hills felsic rocks in relation to SiO_2. Symbols as in Fig. 8.

Fig. 13. Y vs. Zr and CaO vs. Zr diagrams for the felsic igneous lithologies of the Pleasant Hills pluton. Symbols as in Fig. 8.

Fig. 14. Chondrite-normalized REE patterns for the Pleasant Hills pluton felsic lithologies. A: 25-5-1, 25-5-8 = fgpg at northwestern edge of pluton -type C, Chain Lake and E. Branch Economy River; 26-13-6 = fgpg at northwestern edge of the pluton- type A, West Economy river; 4697 = felvol early felsic volcanics/subvolcanics, northeastern margin of pluton; 4865 = sprhy late fine grained phases that cut rapakivi phases, West Bass river. B: 4681 = cgpog main coarse grained at southern edge of Eastern pluton; 42-1-2 = cgpg, main granite in northern western half of the pluton; 4700, 4699 = vcgrog main coarse grained hornblende granite at southern edge of western pluton; C: 4670, 4689 = rg main rapakivi phases, eastern pluton (Gamble Lake area); 4672, 4686 = mgpg in the eastern part of the pluton; 4681 = cgpog main coarse granite at southern edge of eastern pluton.

Fig 15. Chondrite-normalized REE patterns for the Pleasant Hills pluton mafic lithologies. 4282=gabbro; 4674=diorite (Gamble Lake area); 4778=megacrystic diorite; 4649=megacrystic mafic rock from the Folly Lake diorite.

Fig.16. Map showing the geographic distribution of normative anorthite (An) in the felsic rock phases of the Pleasant Hills pluton.

Fig.17. Normative anorthite vs. SiO_2 diagram for the Pleasant Hills pluton felsic lithologies.

Fig. 18. TiO_2 vs. SiO_2 diagram for the Pleasant Hills pluton mafic lithologies.

Fig. 19. Plot of normative composition of Pleasant Hills pluton felsic lithologies on a normative Qz-Ab-Or diagram. Cotectectic lines for water saturated magma after Johannes and Holtz (1990).

Fig. 20. Composition of feldspars from the Pleasant Hills pluton (data from Table 4) plotted on a Or-An-Ab diagram.

Fig. 21. Compositions of biotite from the Pleasant Hills pluton (data from Table 5).

Fig. 22. Electron microprobe backscatter images of zircons. (A) Zoned crystal of zircon with a rim that appears to have reacted with the host magma. (4863, rapakivi granite). (B) Glomeroporphyritic accumulation of zircon crystals poikilitically enclosed by an opaque mineral. Note the lighter and darker zones. (4681, cgpog).

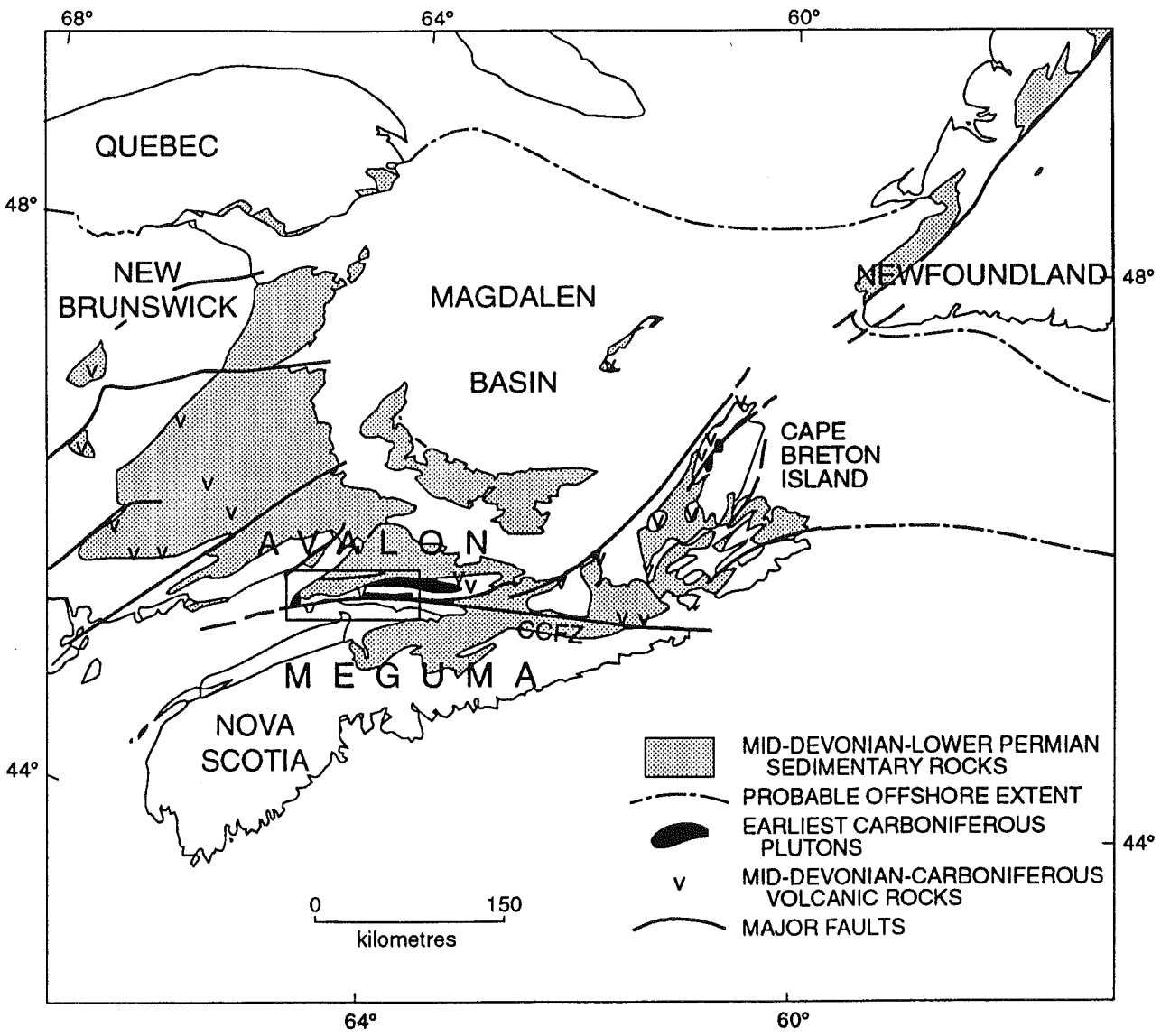

Fig. 1. Map of Magdalen Basin showing location of the Cobequid Highlands (from Piper et al. 1993).

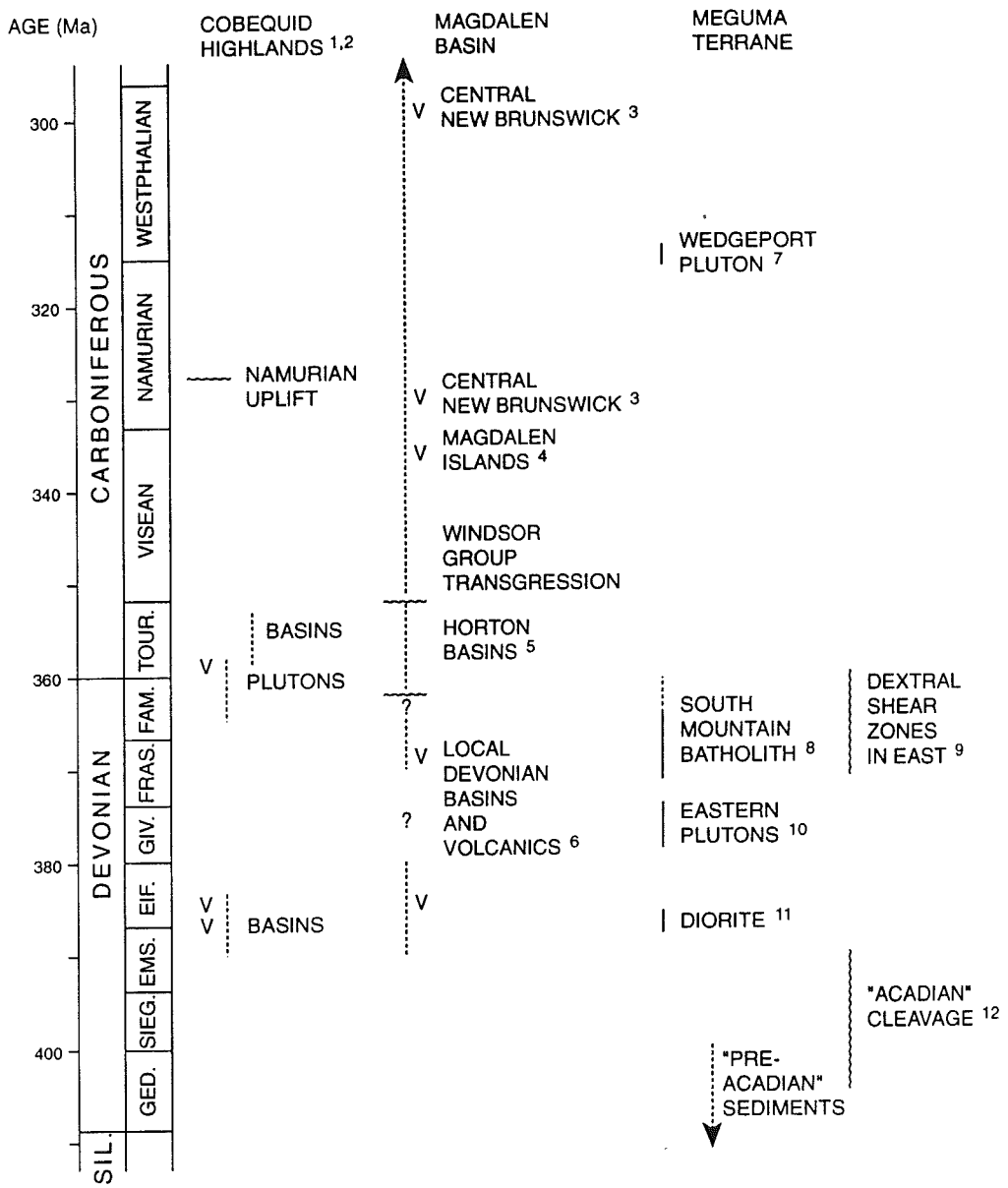

Fig. 2. Chronologic summary of late Devonian - early Carboniferous events in the Cobequid Highlands and adjacent areas (from Piper et al. 1993).

Fig. 3. Map of Carboniferous plutons and Cobequid Fault Zone of the western Cobequid Highlands, showing location of Pleasant Hills pluton in relationship to major faults and other plutons.

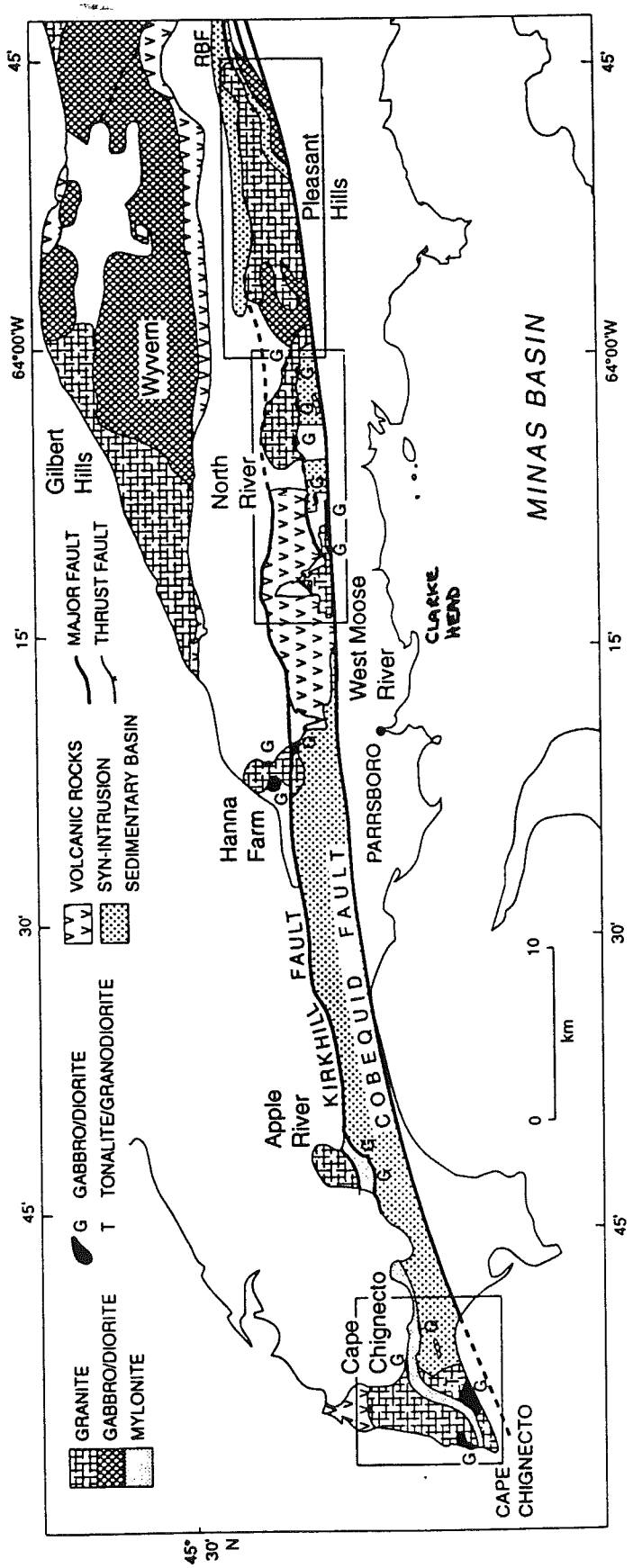

Fig. 4. Map of Pleasant Hills pluton showing main petrologic phases.

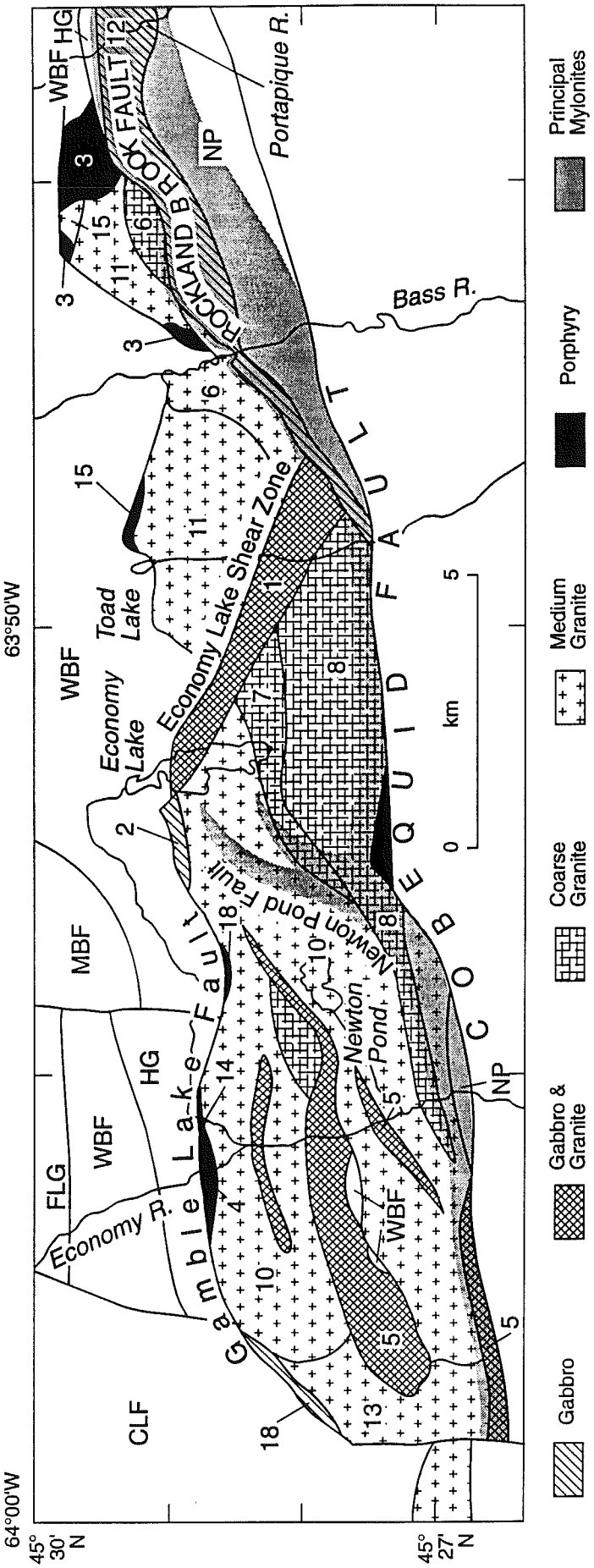

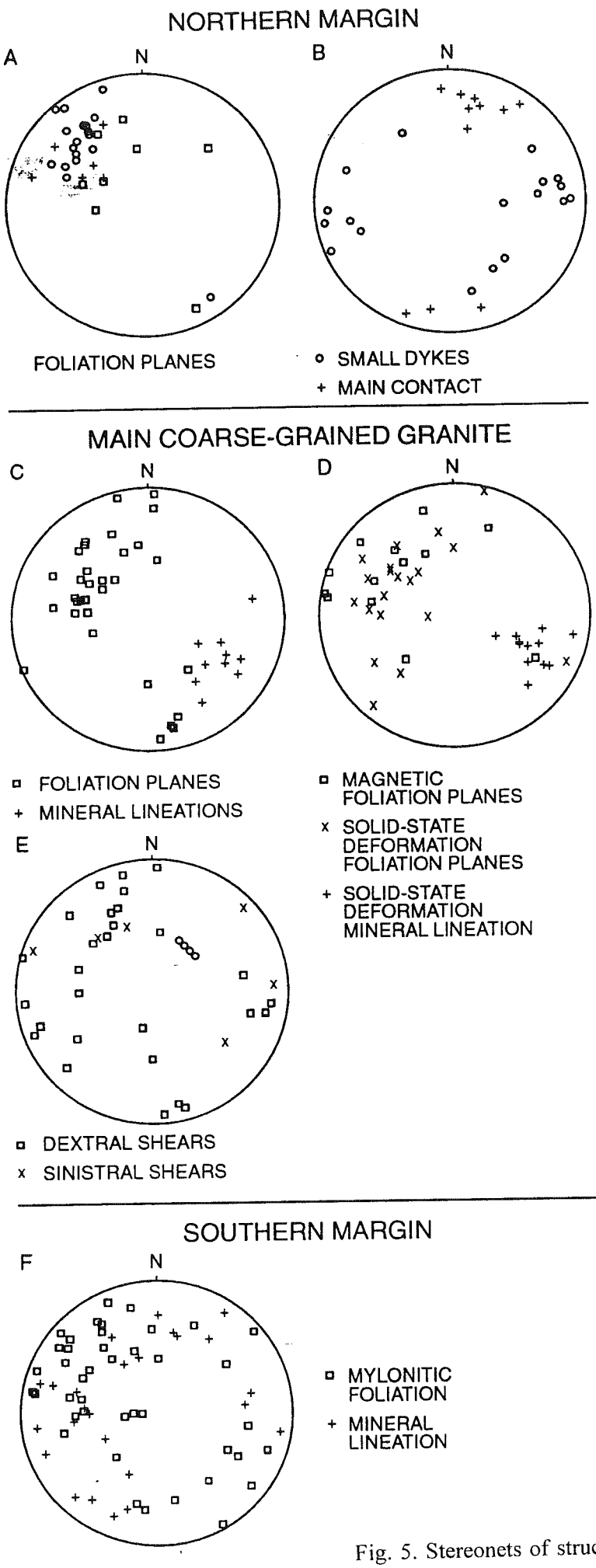

Fig. 5. Stereonets of structural observations in the Pleasant Hills pluton.

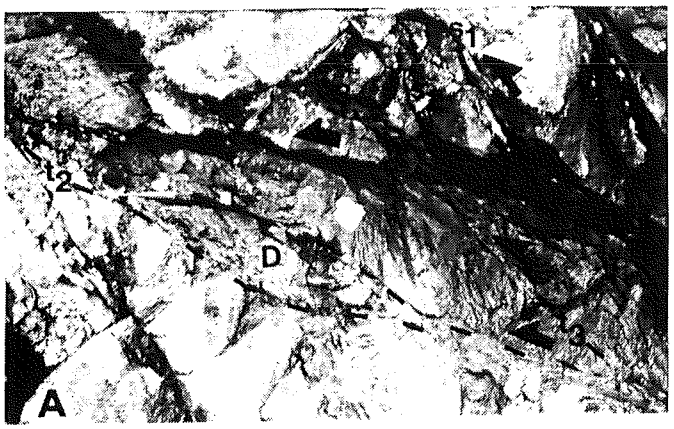

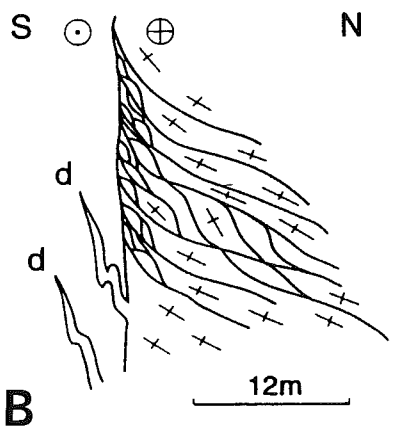

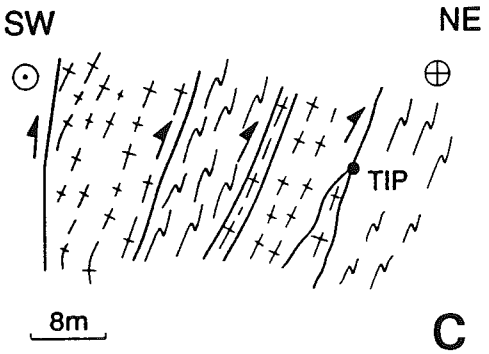

Fig. 6. Structural observations in the Pleasant Hills pluton. (A) Duplex structures. A roof thrust (t_1) and a floor thrust (t_2) define a partly exposed duplex with three splays (s_{1-3}) offsetting the floor of the hanging wall. A smaller, fully exposed duplex is observed in the centre of the photograph. Outcrop is 3.5 m wide. (B) Dextral transpressional contact between granite and diorite, deformed under solid-state conditions. The diorite (d) has acted as a barrier to southward motion of the granite (+ symbol). (C) Cross section of alternating sheets of gabbro (+), in places mylonitic, and metasediment (Z pattern) with late intrusion of granite wedge (TIP indicated). The granite has intruded along a pre-existing contact between gabbro and metasediment at the northern margin of the pluton.

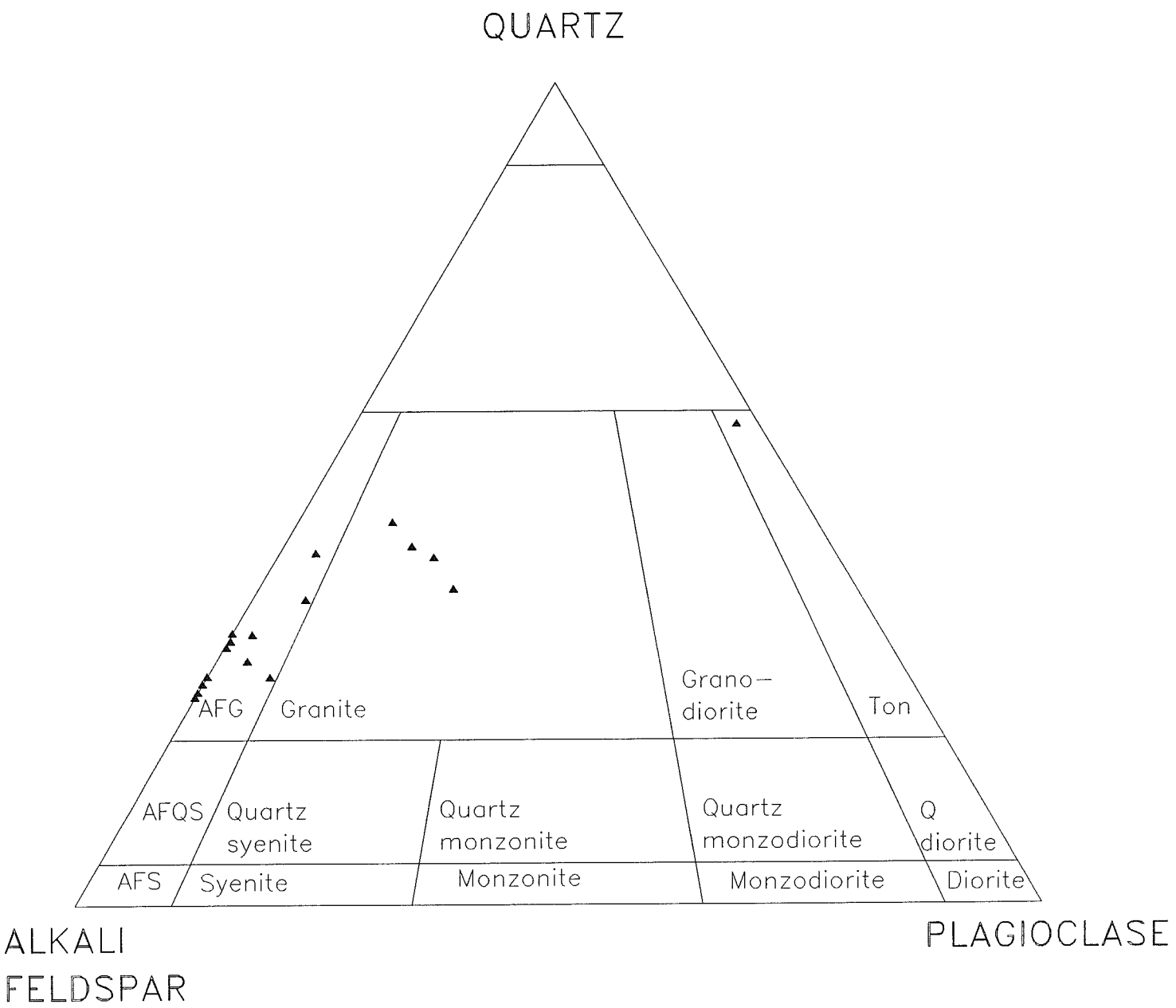

Fig. 7. I.U.G.S. classification of the granitoid rocks, Pleasant Hills pluton, based on modal compositions. Field names after Streickeisen, 1976.

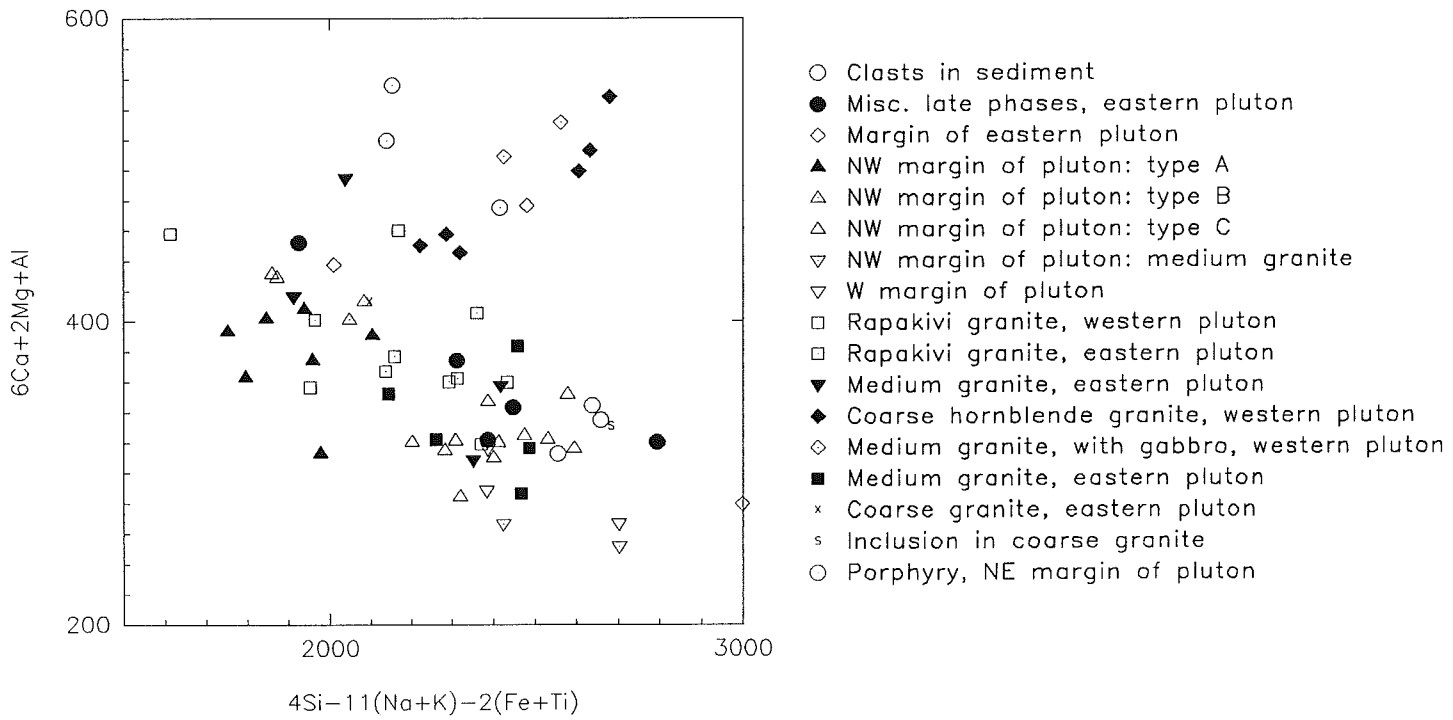

Fig. 8. Major element variation in the igneous rocks of the Pleasant Hills pluton illustrated using the parameters of de la Roche et al. (1980).

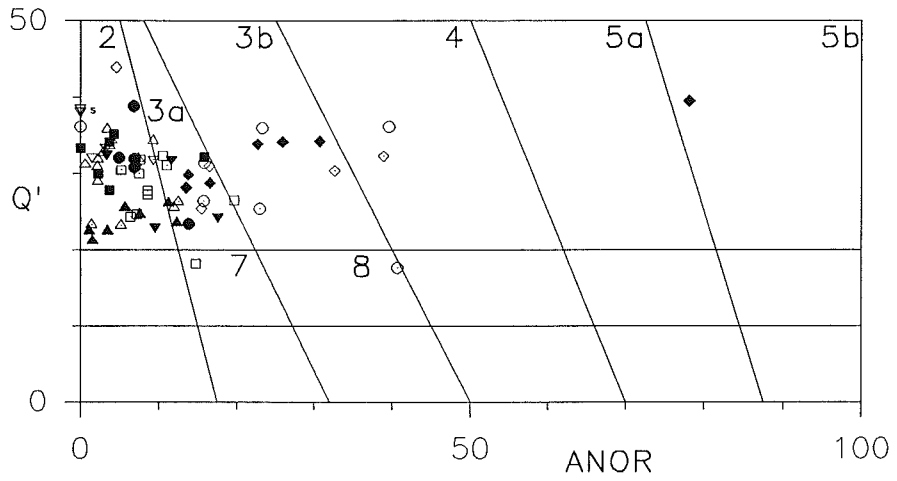

Fig. 9. Normative Q'-ANOR diagram for the Pleasant Hills pluton felsic igneous lithologies. Numbered classification fields after Streckeisen and Le Maitre (1979). Q'=100xQ/(Q+Or+Ab+An); ANOR=100xAn/(Or+An). Symbols as in Fig. 8. 2 = alkali-feldspar granite; 3a = syenogranite; 3b = adamellite-monzogranite; 4 = granodiorite; 5b = tonalite; 7 = quartz syenite; 8 = quartz monzonite.

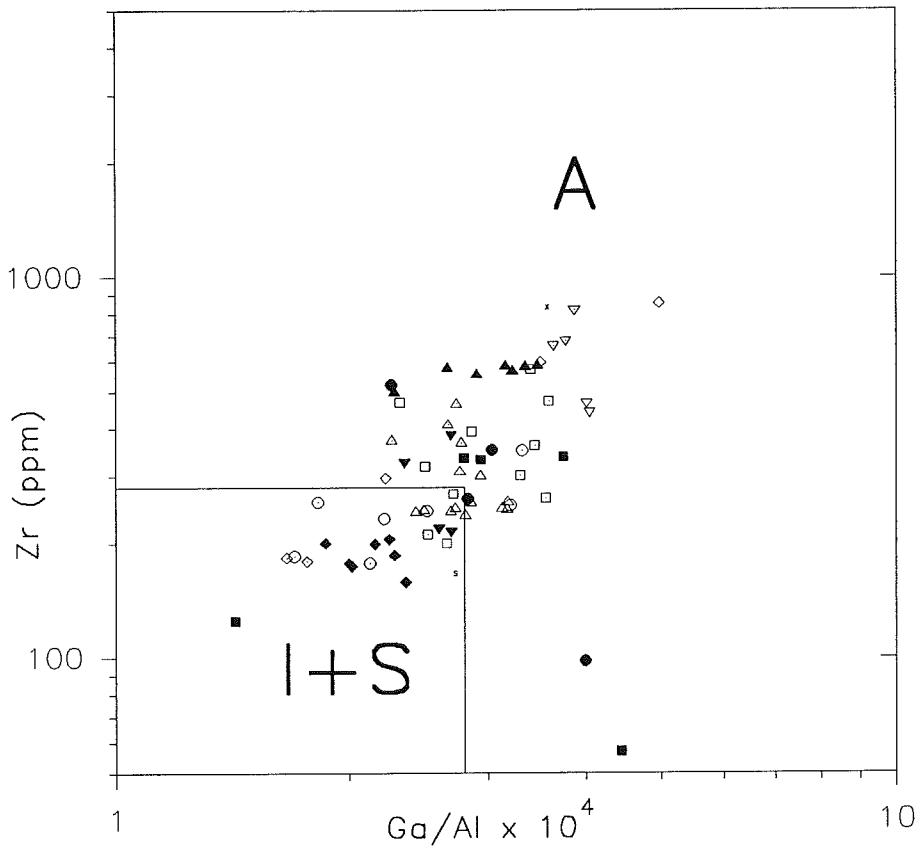

Fig.10. Zr vs. Ga/Al discriminant diagram for recognition of A-type granite (Whalen and others, 1987). A = field for A-type granites; I+S = field for I- and S- type granites. Symbols as in Fig. 8.

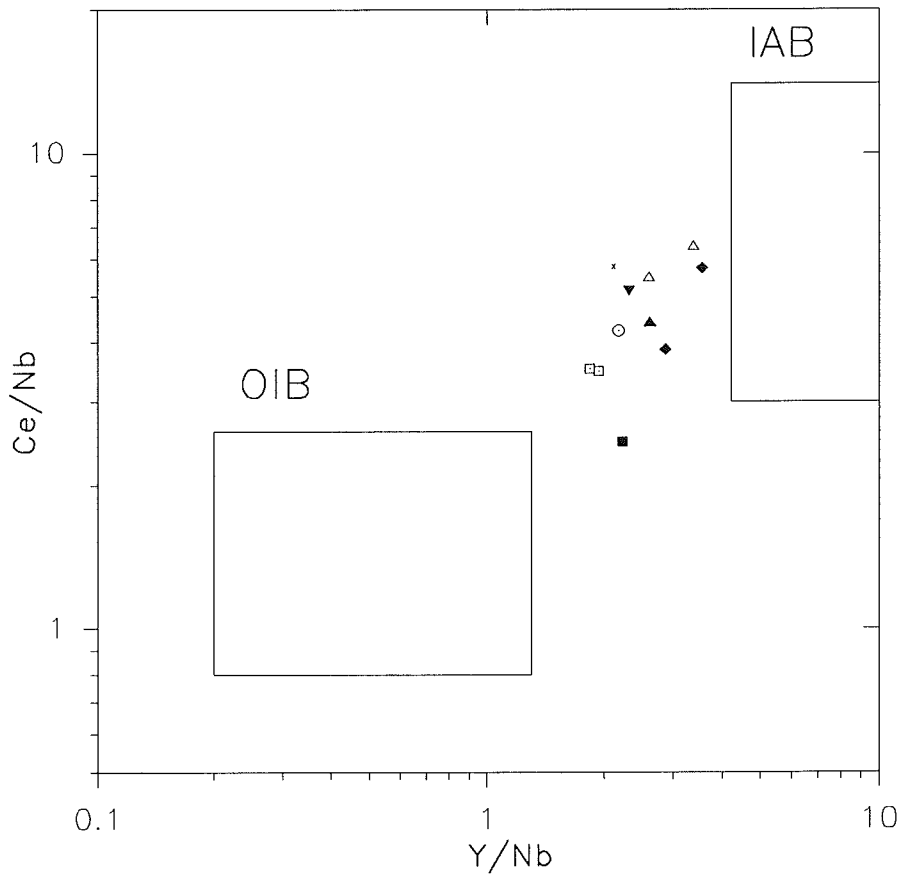

Fig.11. Ce/Nb vs. Y/Nb discriminant diagram for recognition of groups of A-type granitoids. The fields for OIB (oceanic-island basalt) and IAB (island-arc basalt) are after Eby (1992). Symbols as in Fig. 8.

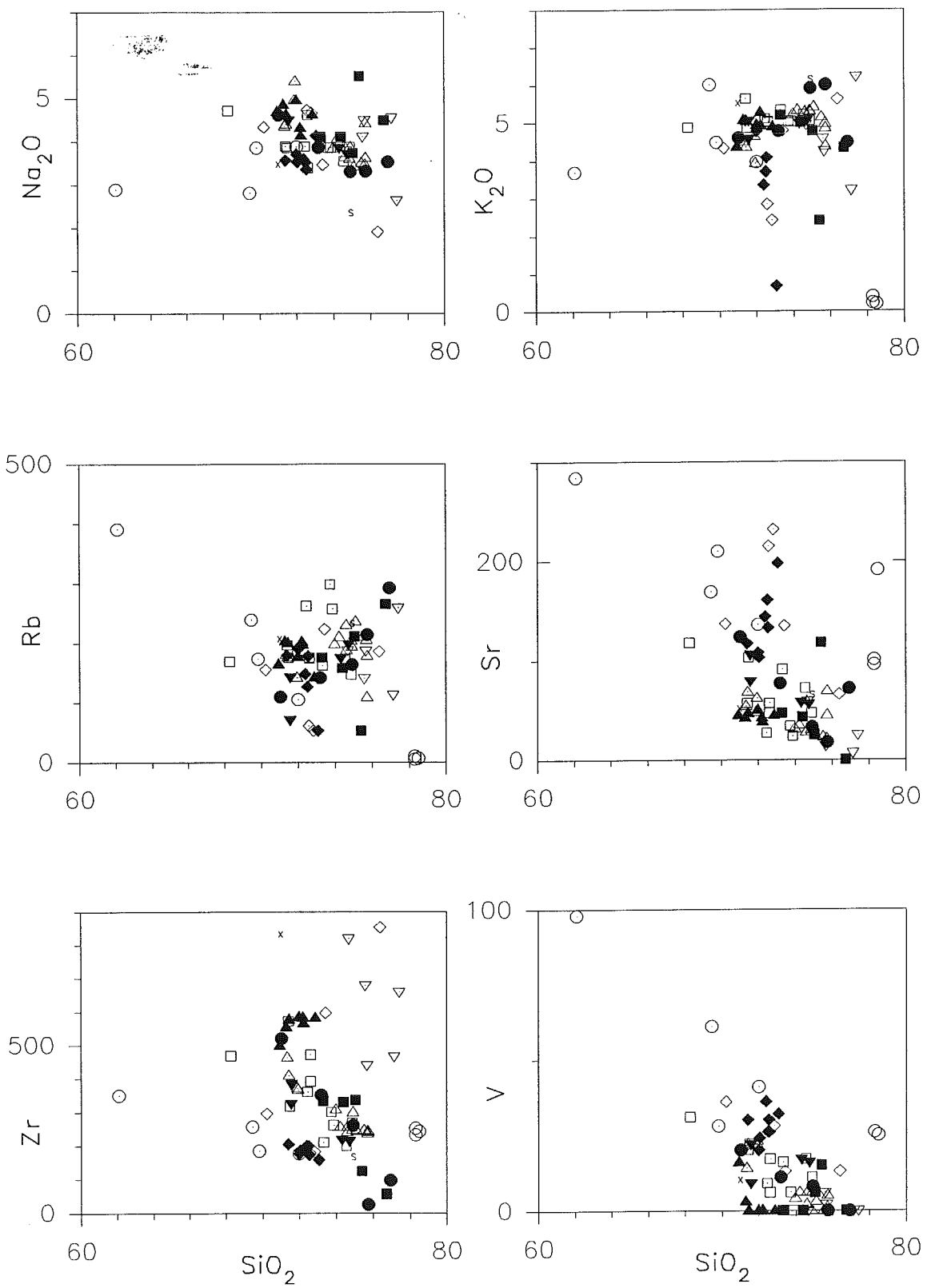

Fig. 12. Major and trace elements variations in Pleasant Hills felsic rocks in relation to SiO_2. Symbols as in Fig. 8.

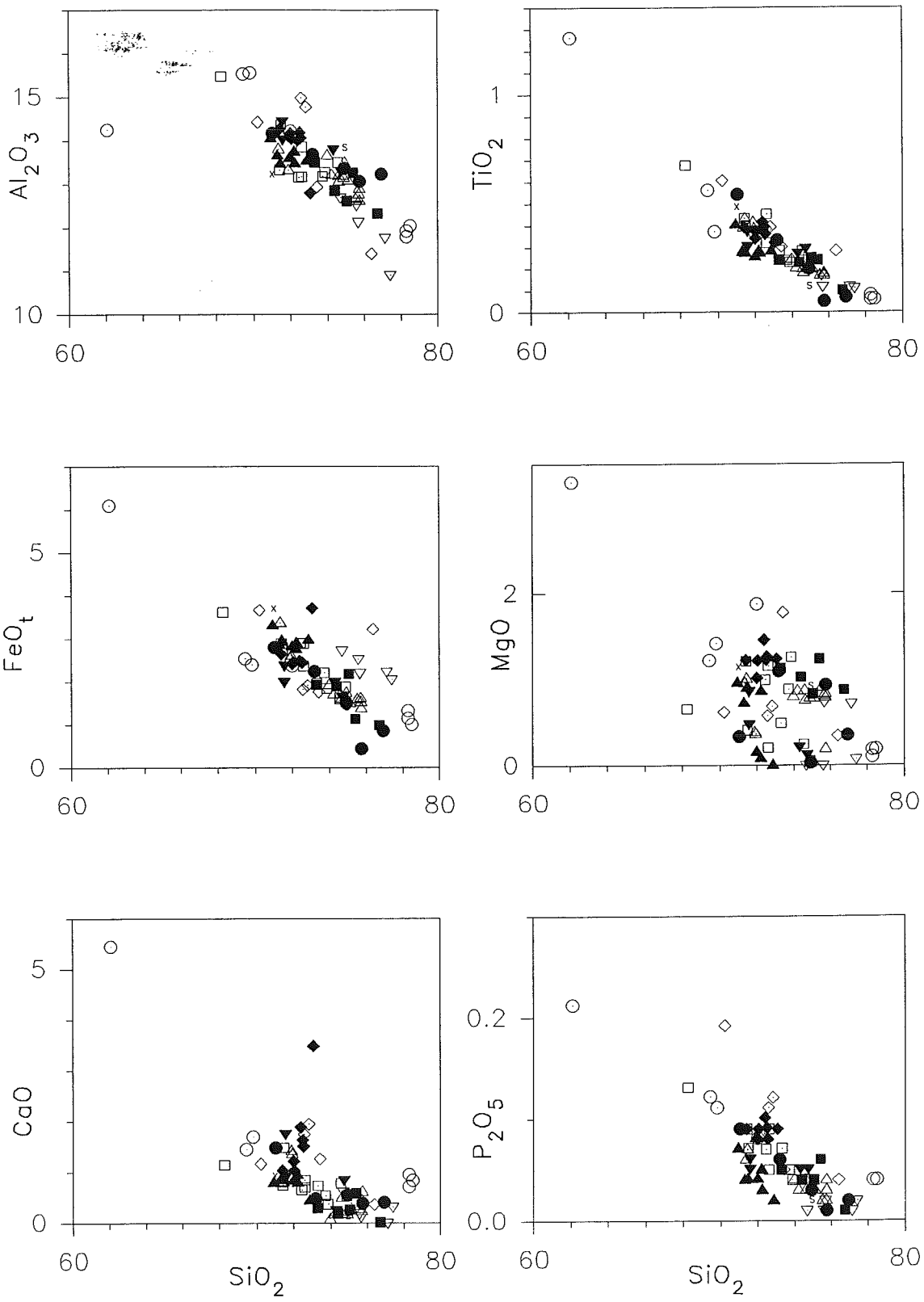
Al_2O_3
15
10
60
80
TiO_2
1
0
60
80
FeO_t
5
0
60
80
MgO
2
0
60
80
CaO
5
0
60
80
SiO_2
P_2O_5
0.2
0.0
60
80
SiO_2

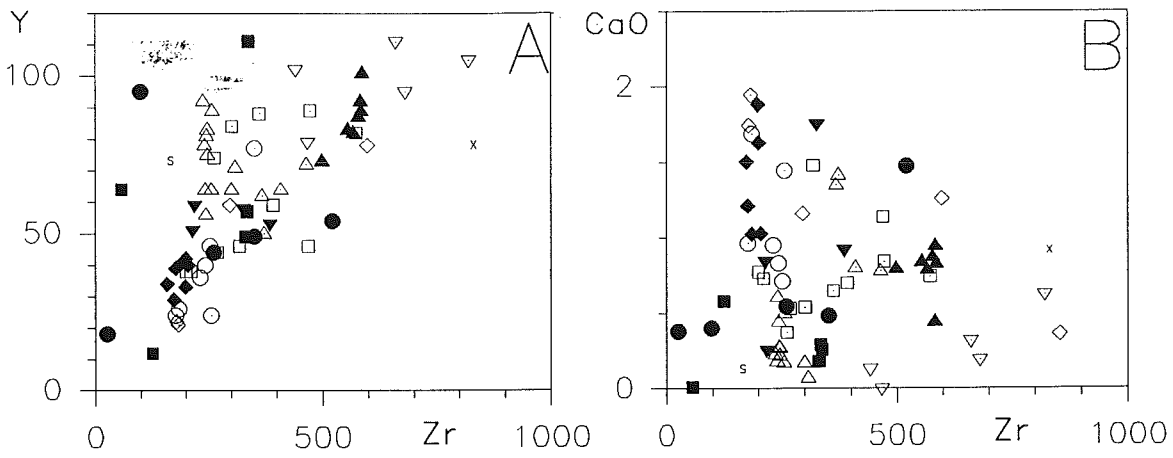

Fig. 13. Y vs. Zr and CaO vs. Zr diagrams for the felsic igneous lithologies of the Pleasant Hills pluton. Symbols as in Fig. 8.

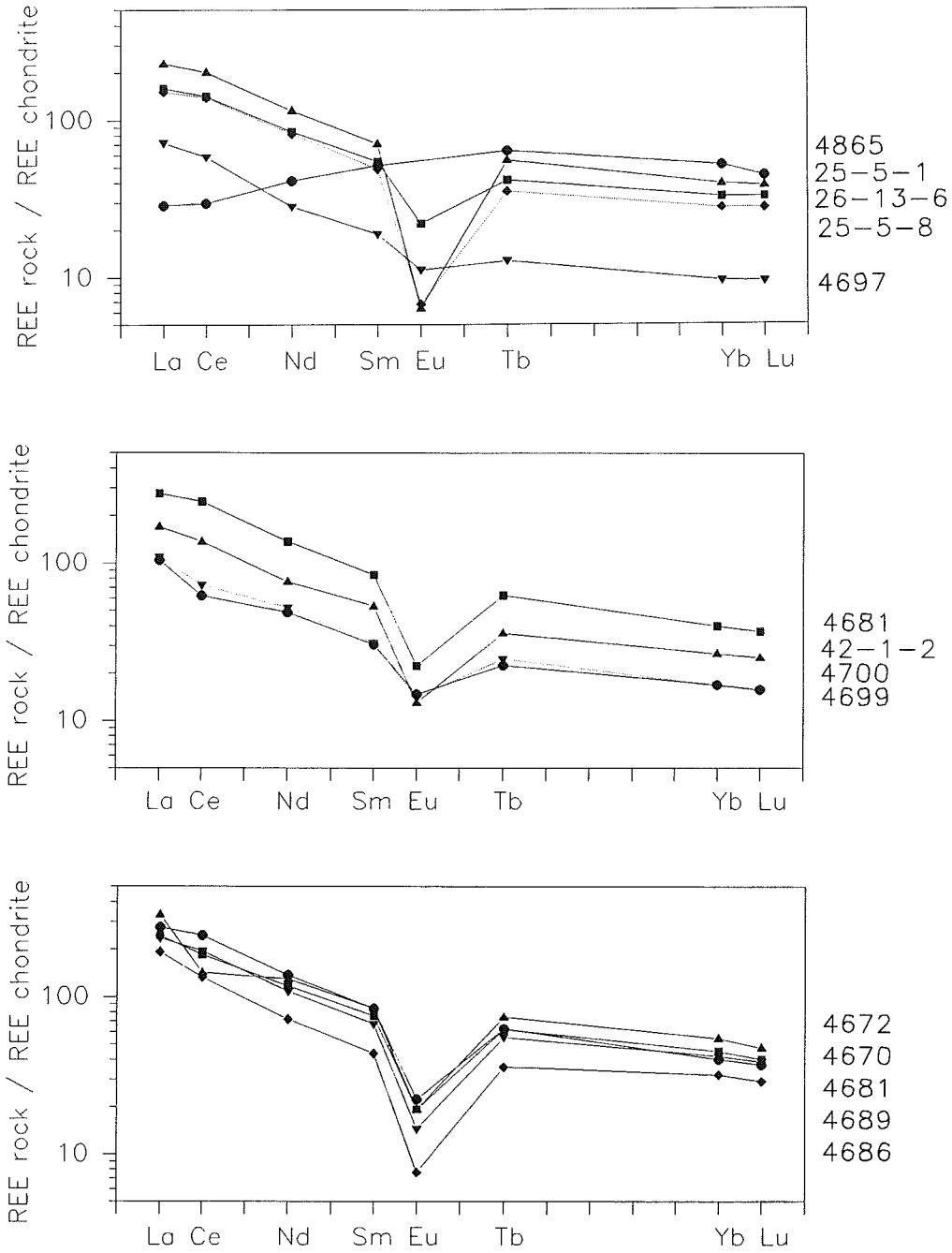

Fig. 14. Chondrite-normalized REE patterns for the Pleasant Hills pluton felsic lithologies. A: 25-5-1, 25-5-8 = fgpg at northwestern edge of pluton -type C, Chain Lake and E. Branch Economy River; 26-13-6 = fgpg at northwestern edge of the pluton- type A, West Economy river; 4697 = felvol early felsic volcanics/subvolcanics, northeastern margin of pluton; 4865 = sprhy late fine grained phases that cut rapakivi phases, West Bass river. B: 4681 = cgpog main coarse grained at southern edge of Eastern pluton; 42-1-2 = cgpg, main granite in northern western half of the pluton; 4700, 4699 = vcgrog main coarse grained hornblende granite at southern edge of western pluton; C: 4670, 4689 = rg main rapakivi phases, eastern pluton (Gamble Lake area); 4672, 4686 = mgpg in the eastern part of the pluton; 4681 = cgpog main coarse granite at southern edge of eastern pluton.

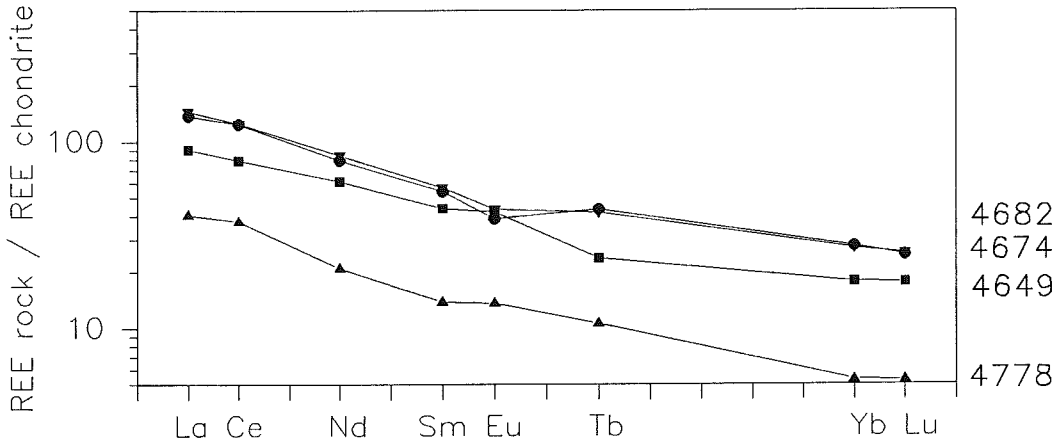

Fig 15. Chondrite-normalized REE patterns for the Pleasant Hills pluton mafic lithologies. 4282=gabbro; 4674=diorite (Gamble Lake area); 4778=megacrystic diorite; 4649=megacrystic mafic rock from the Folly Lake diorite.

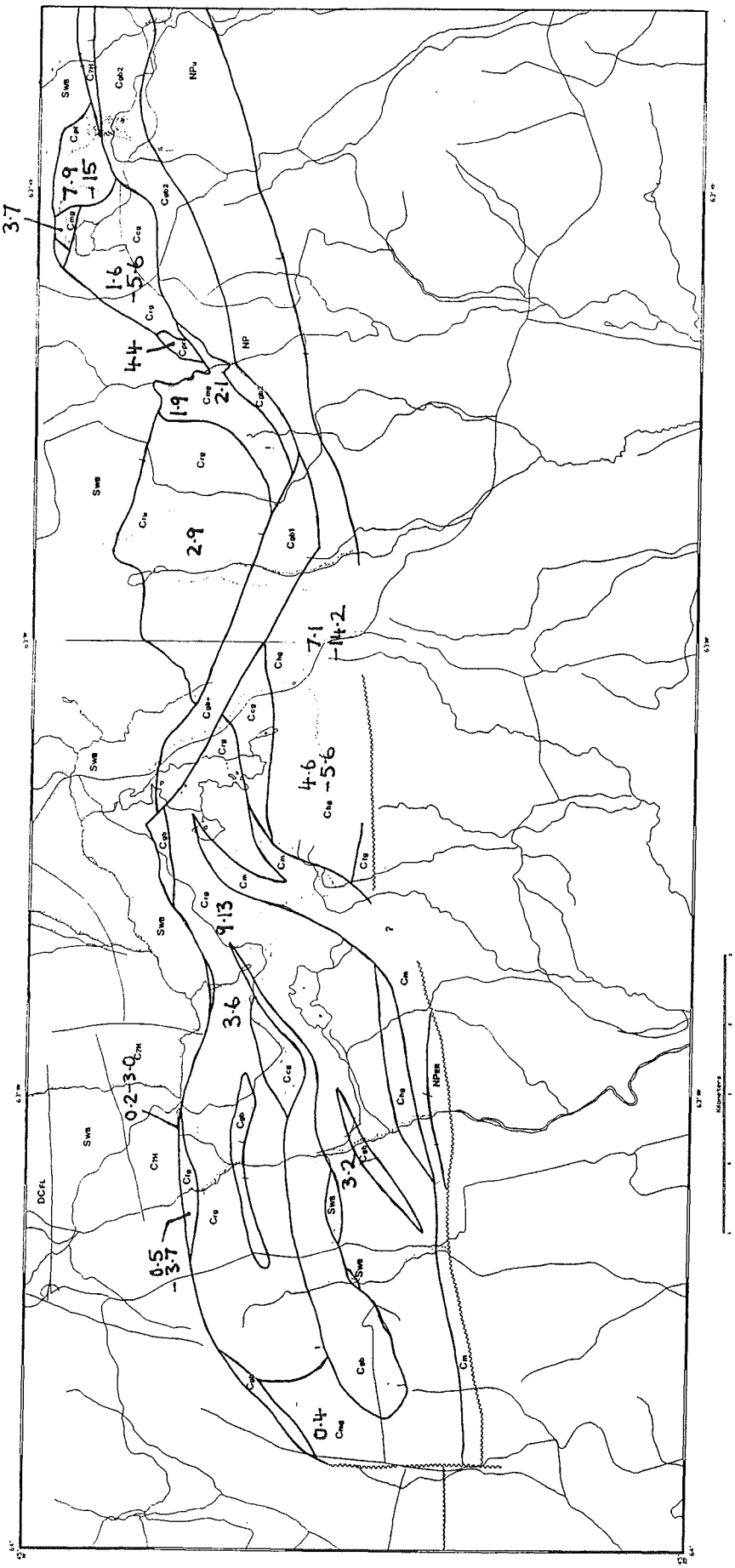

Fig.16. Map showing the geographic distribution of normative anorthite (An) in the felsic rock phases of the Pleasant Hills pluton.

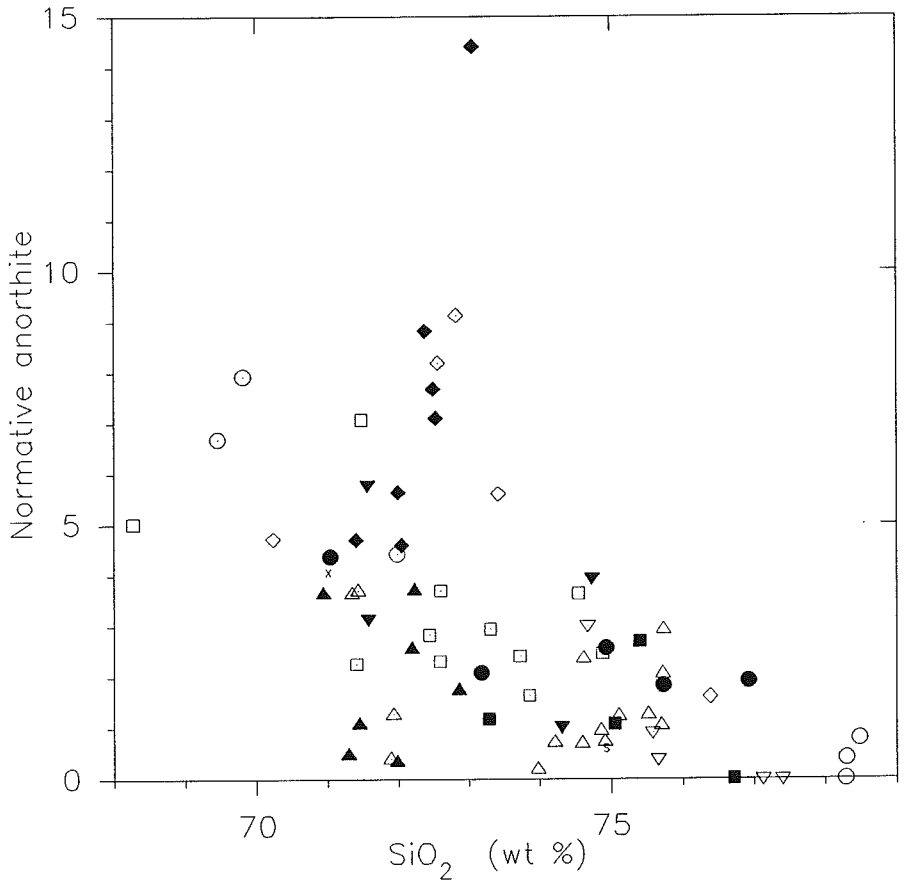

Fig.17. Normative anorthite vs. SiO_2 diagram for the Pleasant Hills pluton felsic lithologies.

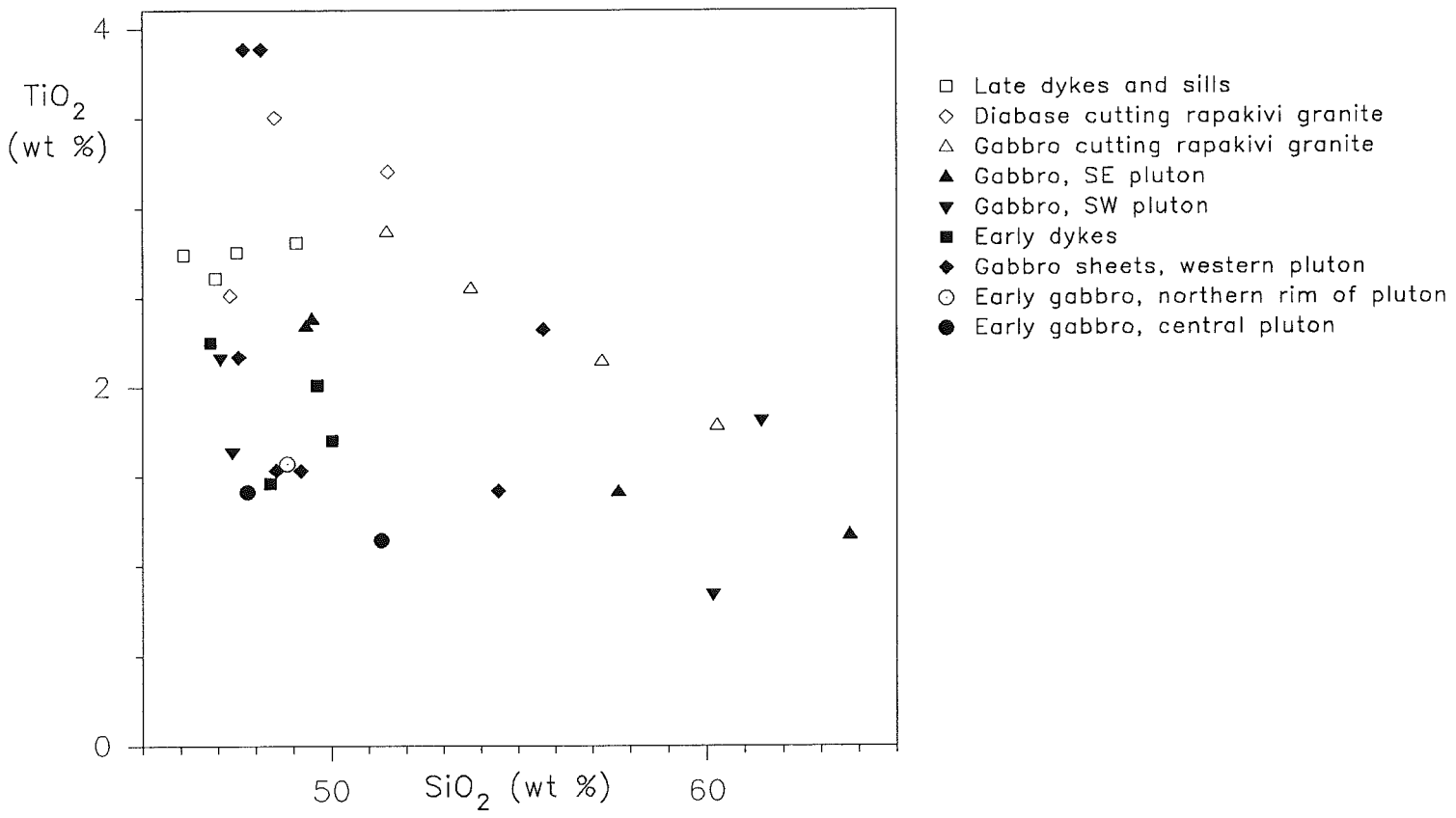

Fig. 18. TiO_2 vs. SiO_2 diagram for the Pleasant Hills pluton mafic lithologies.

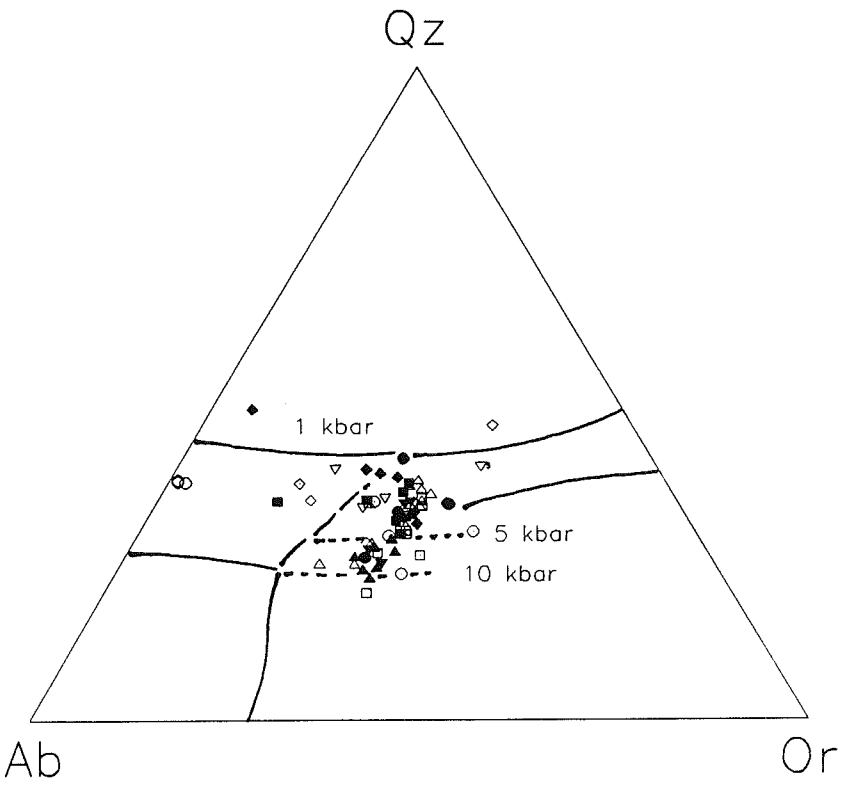

Fig. 19. Plot of normative composition of Pleasant Hills pluton felsic lithologies on a normative Qz-Ab-Or diagram. Cotectectic lines for water saturated magma after Johannes and Holtz (1990).

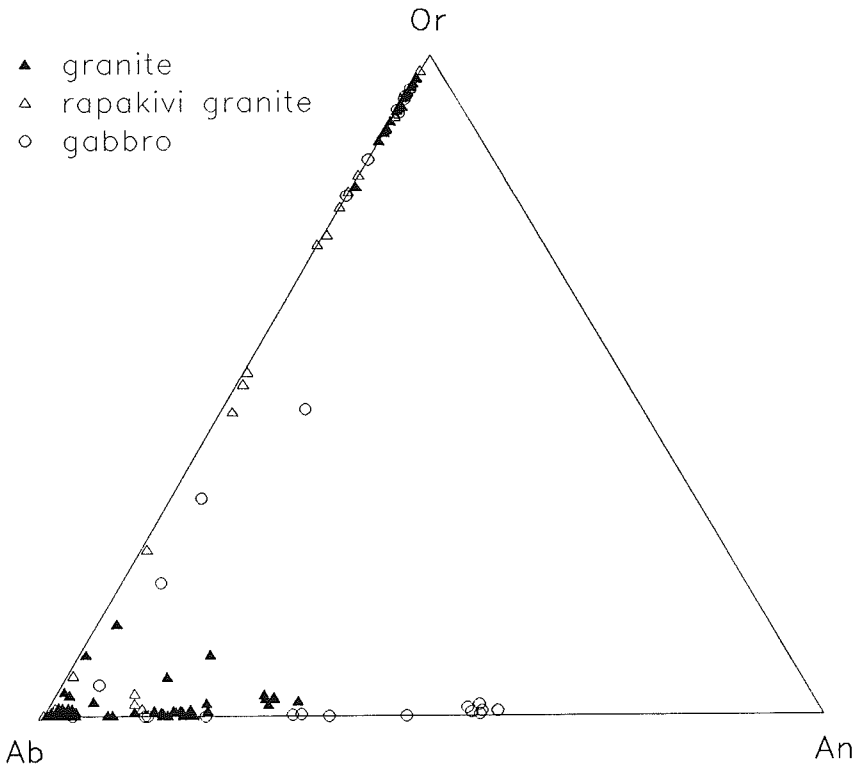

Fig. 20. Composition of feldspars from the Pleasant Hills pluton (data from Table 4) plotted on a Or-An-Ab diagram.

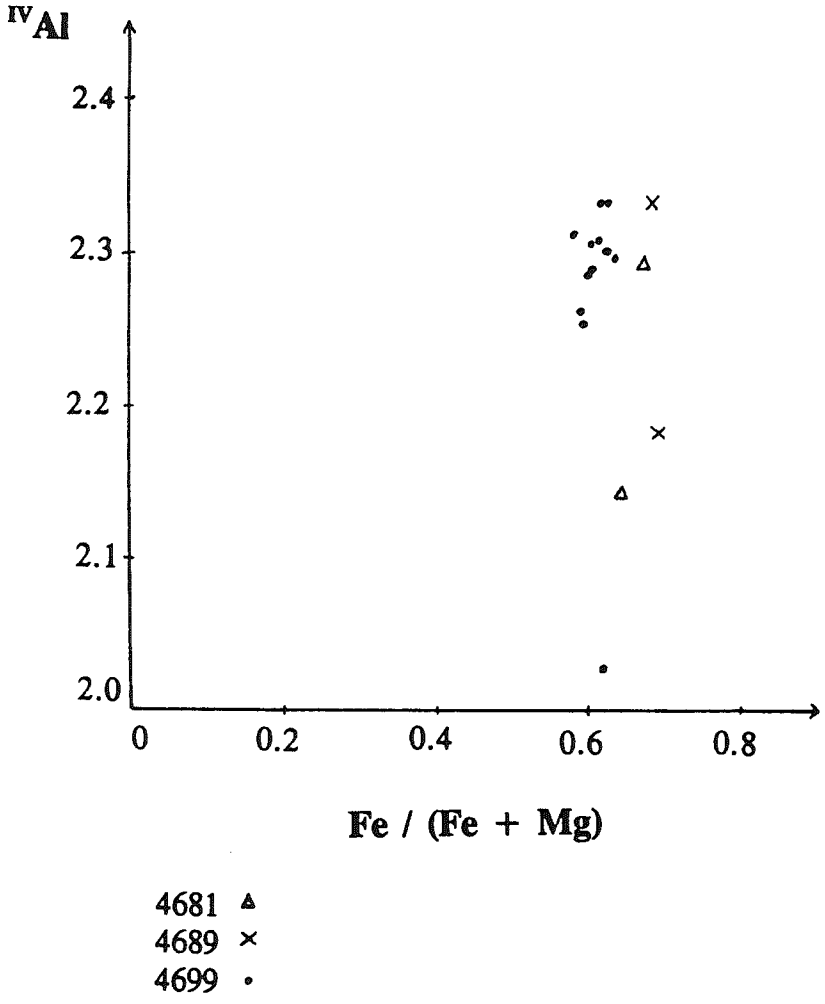

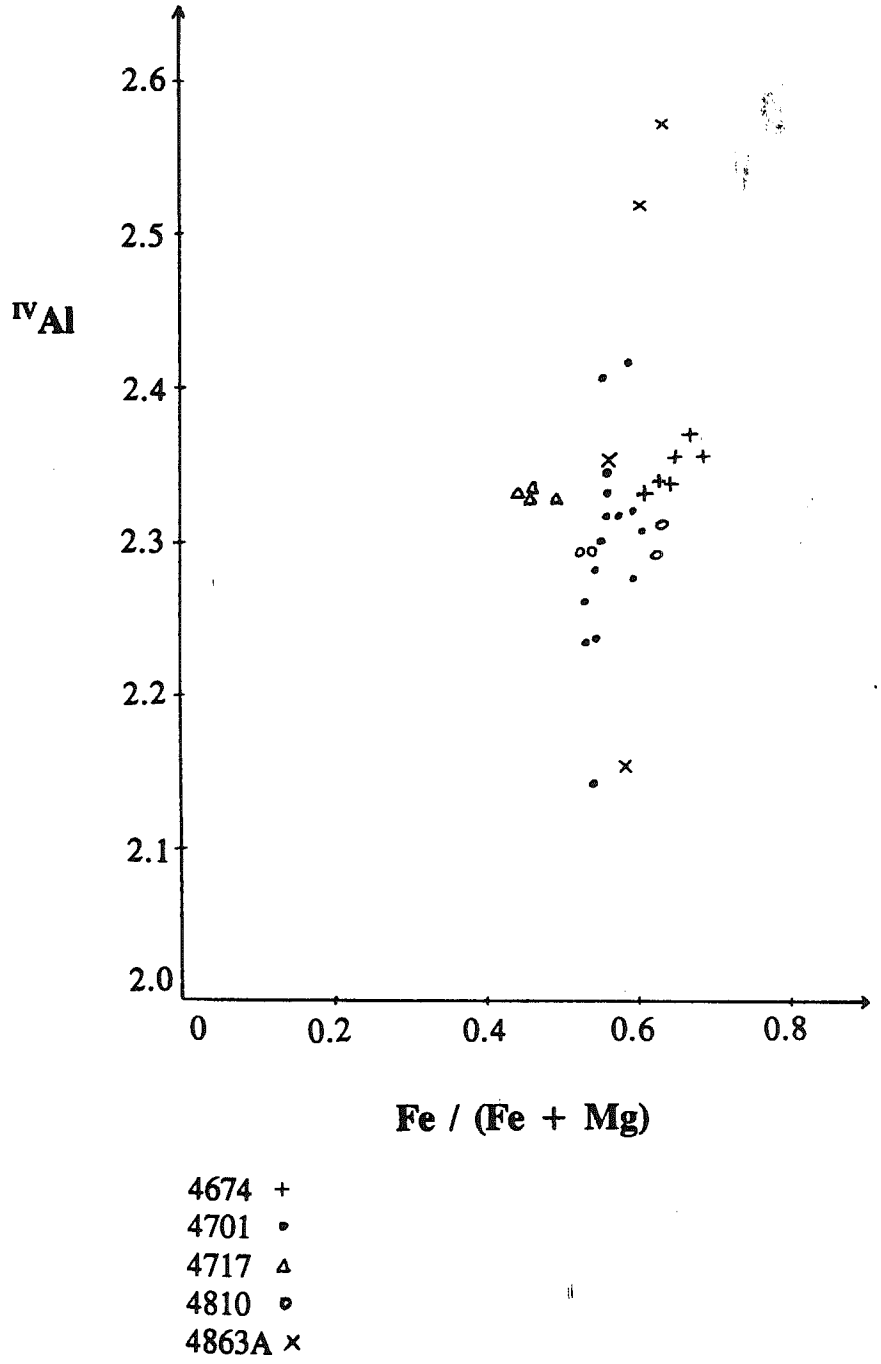

Fig. 21. Compositions of biotite from the Pleasant Hills pluton (data from Table 5).

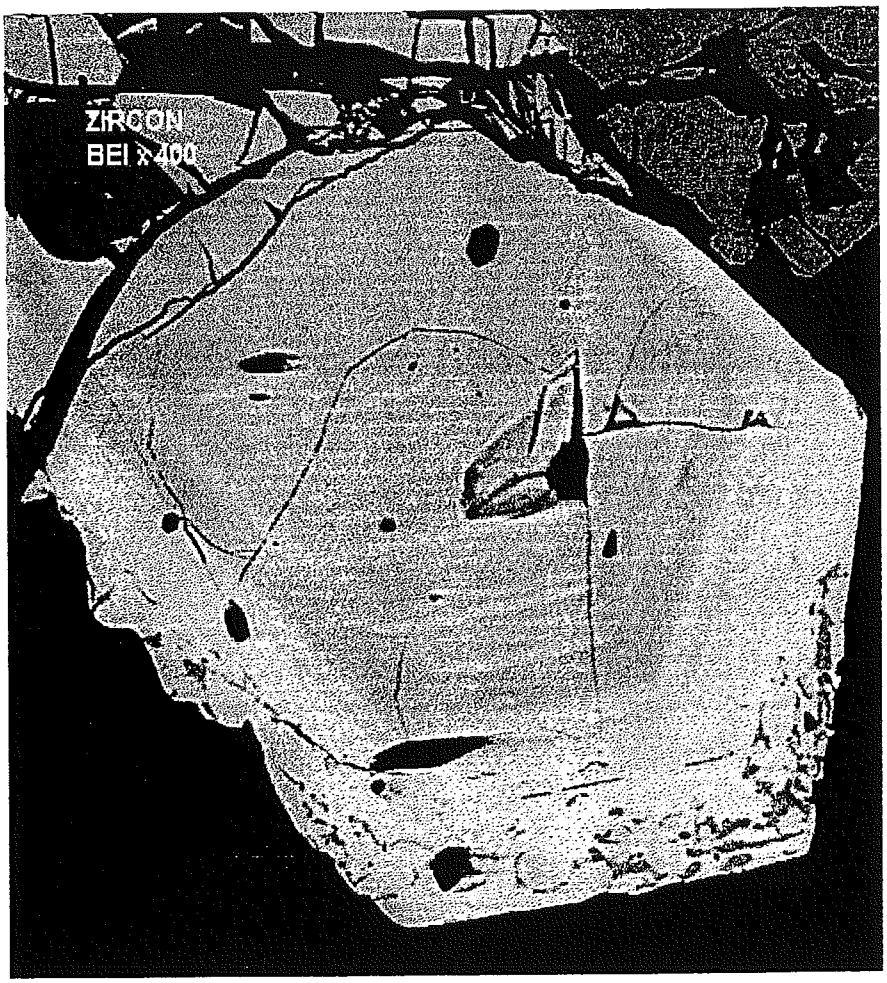

Fig. 22. Electron microprobe backscatter images of zircons. (A) Zoned crystal of zircon with a rim that appears to have reacted with the host magma. (4863, rapakivi granite). (B) Glomeroporphyritic accumulation of zircon crystals poikilitically enclosed by an opaque mineral. Note the lighter and darker zones. (4681, cgpog).

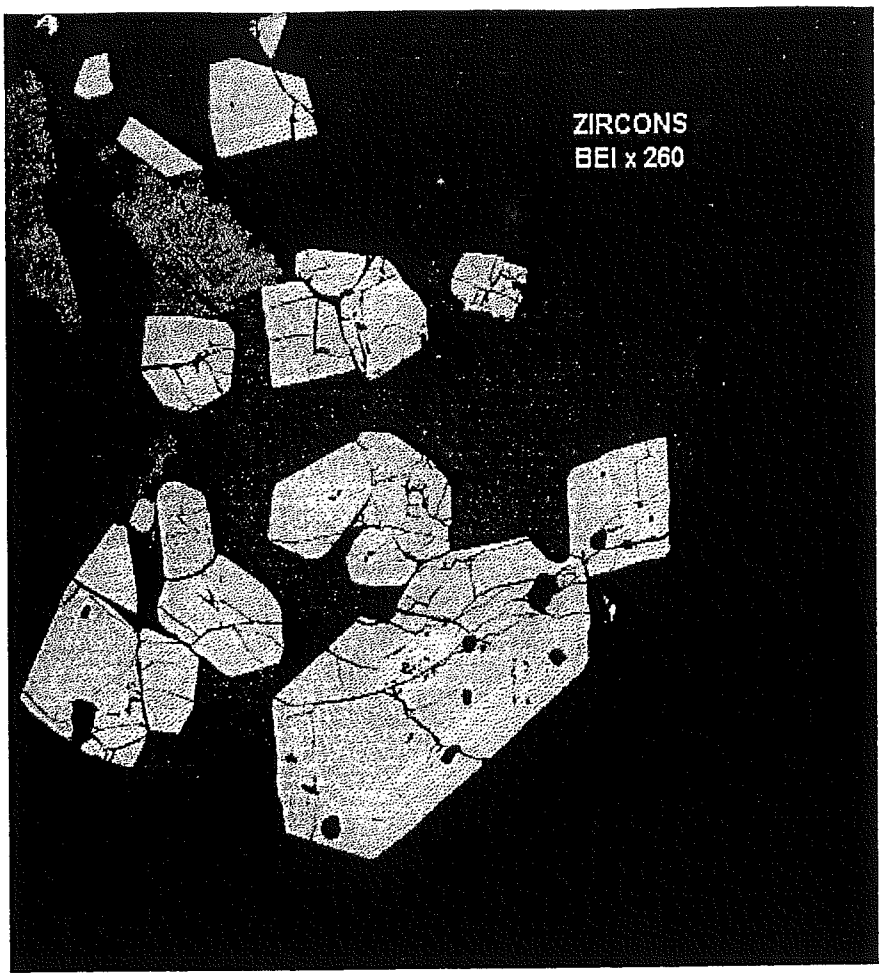
ZIRCONS
BEI x 260

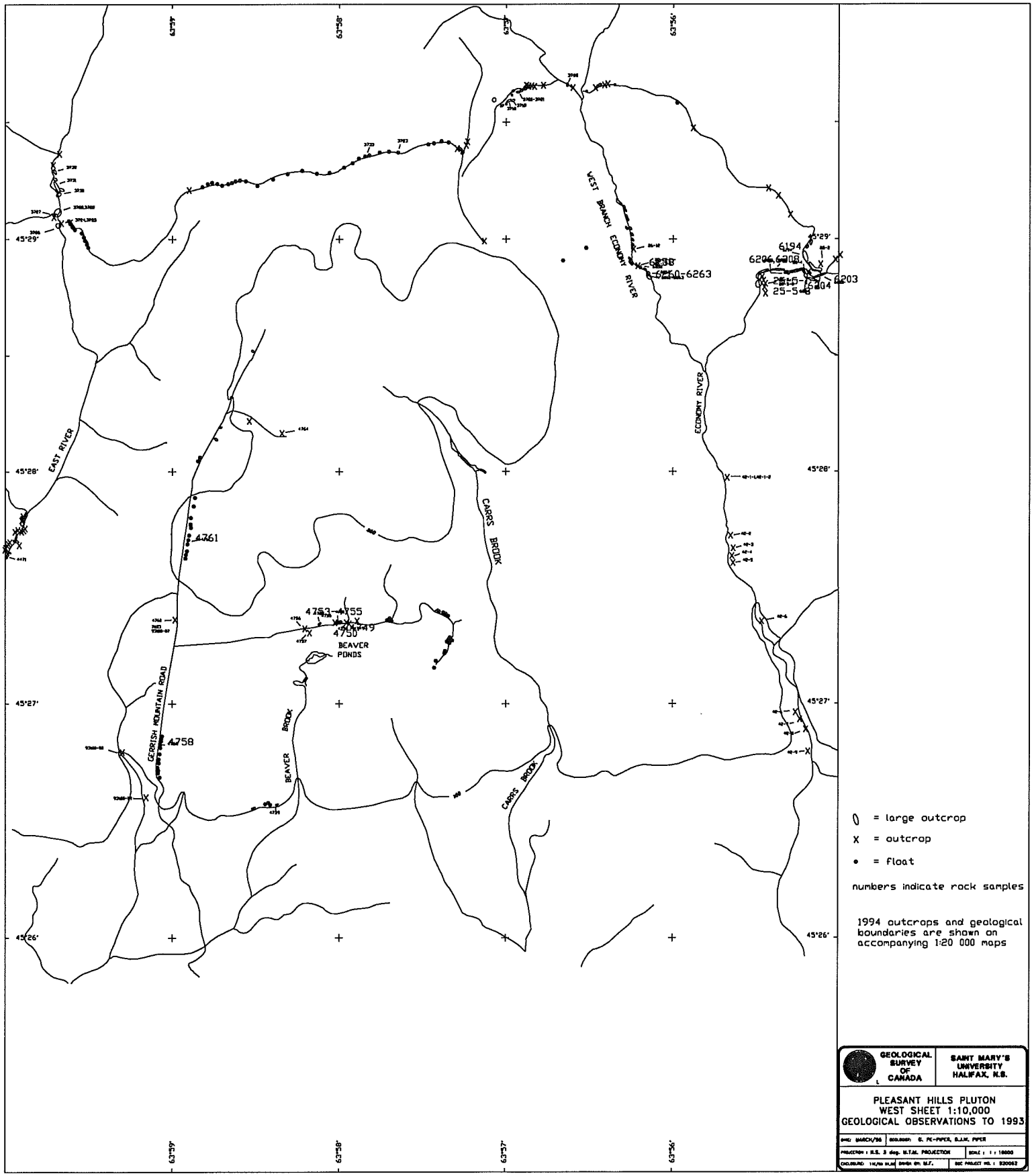
63°59'
63°58'
63°57'
63°56'
45°29'
45°28'
45°27'
45°26'
EAST RIVER
WEST BRANCH ECONOMY RIVER
ECONOMY RIVER
CARRS BROOK
BEAVER BROOK
GERRISH MOUNTAIN ROAD
BEAVER PONDS
4761
4758
4753-4755
4749
4750
6194
6200-6208
6250-6263
6203
6204
25-5-6
25-5-7
25-5-8
= large outcrop
= outcrop
= float
numbers indicate rock samples
1994 outcrops and geological boundaries are shown on accompanying 1:20 000 maps
GEOLOGICAL SURVEY OF CANADA
SAINT MARY'S UNIVERSITY HALIFAX, N.S.
PLEASANT HILLS PLUTON
WEST SHEET 1:10,000
GEOLOGICAL OBSERVATIONS TO 1993

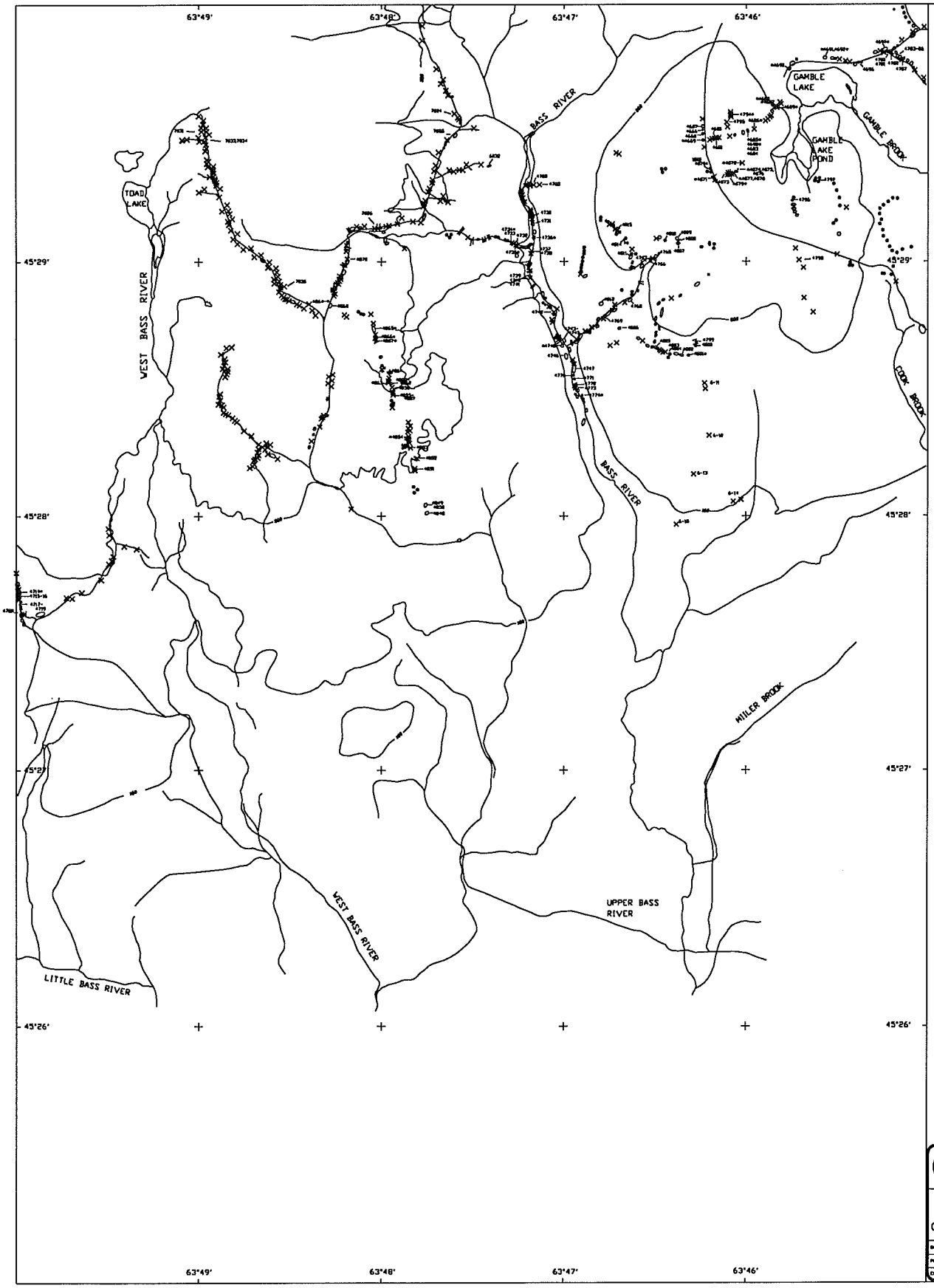

= large outcrop

X = outcrop

• = float

numbers indicate rock samples

1994 outcrops and geological boundaries are shown on accompanying 1:20 000 maps

GEOLOGICAL SURVEY OF CANADA

SAINT MARY'S UNIVERSITY HALIFAX, N.S.

PLEASANT HILLS PLUTON EAST SHEET 1:10,000 GEOLOGICAL OBSERVATIONS TO 1993

DATE: MARCH/96 GEOLOGIST: G. PE-PIPER, D.J.W. PIPER

PROJECTION: N.S. 3 deg. M.T.M. PROJECTION SCALE: 1 : 10000

ENCLOSURE: 1%/96 1%/96 DRAWN BY: M.F. SMC PROJECT NO.: 930052

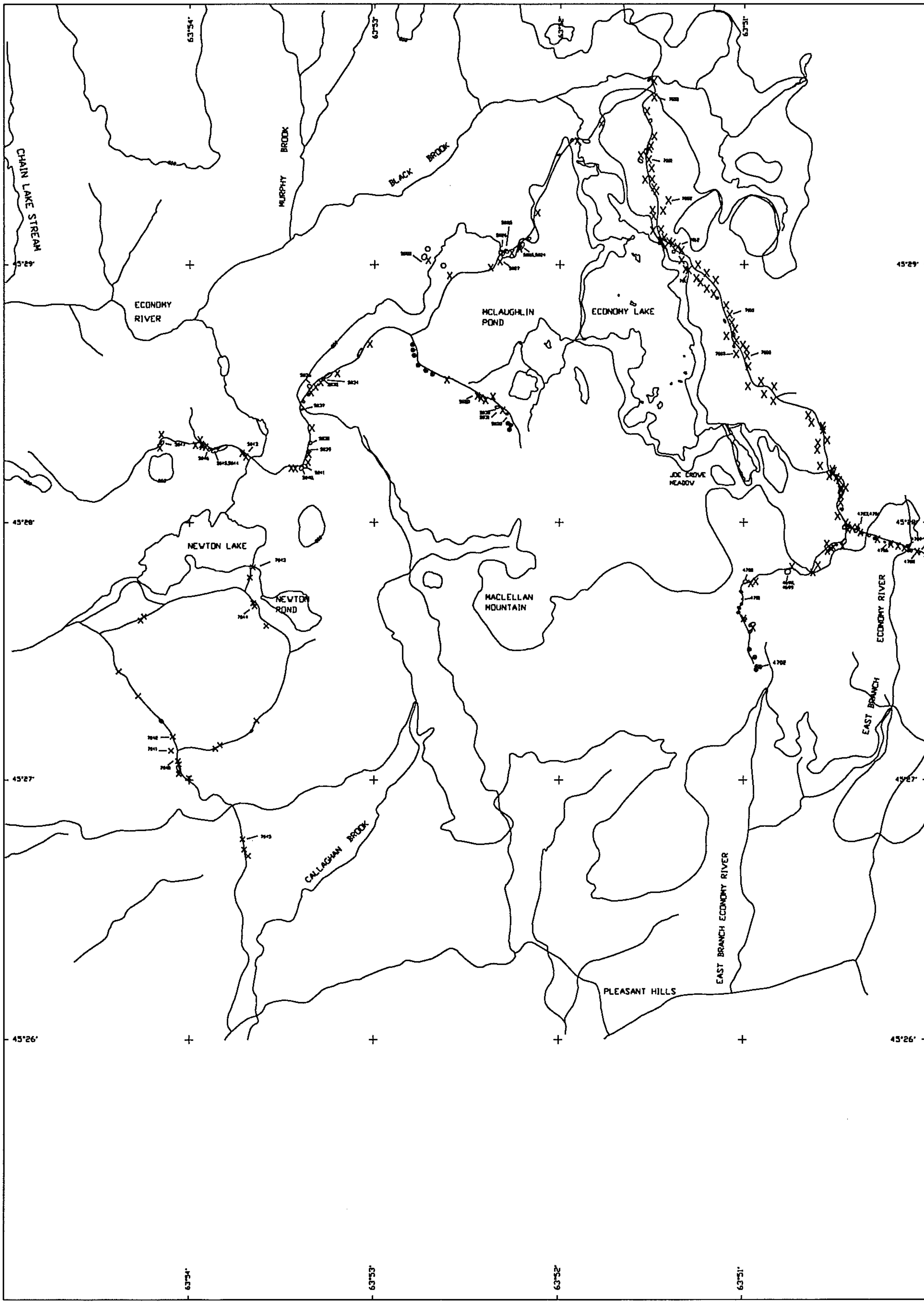

o = large outcrop

X = outcrop

• = float

numbers indicate rock samples

1994 outcrops and geological boundaries are shown on accompanying 1:20 000 maps

GEOLOGICAL SURVEY OF CANADA

SAINT MARY'S UNIVERSITY HALIFAX, N.S.

PLEASANT HILLS PLUTON CENTRAL SHEET 1:10,000 GEOLOGICAL OBSERVATIONS TO 1993

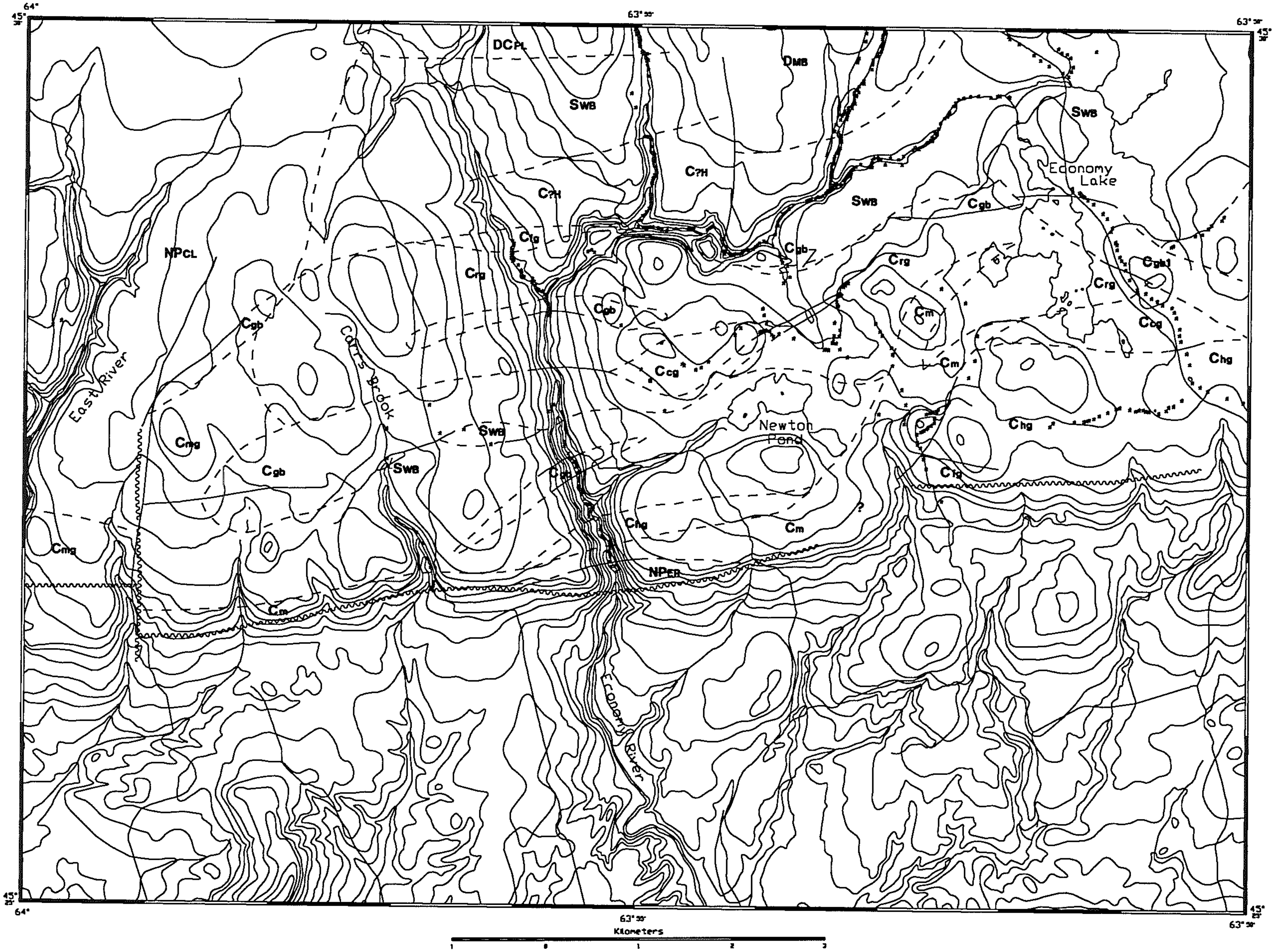

LEGEND

SEDIMENTARY AND VOLCANIC ROCKS

C?H	[illegible] Early Carboniferous
DCFL	Fountain Lake Group [illegible] Late Devonian - Early Carboniferous
DMB	[illegible] Formation. Conglomerate, sandstone and shale. Middle Devonian
SWB	[illegible] Formation. Sandstone and siltstone. Silurian
NPCL	[illegible] Lake Formation. [illegible] Neoproterozoic III

LATEST DEVONIAN - EARLY CARBONIFEROUS PLUTONIC ROCKS

Ccg	Coarse-grained alkali-feldspar granite.
Chg	Hornblende granite, generally coarse grained.
Cmg	Medium-grained alkali-feldspar granite, locally coarser grained.
Crg	[illegible]
Cfg	Fine-grained granite.
Cpr	Porphyritic rhyolite.
Cm	[illegible]
Cgd	Granodiorite.
Cgb	Gabbro, commonly cut by granite veins.
Cgb1	[illegible]
Cgb2	[illegible]

PLUTONIC ROCKS

NPER	Economy River granodiorite, generally strongly foliated.
NPU	[illegible]

(solid line)	Geological boundary
(dashed line)	Geological boundary, assumed
(wavy line)	Major fault

O	Outcrop
L	Large outcrop
S	Several outcrops
A	Disturbed outcrop
F	Float

WESTERN PLEASANT HILL PLUTON

Geological mapping by [illegible] 1994

Scale 1 : 20,000

[illegible]

GEOLOGICAL SURVEY OF CANADA (ATLANTIC)

SAINT MARY'S UNIVERSITY HALIFAX, N.S.

WESTERN PLEASANT HILLS PLUTON 1:20,000 GEOLOGY

DATE: MARCH/96	GEOLOGIST: G. PE-PIPER, D.J.W. PIPER	
PROJECTION: TRANSVERSE MERCATOR		SCALE: 1 : 20,000
ENCLOSURE: 11E/06 II	DRAWN BY: M.F.	GSC PROJECT NO.: 920062

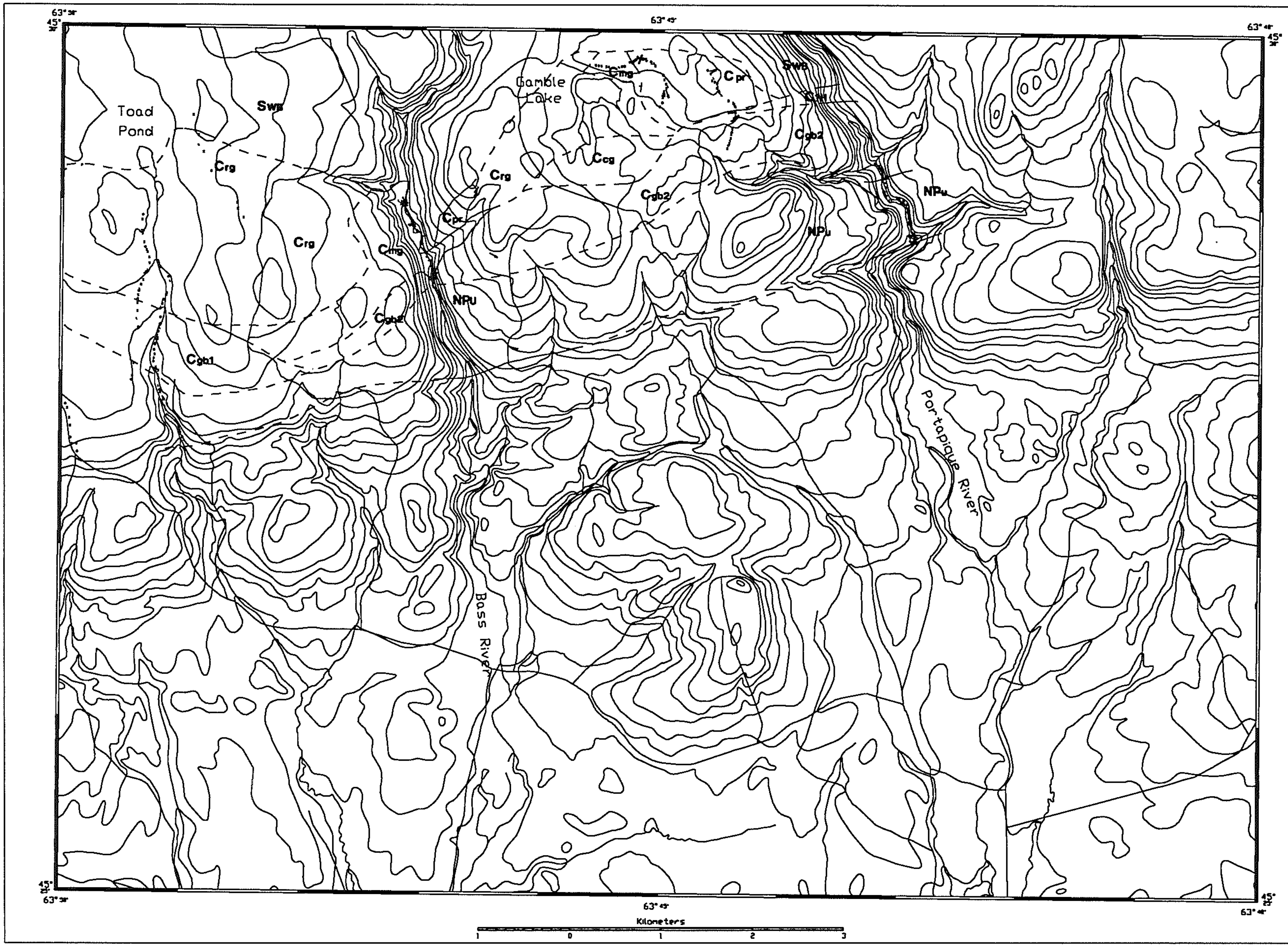

LEGEND

SEDIMENTARY AND VOLCANIC ROCKS

C?H	Horton Group equivalents. Conglomerate, sandstone and siltstone. Early Carboniferous
DCFL	Fountain Lake Group. basalt, rhyolite, lesser red sandstone and conglomerate. Late Devonian - Early Carboniferous.
DMB	Murphy Brook Formation. Conglomerate, sandstone and shale. Middle Devonian
SWB	Wilson Brook Formation. Sandstone and siltstone. Silurian
NPCL	Cranberry Lake Formation. Thin-bedded sandy turbidites. Neoproterozoic III

LATEST DEVONIAN - EARLY CARBONIFEROUS PLUTONIC ROCKS

Ccg	Coarse-grained alkali-feldspar granite.
Chg	Hornblende granite, generally coarse grained.
Cmg	Medium-grained alkali-feldspar granite, locally coarse grained.
Crg	Medium-grained rapakivi granite, associated with lesser alkali-feldspar granite, gabbro and granodiorite.
Cfg	Fine-grained granite.
Cpr	Porphyritic rhyolite.
Cm	Mylonitic granite, locally foliated gabbro and granodiorite.
Cgd	Granodiorite
Cgb	Gabbro, commonly cut by granite veins.
Cgb1	Gabbro, lesser granite and granodiorite, locally foliated.
Cgb2	Gabbro, minor granodiorite and, in the Portapique River, granite, generally strongly foliated.

PLUTONIC ROCKS

NPER	Economy River granodiorite, generally strongly foliated.
NPu	Undivided Neoproterozoic rocks, principally diorite with lesser Gamble Brook Formation quartzite.

Geological boundary

Geological boundary, assumed

Major fault

O Outcrop
L Large outcrop
S Several outcrops
A Disturbed outcrop
F Float

WESTERN PLEASANT HILL PLUTON
Geological mapping by G. Pe-Piper, D.J.W. Piper, [illegible], 1987 - 1994

Scale 1 : 20,000

Locations digitised from 1:10,000 orthophoto maps and may not correspond precisely with geographic locations derived from the 1 : 20,000 digital base. 1994 locations are available in a [illegible] database; pre-1994 locations are shown on the accompanying 1 : 10,000 map sheets.

GEOLOGICAL SURVEY OF CANADA (ATLANTIC)

SAINT MARY'S UNIVERSITY HALIFAX, N.S.

EASTERN PLEASANT HILLS PLUTON
1:20,000
GEOLOGY

DATE: MARCH/96	GEOLOGIST: G. PE-PIPER, D.J.W. PIPER	
PROJECTION : TRANSVERSE MERCATOR		SCALE : 1 : 20,000
ENCLOSURE: 11E/05 N1	DRAWN BY: M.F.	GSC PROJECT NO. : 920062